CHITOSAN PARTICLES FOR THE CONTROLLED RELEASE OF PROTEINS

Li Ruo

DOCTORAL DISSERTATION

DEPARTMENT OF MECHANICS

POLITECNICO DI TORINO

Ph.D Condidate: Li Ruo

Major: Biomedical Engineering

Circle: XXIV

Supervisor: Prof. Gianluca Ciadelli

Department of Mechanics

Politecnico di Torino, Italy

Abstract

Back Ground Chitosan as a natural polymer has been fabulated into a number of formulations such as films, hydrogels and particles based on its excellent properties such as biodegradable, biocompotable, bioadhesive, permeartion-enhancement, antibiotic, antitumor etc. properties. Among them, chitosan microparticles found a lot of applications in pharmaceutics such as vaccine delivery, mucosal delivery and gene delivery, etc. Down to the nanoscale, chitosan nanoparticles have more attractive properties more than that of chitosan microparticles, which further widen the applications of chitosan particles in biomedicine and biopharmaceutics.

Objective of this Thesis This thesis is aimed to prepare chitosan micro or nanoparticles to delivery proteins.

What are the questions this thesis attempted to solve? 1) What are the proper preparation conditions of chitosan micro or nanoparticles? 2) How does the pH value affect the formation and protein encapsulation of chitosan nanoparticles? 3) How to overcome the burst release of chitosan nanoparticles? 4) How to overcome the aggregation disadvantage in the contritional preparation process of TPP-gelated chitosan microparticles? 5) How to construct a composite particles system to realize the sustainable release of proteins?

What are the methods used in this thesis? 1) ionotropic gelation method to prepare chitosan nanoparticles 2) Emulsification-coacervation (NaOH) method to prepare chitosan microparticles 3) a polyelectrolytes coacervation method to prepare chitosan-BSA complexes 4) a microemulsion involved emulsification-coalescence method to prepare TPP-gelated chitosan microparticles 5) a nanoparticles encapsulation method to prepare composite particles.

Results and Conclutions 1) the effect of preparation parameters on the properties of chitosan nanoparticles: 1a) the concentration of chitosan has no siganificant effect on particles yield, positively associated with particles size, size distribution, positively associated with BSA encapsulation efficiency in a specific concentration range; 1b) the mass matio of chitosan to TPP negatively associated with particles yield, positively associated with particle size and size distribution, negatively associated with BSA encapsulation efficiency; 1c) the concentration of BSA has no significant effect on particles yield, particle size or size distribution, negatively associated with BSA encapsulation efficiency in a specific

concentration range. 2) a chitosan polymer chain conformation related mechanism is proposed through the study of the effect of pH value on the formation and BSA encapsulation of chitosan nanoparticles. 3) the most homogeneous and smooth chitosan particles could be obtained at the parameters of: 2% (m/v) chitosan solution, 2/10 w/o volume ratio, 4% Span 85 as susfactant, 5 Krpm homogenization speed and 3 times addition of NaOH solution as a coacervation agent. The obtained particles have a mean diameter of 9.4±1.9 μm. The BSA loading test found that dispersed particles only could be obtained below the BSA concentration of 0.5% under above mentioned parameters. 4) a noval polyelectrolytes complex formed by TPP and BSA is obtained attempted to solve the burst release effect of chitosan nanoparticles. 5) a microemulsion involved emulsification-coalescence method is used to overcome the aggregation problem of TPP-gelated chitosan microparticles. 6) a chitosan nanoparticles encapsulated PLA composite particles are successfully constructed.

What is new in this thesis? 1) to study the formation mechanism and protein encapsulation of chitosan nanoparticles through the study of the effect of pH value on their properties and propose the role of chitosan polymer chain conformation during this process, 2) a noval TPP-BSA polyelectrolytes complex is obtained base on the purpose to overcome the burst release effect of chitosan nanoparticles, 3) apply emulsification-coalescence method in which a microemulsion of cross-linking agent-TPP is used to solve the aggregation problem of TPP-gelated chitosan microparticles, 4) propose a chitosan nanoparticles encapsulated PLA composite particles to control the release of proteins.

Where is the study of this thesis in the field? 1) Chitosan nanoparticles have been extensively investigated in the past few years and the factors which can affect the properties of chitosan nanoparticles have been well documented as well. This thesis provides the evidence from a new side to understand the formation and protein encapsulation mechanisms of chitosan nanoparticles. 2) New and highly effective methods have been proposed by others to prepare protein loaded chitosan microparticles such as sieving and microfluidic methods which can reproduceably scale up the production of monodispersed chitosan microparticles. This thesis just solved a technique problem in the conventional preparation process of TPP-gelated chitosan microparticles. 3) The proposed TPP-BSA polyelectrolytes complex could be an alternative route to overcome the burst release effect of chitosan nanoparticles. 4) The proposed chitosan nanoparticles encapsulated PLA composite particles is one of the solutions among other composite particles proposed by others.

Abbreviations

APCs	antigen-presenting cells
BSA	borvin serium albumin
BSA-CSNPs	BSA-incorporated chitosan nanoparticles
CS	chitosan
CSCL	chitosan hydrochloride
CSMPs	chitosan microparticles
CSNPs	chitosan nanoparticles
DCs	dendritic cells
DD	deacetylation degree
DDS	drug delivery system
DLS	long double-stranded RNA
DMEM	dynamic light scattering
DSC	dulbecco's modified eagle medium
dsRNA	differential scanning calorimetry
ECM	extracellular cell matrix
EE	encapsulation efficiency
EPR	enhanced permeability and retention
FGF-2	fibroblast growth factor-2
FITC	fluorescein isothiocyanate
FTIR	Fourier transformation infrared
GAGs	glycosamine glycans
HLB	hydrophile-lipophile balance number
TPP	tripolyphosphate
LC	loading capacity
LMW	low molecular weight
miRNA	microRNAs
MMW	medium molecular weight
MPs	microparticles

NPs	nanoparticles
PAMAMs	polyamidoamines
PDI	polydispersity index
PBS	phosphate buffered saline
PEC	polyelectrolytes complexe
PEG	polyethylene glycol
pI	isoelectric piont
RES	reticuloendothelial system
SEM	scanning electron microscope
siRNA	small interfering RNAs
SLN	solid lipid nanoparticles
TEM	transmit electro microscope
TPP	sodium tripolyphosphate
VEGF	vascular endothelial growth factor

Table of Contents

Chapter 1 Introduction

Tissue engineering aims at the repairing and restoring damaged tissue function employing three fundamental “tools”, namely cells, scaffolds and growth factors which, however, are not always simultaneously used [1]. There are four fundamental technologies or methodologies that are necessary for tissue engineering. They are preparing artificial scaffold for proliferation and differentiation of cells, drug delivery system (DDS) to preserve the biological activity of growth factors and control their release, efficient isolation and proliferation of cells, a physical barrier to protect transplanted cells and the area to be regenerated from immunological attack and fibroblast infiltration [2]. Some DDSs such as hydrogel, microfluidic system, viral or cellular carriers, and nano- or micro-carriers have been successfully prepared to induct the regeneration of tissues and organs by the controlled release of various biologically active growth factors. Specific DDS has its own advantages and disadvantages respectively. For insistence, hydrogel release system has the advantage of easy fabrication and mass productability, but may have the disadvantage of poor regulation of release profile and activity loss of molecules. Chitosan based micro- or nano- particles as particulate drug delivery system are mainly discussed in this thesis. In order to control the release profile of growth factors in a bioengineering scaffold, CSMPs are prepared in this thesis. Therefore, the preparation methods and biomedical application of CSMPs are reviewed in the third section of this introduction part.

Drug delivery formulations have gained huge support from emerging nanotechnology. Nanotechnology, which is still not a mature technology and thus, more appropriately called nanoscience, usually refers to research at the scale of 100 nm or less [3]. Nanotechnology has been evolving tremendously in last few decades and made enormous impact on many other research scopes. In the human health field, the introducing of nanotechnology gave rise to a novel concept ‘nanomedicine’. In definition, nanomedicine is the process of diagnosing, treating, and preventing disease and traumatic injury, relieving pain, and preserving and improving human health, using molecular tools and molecular knowledge of the human body [4]. Numerous nanomedicine research activities have been dedicated to drug delivery study. Many of the current ‘nano’ drug delivery systems which are remnants of conventional drug delivery systems that happen to be in the nanometer range, such as liposomes, polymeric micelles, nanoparticles, dendrimers, and nanocrystals. Due to the advantages of nanoscaled size, these nanovehicles are capable of overcome tissue barriers in human body, reach specific disease sites and remain there longer to realize larger bioavailability. Some of them

are even able to deliver loaded package to specific organelles. Even so, this research field develops so fast that all above mentioned nanocarriers are already called as ‘first generation’ nanomedicine. Conjugated with special target ligands, such as antibodies, peptides or other adaptors, these nanocarriers are able to target specific cell subsets. Functionalized with various functional groups, some of they become multifunctional nanocarriers, for instance, both capable of imaging and treating, both thermal and pH responsible, and so on. In addition, various nanocarriers such as organic and inorganic nanoparticles are combined to exert multiple functions. All of these refined mono or multiple nanocarriers could be termed as the second generation nanomedicines or even are further subdivided to be ranked as more advanced generation. In this thesis, chitosan nanoparticles (CSNPs) are prepared for delivering protein drugs. Therefore, the preparation methods and biomedical application of CSNPs are introduced in this chapter.

1.1 Particulate Drug Delivery System

In the past few decades, more and more research work has been conducted on particulate drug delivery systems. Particulate systems such as microparticles and nanoparticles have been widely used to delivery a wide range of macro or small molecules to improve their pharmacokinetic and pharmacodynamic in human body. As drug delivery systems, they have the advantages of protecting drug from quick digestion and damage by body fluid, localizing at desired spots and releasing encapsulated drugs. These advantages remarkably enhance drug bioavailability and efficacy, reduce undesired side effects, and consequently improve patients’ comfort and compliance.

1.1.1 Microparticles

Microparticle, also called as ‘microsphere’ or ‘microcapsule’ have many applications in medicine. In most cases, microparticles are used as drug carriers to deliver drug to the areas of interest and slowly release encapsulated drug over a desired period of time to maintain an effective local drug concentration. Microparticles also has novel application in the foods, medical devices, chemical coatings, personal health testing kits, sensors for security systems, biochemical sensors water purification units for manned space craft, and high throughput screening techniques[5]. In this chapter, the application of microparticles will be overviewed only on the aspect of drug delivery.

Immune Adjuvants

Recently microparticles have been well developed as effective immune adjuvants. In order to realize a strong and lasting immune response, many vaccination formulations need the assistance of adjuvants since many antigens couldn't produce sufficient immune responses themselves. Generally microparticles could serve as immune adjuvants via enhancing and/or facilitating the uptake of antigens by antigen-presenting cells (APCs) such as dendritic cells (DCs) or macrophages; storing and controlling the release of loaded antigens, consequently increasing the availability of antigens to the immune cells; induce multiple immune responses by loading antigens combination; protecting sensitive antigen molecules from the degradation effect of surround environment and so on [6]. To date, many polymers [7], copolymers [8], and lipids [9] have been applied to produce microparticulate carriers of many kinds of antigen. Several important factors like particle size, morphology, particle surface properties, antigen loading and release kinetics of microparticles dramatically affect the induced immune responses in the sense of antigen stability, antigen release, particle interaction with APCs, antigen presentation and processing by APCs [10].

Ocular Drug Delivery

Microparticles have also been applied as ocular drug delivery system. The major objective of ocular therapeutics is to maintain sufficient drug concentration and residence time at the site of action. Whereas, the protective mechanisms such as rapid turnover, lacrimal drainage, reflex blinking, and drug dilution by tears lead to poor drug availability and permeation through corner. Considering the efficiency of conventional ophthalmic formulations like eye drops, suspensions, and ointments are badly compromised by the above mentioned physiological barrier, various modern approaches have been proposed. For instance, in situ gel, ocuserts, nanosuspension, microparticles, nanoparticles, liposomes, niosomes, and implants improve the ophthalmic bioavailability of the drugs and controlled the release of the ophthalmic drugs to the anterior segment of the eye [11]. Among them, Microparticles extend precorneal residence time, which leads to continuous and sustain release of the drug and consequently improve ocular bioavailability of the drug and reduced dosing frequency. Some natural or synthetic materials with good biodegradability, biocompatibility and bioadhesion like gelatin [12], chitosan [13] and hyaluronate esters [14] have been used to prepare these microparticles.

Pulmonary Drug Delivery

Pulmonary drug delivery (PDD) has several advantages which the pulmonary route offers over the others routes of drug administration, i.e. reduces first-pass metabolism or gastrointestinal degradation (such as proteins and peptides). In addition, less invasiveness and lower side effects of pulmonary

administration increase patient compliance and reduce systemic exposure. However, PDD may has limitations due to a series of defenses of respiratory tract against inhaled materials such as mucociliary clearance, alveolar macrophages clearance, enzymatic metabolism and low permeability. All these barriers could lead to insufficient drug local concentration or bioavailability and consequently frequent drug administration is required. Particulate drug carriers such as liposomes, microparticles and nanoparticles can be/have been used to improve the therapeutic index of new or established drugs by modifying drug absorption, reducing metabolism, prolonging biological half-life or reducing toxicity [15].

1.1.2 Nanoparticles

Nanotechnology has been vastly applied in fiber and textiles, agriculture, electronics, forensic science, space and medical therapeutics [16]. The application of nanotechnology in medicine gave the birth of a new concept—nanomedicine. To date, many nanomedicine formulations have been developed, i.e., nanoparticles, nanocapsules, micellar syatems and dendrimers [16]. These nanoscaled formulations improve drug bioavailability, prolong drug in vivo circulating half-live and decrease drug size effect as a DDS. In addition, nanomedicine has specific advantages due to its nanoscaled size and targeted drug delivery is one of them.

Targeted Drug Delivery

The targeted drug delivery of nanomedicine could be achieved through passive or active targeting route. Generally the passive targeting is based on the enhanced permeability and retention (EPR) effect of the physiology of diseased tissues such as tumor or inflammation tissues. Whereas, nanomedicines have a longer EPR effect in tumor tissues for weeks than that in inflammation sites for few days. This could be contributed to the lymphatic drainage system is still operative in inflammation sites, thus swelling may dissipate in a matter of a few days. While, cancer is like inflammation that never ceases but grows [17], which results in a consequential long period of EPR effect. The EPR effect has been applied to develop a number of passively targeting nanocarrieres and one example is PEGylatyed liposome-Doxil which encapsulates an antitumor drug—doxorubicin. It has shown a long drug retention, circulation time and 6 times more effective in comparison with free doxorubicin [18].

On the other hand, active targeting requires the conjugation of receptor specific ligands to realize diseased sites targeting. It could be achieved by molecular recognition of the diseased cells by various signature molecules overexpressed at the diseased site either via the ligand-receptor, antigen-antibody

interactions or by targeting through aptamers. Thus, specific ligands-conjugated nanocarriers could overcome the physiological barriers and access different tissues followed by an efficient cellular uptake and intracellular internalization. Kocbek et al. [19] reported a monoclonal antibody-conjucated PLGA nanoparticles to actively target cancer cells. Their results indicated good cancer cell recognition of surface-modified nanoparticles than that of noncoated nanoparticles.

The Medical Applications of Nanoparticles

Nanoparticles have been widely applied in therapeutics, diagnostics and imaging in medical and pharmaceutical fields. In therapeutics, surface-modified or multifunctional nanoparticles have been used to delivery various therapeutic drugs such as cancer therapeutics, vaccines, nucleic acids. They increase the effective drug concentration at desired diseased sites and decreased undesirable side effects of the current therapeutic. For example, the most frequently used chemotherapeutic antitumor drugs such as carboplatin, paclitaxel, doxorubicin and etoposide, etc., have been successfully loaded onto NPs and dramatically decrease their side effect to tumor-suffered patients.

Molecular diagnostics and imaging emerged with the combination of nanomaterials, noanotechnology and modern advanced analysis instrumentation. The emergence of molecular diagnostics not only tremendously improves the medical diagnostic lever, provides more solid evidences for doctors, and also accelerates the development of cell and molecular biology. Nanoparticle is a major member of molecular diagnostics agents, i.e., gold (Au) NPs [20] and quantum dots (QDs) [21]. They are capable to detect cancer markers in blood assays or cancer tissue biopsies at pg/mL scale. On the other hand, the conjugation of various fluorescent molecules on nanparticles could be as imaging agents to track and image nanoparticles from systemic to subcellular lever.

The Classification of Nanoparticles in Nanomedicine

As discussed above, many types of nanoparticles have varying formulations can be formulated from diverse materials with unique architectures to treat a particular disease. Polymeric nanoparticles are the most frequently used nanoscaled DDS. Based on various chemical structures, a number of synthetic and natural polymers such as polylactide (PLA) [22], (PCL) [23] poly D, L-lactide co-glycolide (PLGA) [24] chitosan [25], and alginate [26] have been formulated by varying processes into nanoparticles/nanosphrees or nanocapsules. These Biodegradable materials used for the formulation of nanoparticles allow sustained drug release within the target site over a period of days or even weeks. In addition, the polymeric nanoparticles surface could be conveniently conjugated with various functional groups and other ligands, thus it makes targeting specific diseased sites possible.

Solid lipid nanoparticles (SLN) which are formulated from solid lipids such as triglycerides, complex glyceride mixtures and waxes have been used as controlled release DDS since 1990s [27]. SLN have been applied for topical, oral, pulmonary, parenteral application routes due to their good tolerability and biodegradability [28].

Recently, ceramic nanoparticles as inorganic particles are more and more used for drug delivery due to their ultra fine size (generally below 50nm) and porous structure. They can avoid the uptake by reticuloendothelial system (RES) due to their very small size [28]. Further more, they can also effectively protect various bioactive molecules from the denaturation caused by changes in the external pH and temperature due to their stability on external conditions. The biocompatible materials such as silica [29], alumina [30], titania [31], etc. have been formulated into ceramic nanoparticles. In addition, the particle surface could be conveniently modified by various targeting moieties to be processed as active targeting vehicles [32].

Magnetic nanoparticles are important nanocarriers in the biomedical and biological field, which is mainly contributed to their specific targeting functions. For instance, the antitumor drug loaded magnetic nanoparticles could be specifically concentrated at tumor sites by the introduction of external an external agent (magnetic fields, light, radiation, etc…) to improve the efficiency of chemotherapeutics and decrease undesirable side effects [33]. Magnetic nanoparticles are always used in the formulation of magnetic colloids which consist of magnetic nanoparticles and a dispersant such as water [34]. Thus, the stability of colloid is very important for magnetic colloid. In order to increase the repulsive force between particles to avoid flocculation, synthetic or natural polymers are always used to coat the particle surface [35].

Polymeric micelles are nanoscaled core/shell structures formed by amphiphilic block copolymers. Polyethylene glycol (PEG) [36] is always used as the hydrophilic block, meanwhile, poly (propylene oxide), poly (L-amino acid)s and poly (ester)s are most frequently used as the hydrophobic blocks [37]. The polymeric micelles used for drug delivery have shown the abilities to attenuate toxicities, enhance delivery to desired biological sites and improve the therapeutic efficacy of active pharmaceutical ingredients. These probably are contributed to their small size and hydrophobic shells which can avoid the uptake by RES.

Dendrimers, also called arborols or cascade molecules, are macromolecules composed of multiple perfectly branched monomers that emanate radially from a central core [38]. On architecture, dendrimers consist of three major domains including a multivalent surface which contains a large

number of reactive sites, the interior shells surrounding the core and the core which the dendrons are attached on. Dendrimers could serve as potential targeting nanocarriers due to the presence of a large number of surface functional groups. In addition, the solubility of dendrimers could be modulated by varying end groups on surface. On the other hand, the core could be also tailored to encapsulate aqueous soluble or hydrophobic drugs to achieve sustained drug release. Many polymers have been used to prepare dendrimers such as polyamidoamines (PAMAMs), polyamines, polyamides (polypeptides), poly (aryl ethers), polyesters, carbohydrates and DNA. Among them, the commercially available polyamidoamine (PAMAM; Starburst™) dendrimers [39] and poly (propylenemine) (also called PPI, DAB; Astramol®) dendrimers have been most widely studied for biomedical use.

1.2 The Application of Chitosan on Biomedical Engineering

1.2.1 Structure and Physicochemical Properties of Chitosan

Chitosan is a linear copolymer composed of Nacetyl-d-glucosamine and d-glucosamine units available in different proposion depending upon the degree of deacetylation (Fig. 1). The history of chitosan dates back to the 19th century, when Rouget discussed the deacetylated form of chitin in 1859 [40]. It is obtained by the deacetylation of chitin which is an abundant natural source widely found in the shells in insects, crustaceans and several fungi. Chitin is insoluble in aqueous solution or organic solvents. However, chitosan can be dissolved in weekly acetic aqueous solution due to the protonation of amino groups. After refinement, chitosan has a rigid crystalline structure through inter- and intra-molecular hydrogen bonding.

The primary amino groups offer chitosan some special properties such as water-solubility, hemocompatibility, and cationic groups which could react with a big number of anions or other negatively charged molecules. And also based on the cationic property, chitosan-based or coated formulations could adhere to negatively charged biosurfaces or membranes. The hydroxyl groups could serve as the modification sites by other molecules or polymers, by which a verity of chitosan derivatives have been developed [41].

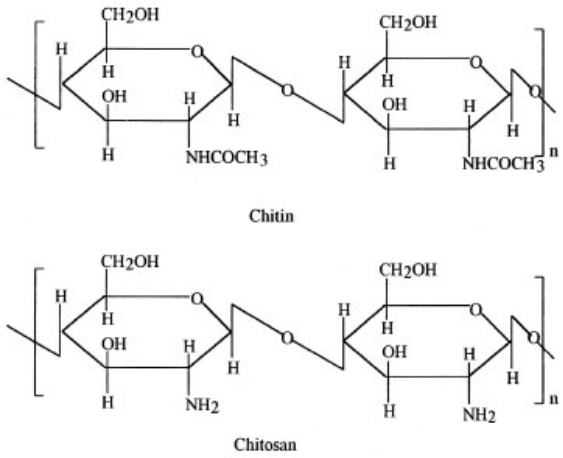

Fig. 1.1 Chemical Chemical Structure of Chitin and Chitosan.

1.2.2 Biodegradability, Biological Properties and Toxicity of Chitosan

Chitosan could be degraded by acid catalyzed degradation, for instance, in stomach. In addition, enzymes such as lysozyme, bacterial enzymes in the colon [42] and some chitosanases [43] can degrade chitosan by hydrolyzing the glucosamine–glucosamine, glucosamine–Nacetyl-glucosamine and N-acetyl-glucosamine–N-acetylglucosamine linkages in vertebrates [44]. Some studies revealed that the biodegradability of chitosan is deacetylation degree-dependent and the higher the deacetylation degree, the less the degradation is [45, 46].

Chitosan has some favorable biological properties including mucoadhesion, enhanced mucosal epithelial permeability, and immune adjuvant effects [47]. The mucoadhesive property of chitosan enhances or prolongs drug absorption and thus permits maximal drug availability to the mucosal epithelium. Smith et al. proposed that chitosan could enhance the epithelial permeability by transiently opening the cell tight junction [48]. While, chitosan as an immune adjuvant have been found to enhance local and systemic immune responses to influenza, tetanus toxoid, diphtheria and pertussis vaccines when delivered intranasally [49-52]. In addition, chitosan was found to be toxic for some bacteria [53], therefore, it can serve as an antibiotic material.

1.2.3 The Biomedical Applications of Chitosan

Chitosan has been extensively used in tissue engineering including bone, cartilage, liver, and nerve tissue engineering [54]. Tissue engineering is aimed to develop biocompatible substitutes to restore, maintain, or improve biofunction of dysfunctional human tissues or organs. Since chitosan is

biodegradable and nontoxic, it has been formulated into a verity of forms such as film, powder, gels. In addition, various modification of chitosan could be made to improve the cell seeding. In bone tissue engineering, chitosan has been shown to promote cell growth and mineral rich matrix deposition [55]. In cartilage tissue engineering, glycosamine glycans (GAGs) plays a pivotal role in modulating chondrocytes morphology, differentiation, and function [56]. While, chitosan is chosen as scaffold material in cartilage tissue engineering due to its structural similarity to GAGs [57]. In live tissue engineering, the bioartificial liver needs to provide an extracellular cell matrix (ECM) like surrounding for the seeded primary hepatocytes or liver stem cells. Also for the similarity with GAGs which are components of ECM, chitosan frequently serves as the scaffold material for hepatocytes culture [58, 59]. In nerve engineering, artificial tubes are the effective means to repair injured nerves by bridging of nerve stumps. Chitosan is suitable for nerve regeneration due to its biocompatible and biodegradable properties. In addition, bioadhesive chitosan could favour the adhesion of nerve cells to the tube lumen [60].

Chtiosan has been widely applied in drug delivery in a verity of forms such as film or membrane [61], hydrogel system [62] and particulate system [63]. A big number of drugs and biomolecules could be delivered by chitosan-based drug delivery systems, i.e., proteins/peptides, genes, antibiotics and chemotherapeutics. With the favorable biodegradable and nontoxic properties, chitosan could be fabricated to hydrogel through gel gelation without the use of cross-linking moieties through electrostatic, hydrophobic, and hydrogen bonding forces between polymer chains or covalently cross-linking available $–NH_2$ and –OH groups on chitosan by various cross-linkers such as small molecule cross-linkers, polymers or photosensitive agents. For example, genipin, a naturally derived cross-linking agent is effective to cross-link chitosan which contains amino groups [64]. The chitosan-based particulate systems will be discussed in the following section.

Besides tissue engineering and drug delivery applications, chitosan also has been used in wound-healing formulations. For a wounding-healing formulation, it should protect the wound from bacterial infection as well as promote healing process. Chitosa was found to induce wound-healing on its wound and produce less scarring due to its antibiotic property [65]. In addition, endothelial cell proliferation enhanced growth factors such as fibroblast growth factor-2 (FGF-2) could be enclosed in the formulation to accelerate this wound-healing process [66].

Because of the excellent non-toxic, hygrophilic and cationic properties, chitosan has also been frequently used in bioimaging. As discussed before, some metal or magnetic based imaging agents are

commonly in a colloid form to avoid agglutination. Chitosan are always used as coating or conjugation material to stabilize these imaging agents and decrease their toxicity [67]. Besides as coating material, the imaging agents such as super paramagnetic iron oxide [68], gadolinium [69] etc. could be encapsulated or entrapped in chitosan particles as well.

1.3 Chitosan Microparticles

Chitosan particles have found a verity of applications in biomedical and pharmaceutical fields in past few decades. In this section, beginning with the application of chitosan in biomedical engineering, the emphasis is put on chitosan microparticles.

1.3.1 The Preparation Methods of Chitosan Microparticles

Microparticles, also called microspheres were used to extend the life span of active drugs and control the drug release. The total dose and release kinetics can be manipulated to achieve desired result by varying the copolymer ratio, molecular weight, polymer concentration etc. First, the preparation methods of chitosan microparticles are discussed in this section. Fig. 2 represents these methods [70].

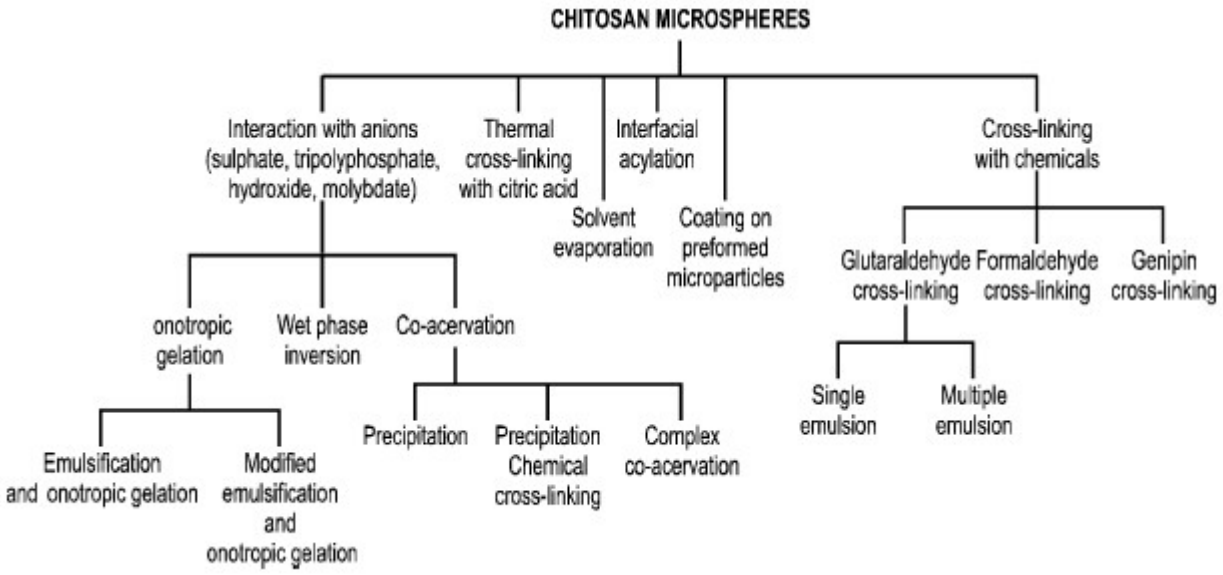

Fig. 1.2 Methods for the Preparation of Chitosan Microparticles. Adopted from V.R. Sinha et al., 2004, International Journal of Pharmaceutics.

Ionotropic Gelation

The polycationic chitosan in weak acetic solution could be gelated by a verity of counterions including low molecular weight anions such as diphosphoric acid, tripolyphosphate, etc., hydrophobic

counterions such as alginate, κ-carragenan, poly-1-hydroxy-1-sulphonate-propene-2, polyaldehydro-carbonic acid, high molecular weight ions such as octyl sulphate, lauryl sulphate, hexadecyl sulphate, and cetylstearyl sulphate [71]. Chitosan solution was extruded dropwise through a needle into various counterions aqueous solutions under magnetic stirring.

Emulsification and Ionotropic Gelation

In this method, a water-in-oil (w/o) emulsion is obtained firstly by emulsifying chitosan aqueous solution in an oil phase containing proper surfactant. Thereafter, various counterions solutions are added to solidify chitosan emulsion droplets [72]. The particle size could be manipulated by controlling the size of chitosan emulsion droplets, which can be realized by using different emulsification means, i.e. magnetic stirring, homogenization or sonication. In addition, the quantity and concentration of cross-linking agents influence the final particle size as well. This method may have disadvantages of the use of organic solvent and harsh mechanical shear force.

Coacervation/Precipitation

Since chitosan is insoluble in alkaline medium, chitosan microparticles can form when chitosan solution comes in contact with alkaline solution [73]. This method avoids the use of unfavorable organic solvent used in emulsification method. However, it still has the drawback of the use of strong base which could compromise the activity of biomolecules. Besides, chitosan microparticles could also be obtained by the addition of a precipitant, i.e., sulfate to precipitate chitosan out from solution [74]. This method avoids the use of toxic organic solvents and glutaraldehyde which is used as a covalent cross-linked. But, the obtained particles by this method may have a weak mechanical property and irregular morphology.

Spray-drying

Spray-drying method is commonly used to produce powders, granules from the mixture of drug and excipient. The microparticles are obtained by the atomization of drug-excipient mixture in a stream of hot air or by immediate evaporation of excipient. Several parameters could affect the particle size, for instance, the nozzle size, spraying flow rate, atomization pressure, inlet air temperature and extent of cross-linking. For preparing chitosan microparticles, the drug could be dissolved or dispersed in chitosan solution followed by the addition of a proper cross-linking agent. Afterwards, this solution or dispersion is atomized in a stream of hot air which leads to instantaneous formation of free flowing particles [75].

Sieving Method

Agnihotri et al. proposed a novel sieving method to produce chitosan microparticles [76]. As shown in Fig. 3, a 4% (m/v) chitosan pre-crosslinked hydrogel was pushed to pass through a sieve with micropores under certain pressure to form chitosan microparticles. Using this method, chitosan microparticles could be simply produced in a large scale. Further more, the obtained particles could have a very narrow size distribution due to the homogeneous pore size of the sieve.

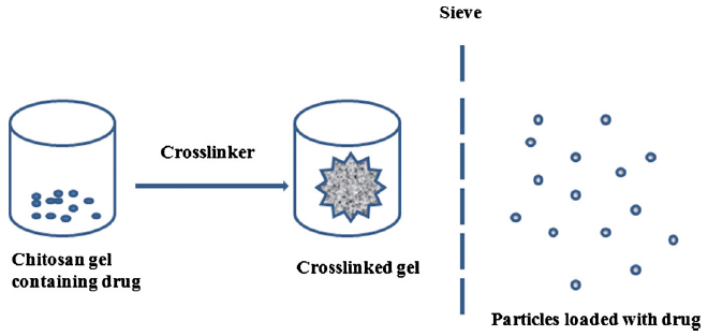

Fig. 1.3 Schematic Representation of Preparation of Chitosan Particulate Systems by Seiving Method. Adopted from Agnihotri SA, Aminabhavi TM, 2004, J Control Release.

Microfluid Chip Technology

The conventional methods for preparing chitosan microparticles such as ionic gelation, emulsification, coaervation and spry drying etc. generally have disadvantages such as unstable yield, tedious procedures and wide size distribution. In order to realize a reproducible and practical method for the pharmaceutical industry, microfluidic chip technique is introduced to the field. Microfluidic chip (containing cross-junction microchannel) emulsification is a relatively new technique for preparing water-in-oil (w/o) and oil-in-water (o/w) emulsions in these years. Yang et al. [77] applied a cross-junction microchannel of a microfluidic device coupled with gelation reaction to control the performance of uniform TPP-chitosan microspheres (Fig.4). The obtained chitosan microparticles by their device had a narrow size distribution (polyindex = 1) which was suitable to provide the optimal release rate in the administration of controlled release drugs. Therefore, it was included that microfluidic chip is capable of generating relatively uniform micro-droplets and has the advantages of actively controlling the droplet diameter, and having a simple and low cost process, with a high throughput.

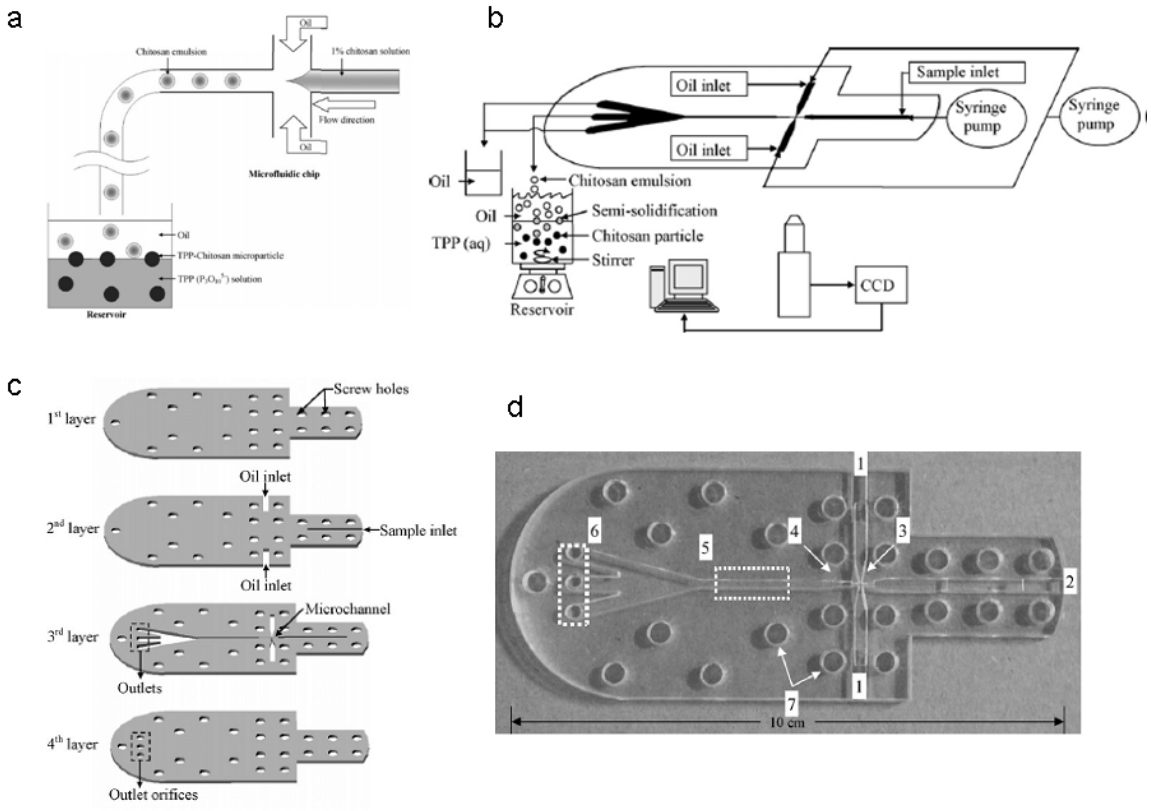

Fig. 1.4 Using a Cross-flow Microfluidic Chip and External Crosslinking Reaction for Monodisperse TPP-chitosan Microparticles. (a) Schematic presentation of the formation of chitosan emulsion in a cross-junction microchannel. Based on microfluidics to exert control over the focusing force, a large set of uniform self-assembling spheres can be obtained. The emulsions are gelled upon contact with 10% (w/v) $P_3O_{10}^{5-}$, and the chitosan molecules entrapped in the micro container (emulsion) are transformed into TPP-chitosan particles in the reservoir. (b) Experimental setup of a microfluidic chip system for the generation of TPP-chitosan microparticles. Schematic presentation and photo image of microfluidic chip: (c) the chip in expanded view and (d) the photo image of the chip: 1, oil inlet; 2, sample inlet; 3, cross-junction channel; 4, broadened channel; 5, observation chamber (1200μm in width channel); 6, outlets; 7, screw holes for bonding. Adopted from Yang et al., 2007, Sensors and Actuators B.

1.3.2 The Application of Chitosan Microparticles

As a DDS, chitosan microparticles find a number of applications in pharmaceutics. This is mostly contributed to the biodegradable, nontoxic and bioadhesive properties of chitosan. The major applications of chitosan microparticles are discussed below, generally from the administration route point of view.

Oral Drug Delivery

Oral drug delivery has the advantages of ease of administration and improved patient convenience and compliance. Chitosan microparticles have been developed to deliver various drugs via oral route. Chitosan has been shown to effectively bind DNA in saline or acetic acid solution and protect DNA from nuclease degradation. Ülker Guliyeva et al. [78] reported that plasmid DNA could be encapsulated into chitosan microparticles without damage by oral administration. I.M. van der Lubben et al. reported an ovalbumin loaded chitosan microparticles prepared by coacervation/precipitation method [79] as an oral vaccine. Their results indicated that chitosan microparticles showed suitable in vitro and in vivo characteristics for oral vaccination.

Nasal Drug Delivery

Nasal drug delivery offers several benefits such as highly vascular mucous membrane, lower enzymatic degradation compared to oral route, and better patient compliance. However, mucocilliary clearance and insufficient drug uptake are the major barriers for nasal drug delivery. Chitosan microparticles have been studied as vaccine carriers in nasal vaccination. Some investigations evidenced that chitosan microparticles could enhance the immune response of encapsulated vaccines by improve the vaccine uptake by specialized M cells and Peyer's patches of mucosal associated lymphoid tissues (MALTs) [80].

Colon and Intestinal Drug Delivery

Chitosan microparticles could be used for colon- and intestinal-specific drug delivery, because chitosan can be degraded by microflora which exist in colon. Lorenzo-Lamosa et al. [81] reported a chitosan microcore encapsulated acrylic microspheres which took advantages of the colon-specific degradation of chitosan microscore (microparticles, 2~3 μm) and pH dependent property of acrylic materials. Mladenovska et al. [82] reported chitosan-Ca-alginate microparticles to specifically deliver 5-aminosalicylic acid to colon. The non-solubility of chitosan at pH values higher than 6.5 leads to slow erosion of chitosan-alginate complex and consequential controlled drug release in the colon where the pH value is in the range of 6.5-7.0.

1.4 Chitosan Nanoparticles

Chitosan nanoparticles have been extensively applied to deliver a large range of chemicals and biomacromolecules based on the excellent properties of chitosan discussed above. Many methods have also developed to prepare chitosan nanoparticles. According to different preparation methods and drug

delivery purposes, chitosan nanoparticles found a verity of applications in pharmaceutics.

1.4.1 The Preparation Methods of Chitosan Nanoparticles

Even though some preparation methods of chitosan microparticles can be used to prepare nanoparticles, whereas, down to nanoscale size, some parameters like the concentrations of chitosan and ionotropic gelation agents and input energy have to be accordingly modified. Here, the most frequently preparation methods are presented as follows.

Emulsification Solvent Diffusion Extraction

El-Shabouri et al. reported using emulsification solvent diffusion extraction method to prepare chitosan nanoparticles [83]. An oil-in-water emulsion was obtained by adding an organic solvent partially miscible into chitosan solution containing a stabilizing agent under magnetic stirring, followed by high-speed homogenization. The resulting emulsion was diluted in a large amount of water to extract the organic solvent. Nanoparticles were obtained as a result of the diffusion of the organic solvent into water. The particle size of obtained particles was between 104-148nm and showed a zeta potential of +31.2 mv. The bioavailability and biological effect of the highly lipophilic drug (cyclosporin-A) showed a significant increase in comparison to the reference Neoral microemulsion.

Emulsion-droplet Coalescence

Tokumitsu et al. [84] firstly reported an emulsion-droplet coalescence technique to prepare chitosan nanoparticles. In this method, both chitosan and NaOH solution were emulsified into the same oil phase under the conditions to prepare two emulsions. The two emulsions were then mixed and stirred at high rotating speed to form chitosan nanoparticles. The hydrophilic drug- gadopentetic acid encapsulated chitosan nanoparticles had a diameter of 452 nm and were proved suitable to be intravenously injected.

Ionotropic Gelation

Based on ionotropic gelation, chitosan can be ioniclly cross-linked by counterions such as $Fe(CN)_6^{4-}$, $Fe(CN)_6^{3-}$, citrate and sodium tripolyphosphate (TPP) etc. to form hydrogel and microparticles like discussed above. When the concentrations of chitosan and these anions decrease to enough low values, nanoparticles are able to generate. This method allows the preparation of chitosan nanoparticles in aqueous solution and avoids the use of organic solvents and high dispersion energy which may compromise the drug activity, therefore, once upon reported, it has drawn extensive attention and has been used to encapsulate a number of chemical or biological molecules which are sensitive to the preparation conditions. This method was firstly reported by Calvo et al. in 1997 [85]. Following studies

revealed that chitosan nanoparticles could form with specific concentrations of chitoan and TPP solution and amount ratio between them. When chitosan concentration is too low, the suspension is translucent, which means no particles generate. When chitosan concentration is too high, the suspension may too instable to form aggregates. When chitosan solution is in a appropriate concentration range, the opalescent suspension is obtained in which nanoparticles can be further proved. The main drawbacks of the chitosan nannoparticles produced by this method are drug burst release effect and low particles yield.

Complex Coacervation

Similar to ionotropic gelation method, complex coacervation method has been used to prepare chitosan nanoparticles through the ionic reaction between cationic chitosan and anionic polyanions, polymers or biomacromolecules rather than anions adopted by the former. Hu et al. [86] repoted chitosan–poly(acrylic acid) nanoparticles which were affected by the ratio between the two polyelectrolytes. Chtiosan/Alginate nanoparticles have been developed to deliver bioactive molecules such as proteins and nucleic acids [87]. chitosan and nucleic acid molecules can form nanoparticles at appropriate ratio to serve as a nonviral gene nanovehicle [88].

Self-assembling Micelles

As discussed above, amphiphilic block copolymers can form micelles. To date, chitosan has been modified into numerous hydrophobic chitosan derivatives to prepare into chitosan micelles. For example, Kim et al. [89] reported a 5β-cholanic acid modified glycol chitosan to deliver an anticancer drug-paclitaxel.

1.4.2 The application of chitosan nanoparticles

Oral, Nasal and Pulmonary Drug Delivery

As discussed in the section of chitosan microparticles, the oral drug delivery has the advantages of convenience and good patient compliance. However, the enzymatic digestion and low mucosal absorption are the main barriers for some drugs which are sensitive to these harsh conditions. Based on the favorable bioadhensive and enhanced permeability properties chitosan, it has been formulated to nanoparticles to deliver these drugs. Beside above mentioned advantages of chitosan microparticles, chitosan nanoparticles also has its size advantages which can allow them more easily absorbed by mucosal epithelium cells. Sarmento et al. reported that [90] alginate/chitosan nanoparticles administered orally to diabetic rats were found effective for oral insulin delivery. Zang et al. [91]

reported that water-soluble chitosan nanoparticles enhance and prolong the intestinal absorption of bovine serum albumin

Pulmonary and nasal drug administrations are also frequently used means due to their large absorbance surface area. Al-Qadi et al. [92] reported a new dry powder system consisting of microencapsulated insulin-loaded chitosan nanoparticles. The mild preparation conditions of chitosan nanoparticles protected the insulin bioactivity well, whereas, the final spray dried powder provided an adequate aerodynamic property for deposition in deep lungs. The assessment of the plasmatic glucose levels following intratracheal administration to rats revealed that the microencapsulated insulin-loaded chitosan nanoparticles induced a more pronounced and prolonged hypoglycemic effect compared to the controls.

Shahnaz et al. [93] et al. reported a thiolated nanoparticle to enhance the bioavailability for the nasal application of leuprolide. The inter- and/or intramolecular disulfide formation within the NPs network stabilized obtained nanoparticles and achieved a sustained leuprolide release over 6 hours. Ciliary beat frequency study demonstrated that thiolated chitosan nanoparticles could be considered as suitable additives for nasal drug delivery systems.

Ocular Drug Delivery

The short residence time, drug drainage and frequent instillation are the major drawbacks of the conventional drugs for ophthalmic diseases. Chitosan nanoparticles have been used to deliver ocular drugs to solve above limitations. De la Fuente et al. [94]. reported a hyaluronic acid-chitosan nanoparticles to deliver genes to the cornea and conjunctiva. Both of chitosan and hyaluuronic are the polysaccharide with good bioadhisive and permeability enhancement properties, besides, hyaluronic acid is known for its implication in several processes, such as the regeneration of corneal and conjunctival epithelial cells, through an interaction with the CD44 receptor. Their results indicated that hyaluronic acid-chitosan nanoparticles were able to target and further transfer genes to the ocular surface.

Vaccine Delivery

Nanoparticles often present significant adjuvant effects in parenteral vaccine delivery due to their effective uptake by antigen presenting cells. The nanoscaled size allows nanoparticles to be taken up by M-cells in mucosa-associated lymphoid tissue (MALT), i.e., gut-associated, nasal-associated and bronchus-associated lymphoid tissues, to initiate vigorous immunological responses. Chitosan nanoparticles have been used in vaccine delivery due to their bioadhesive, biocompatible,

biodegradable and permeation-enhancement properties. They can be effectively uptaken by phagocytotic cells inducing strong systemic and mucosal immune responses against antigens. Zheng et al. [95] investigated the immune stimulation mechanisms of ovalbumine (a frequently used antigen model) loaded chitosan nanoparticles. They suggested that chitosan nanoparticles had a strong potential to increase both cellular and humoral immune responses and elicited a balanced Th1/Th2 response, and that chitosan nanoparticles may be a safe and efficacious adjuvant candidate suitable for a wide spectrum of prophylactic and therapeutic vaccines.

Gene Delivery

As a nonviral gene carrier, chitosan nanoparticles are able to reduce the risk of cell toxicity and even induce strong immune responses. To date, chitosan nanoparticles have been applied to deliver DNAs, and RNAs mainly through the complex coacervation between polycationic chitosan and polyanionic nucleic acid molecules. Among them, one hot scope in life biology since the last decade of 20^{th} century is the gene silencing technique which is induced by long double-stranded RNAs (dsRNA), small interfering RNAs (siRNA) or microRNAs (miRNA). One limitation of the delivery of siRNAs into cells is rapid degradation and poor cell absorption of these small molecules. Katas et al. [96] reported a 100% protecting of siRNAs from nuclease degradation by chitosan nanoparticles. However, generally gene transfection efficiency of chitosan nanoparticles is lower than that of viral gene carriers. Improving transfection efficiency is a challenge for using chitosan nanoparticles as a gene carrier. Mansouri et al. [97] reported a folic acid modified chitosan nanoparticles to improve gene tranfection efficiency. Their results revealed that the obtained folic acid-modified chitosan nanoparticles showed a low cell toxicity and were able to condense DNA effectively with ideal size and zeta potential.

Chapter 2 Chitosan Nanoparticles for the Controlled Release of Proteins

2.1 Aim of the Study

In this section, protein-incorporated CSNPs were prepared for the preservation, delivery and controlled release of protein molecules. Since quite a few factors could influence the features of CSNPs as a protein nanocarrier, in order to achieve ideal particulate characters, protein payload and release profile, the primary influent factors such as CS concentration, CS/TPP mass ratio, BSA concentration, pH value are investigated. Some extra characterizations of CSNPs are also performed to have a glance of the formation mechanism of CSNPs. In the end, as a perspective, some preliminary trials are preformed on the purpose to overcome the burst release effect of CSNPs.

2.2 Materials and Methods

2.2.1 Materials

Low molecular weight chitosan supplied by Sigma (448869) with a deacetylation degree (DD) of 75-85% and viscosity of 20-300 cP (1% in 1% acetic acid) was used in section 2.3.1, 2.3.2, 2.3.3, and 2.3.6. PROTASAN UP CL 113 (soluble chitosan chloride) supplied by NovaMatrix/FMC Corporation with a DD of 75-90% was used in section 2.3.4 and 2.3.5. Albumin from bovine serum (BSA) with molecular weight ~66 KDa was supplied by Sigma. VEGF was kindly provided by Prof. Giacca (International Centre for Genetic Engineering and Biotechnology, ICGEB). Sodium tripolyphosphate (TPP), phosphoric acid, brilliant blue acetic acid, ethanol, phosphate buffered saline (PBS, pH 7.4, tablet) were supplied by Sigma.

2.2.2 Instruments

Magnetic stirrer (RCT-Basic) was purchased from IKA Corporation. Centrifuge (Mikro 220) was purchased from Hettich Corporation. Lyophilizer (CoolSafe) was purchased from Scanvac Corporation. Zetasizer (Nano S90) for particle size measurement was purchased from Malvern Corporation. Fourier

transformation infrared (FT-IR) spectrometer (Frontier) was purchased from Perkin Elmer Corporation. Scanning electron microscope (SEM, 1450VP) for morphological observation of particles is the product of LEO Corporation. Ultraviolet/Visible spectrophotometer for the measurement of protein concentration is the product of Perkin Elmer Corporation. Differential scanning calorimeter (DSC-Q20) is the product of TA Corporation. Incubating shaker (KS 4000ic -3510100) was purchased from IKA Corporation.

2.2.3 Methods

Preparation of Chitosan Nanoparticles

Here, CSNPs were prepared according to an ionic gelation method adopted by Calvo et. al. [98] to prepare CSNPs. For section 2.3.1, 2.3.2, 2.3.3, 2.3.6., low molecular weight chitosan was dissolved in Milli-Q water containing 0.4% (m/v) acetic acid to a concentration of 4 mg/ml as stock solution. TPP was dissolved in Milli-Q water to a concentration of 2.5 mg/ml as stock solution. Both of the two stock solutions were tuned to pH 5. Two milliliters of TPP solution was added to 5 ml chitosan solution under continuous stirring at 500 rpm for 30 minutes at room temperature. The reactions were performed in a 10 ml-beaker. CSNPs spontaneously formed via the electrostatic attraction between positively charged primary amino groups on chitosan chains and reversely charged polyanions. The resulting opalescent suspensions were determined as CSNPs. The concentrations of chitosan, TPP, BSA were adopted according to Table 1. Every sample was prepared in triplicate. The resulting nanoparticles suspensions were stored at 4 C for further analysis. Considering that many factors except for above mentioned ones could influence the formation of colloidal CSNPs, for instance, temperature, stirring rate, the same beaker, magnetic stirrer, and stirrer bar were always used for all samples.

In the above study using low molecular weight chitosan as the material for the preparation of CSNPs, impurities remaining in material which could influence light absorbance of sample were found in protein concentration determination step. In order to investigate more accurately the influence of pH value on the formation of CSNPs, a more purified soluble chitosan chloride was chose in section 2.3.4 and 2.3.5. The volume of reaction system was also increased to obtain a increased amount of nanoparticles. In this case, 28 ml TPP solution was mixed with 70 ml chitosan solution in a 100 ml-beaker under continuous stirring at 600 rpm.

For the preparation of VEGF-incorporated CSNPs, LMWCS was used as preparation material and the preparation parameters were as follow: 2 mg/ml CS solution (pH 5), 1.67 mg/ml TPP solution (pH

5), CS/TPP volume ratio: 5/2 (mass ratio: 3/1), amount of VEGF: 46μl 5 ng/μl, total reaction volume: 23 ml.

Table 2.1 The Concentrations of Chitosan, TPP, and BSA in the Preparation of CSNPs in section 2.3.1, 2.3.2, 2.3.3, and 2.3.6.

Sample	Chitosan (mg/ml)	TPP (mg/ml)	CS/TPP Mass ratio	BSA (mg/ml)
1	2	1	5	0
2	2.5	1.25	5	0
3	3	1.5	5	0
4	3.5	1.75	5	0
5	4	2	5	0
6	2	1	5	1.5
7	2.5	1.25	5	1.5
8	3	1.5	5	1.5
9	3.5	1.75	5	1.5
10	4	2	5	1.5
11	3	2.5	3	0
12	3	1.875	4	0
13	3	1.5	5	0
14	3	1.25	6	0
15	3	1.071	7	0
16	3	2.5	3	1.5
17	3	1.875	4	1.5

18	3	1.5	5	1.5
19	3	1.25	6	1.5
20	3	1.071	7	1.5
21	3	1.5	5	0.5
22	3	1.5	5	1
23	3	1.5	5	1.5
24	3	1.5	5	2
25	3	1.5	5	2.5

Yield Analysis of CSNPs

Eppendorf (EP) tubes being of the size of 1.5 ml were weighed on electronic balance. One milliliter CSNPs suspension of each sample was centrifuged at 15,000 rpm for 20 min. at room temperature. After supernatant was completely removed, EP tubes bearing particles pellets underwent vacuum drying over night at room temperature. Afterword, tubes were weighed again. All the samples were repeated in triplicate. The yield of CSNPs/BSA-CSNPs were determined according to the equation as follows:

$$Yield\ (\%) = \frac{Weight\ of\ Particles}{Total\ Weight\ of\ Used\ Materials} \times 100\%$$

Particle Size Measurement

Particle size measurement of CSNPs was performed by Zetasizer S90 based on dynamic light scattering (DLS) technique. One milliliter suspension of each sample was filled in a disposable polystyrene vial to be analyzed. Particle size values were given in the term of Z-average size (by intensity) along with a polydispersity index (PDI).

Determination of Encapsulation Efficiency of CSNPs

One milliliter particles suspension was centrifuged at 15,000 rpm for 20 min. at room temperature. 100 ml supernatant was used for the measurement of protein concentration using Bradford protein assay [99]. Briefly, spectrophotometer was warmed up before use. A set of BSA standards (0.1, 0.3, 0.6, 0.9, 1.2 mg/ml) were prepared to plot a standard curve (see Fig.2.1). 5 ml dye regent (dissolve 100 mg

Coomassie Brilliant Blue G-250 in 50 ml 95% ethanol, add 100 ml 85% (w/v) phosphoric acid, dilute to 1 liter when the dye has completely dissolved) was added to 100 µl sample solution. The mixture was agitated followed by incubation for 5 min. The absorbance of sample was measured at the wavelength 595nm by spectrophotometer. The encapsulation efficiency (EE) and Loading Capacity (LC) of CSNPs was determined according to the equation as follows

$$EE\ (\%) = \frac{Theoretical\ \mathrm{Pr}otein\ Amount - \mathrm{Pr}otein\ Amount\ in\ Supernatant}{Theoretical\ \mathrm{Pr}otein\ Amount} \times 100\%$$

$$LC\ (\%) = \frac{Weight\ of\ Loaded\ BSA}{Weight\ of\ BSA-CSNPs-Weight\ of\ Loaded\ BSA} \times 100\%$$

Each CSNPs sample was used as the control of its BSA-CSNPs counterpart.

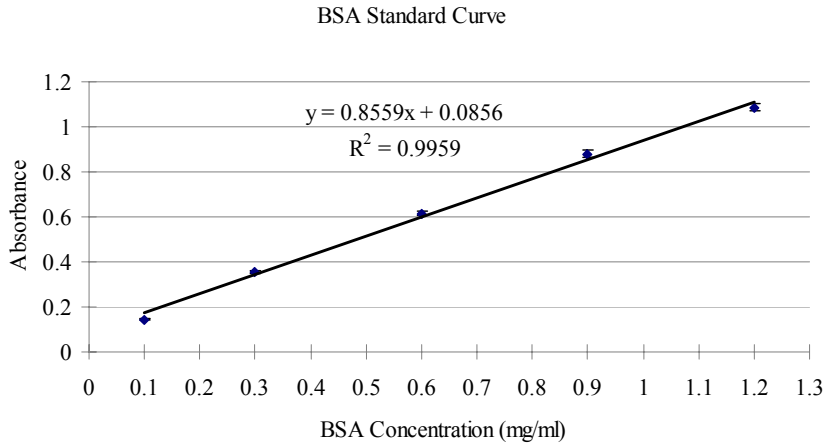

Fig. 2.1 BSA Standard Curve by Bradford Protein Assay.

Scanning Electron Microscpy (SEM) Analysis

CSNPs were analyzed using SEM (LEO 1450VP). One drop of freshly prepared particles suspension was deposited on sample stub covered with carbon tab. The sample was air-dried followed by covered with gold. Low voltage was set to observe CSNPs since at high voltage e.g. usually used 20 KV, CSNPs are highly heated by strong electron stream then deform or even decompose rapidly. In our study, 10 KV is found harmless to CSNPs.

Transmission Electron Microscopy (TEM) Analysis

Morphological characteristics of the nanoparticles were examined using a high resolution Transmission Electron Microscope (TEM) machine. One-drop sample was placed on a carbon coated film 300 mesh copper grid, allowing sitting for 10 min until air-dried. The sample was stained with 1M uranyl acetate solution for 1.5 min at 7 °C and any excess uranyl acetate was removed with filter paper

before observation on the TEM machine.

Fourier Transformation Infrared (FTIR) Spectrometry Analysis

FTIR analysis was performed using a Frontier PerkinElmer FT-IR spectrophotometer with universal ATR module (Diamond/KRS-5 crystal). The instrument was operated with resolution of 4 cm^{-1} and 32 scans with frequency range of 400-4000cm^{-1}.

Differential Scanning Calorimetry (DSC) Analysis

DSC analysis was performed using a TA DSC-Q20 instrument. Each freeze-dried sample (5-10 mg) is run at a scanning rate of 20 °C/min under nitrogen atmosphere. The temperature for the scan ranged from 20 to 280 °C.

In vitro Release of BSA-CSNPs

According to the yield of BSA-CSNPs, 2 mg BSA-CSNPs was collected in a 1.5 ml-size EP tube by centrifugation. The supernatant was completely removed away followed by resuspension in 1 ml PBS (pH 7.4). The suspension was put in an incubating shaker under continuous shaking at 37°C. At the time interval of 1, 3, 6, 24 hours, each sample was centrifuged and 200 μl supernatant was collected followed by refilled with 200 μl fresh PBS and resuspended. The concentration of released BSA was determined by Bradford protein assay. All samples are performed in triplicate.

For the in vitro release of VEGF, an enzyme-linked immuno sorbent assay (ELISA) kit was used to measure its concentration at the time interval of 1, 3, 6 and 24 hours and 3, 5, 7, 10, 15, 20 and 30 days in Dulbecco's modified eagle medium (DMEM) culture media.

2.3 Results and Discussion

2.3.1 The Effect of Chitosan Concentration on the Particle Size and BSA Encapsulation Efficiency of CSNPs

When other preparation parameters were fixed, the effect of CS concentration on the features of CSNPs was investigated. In this section, these fixed parameters are: CS/TPP mass ratio (5/1), BSA concentration (1.5 mg/ml). Five CS concentrations were chosen: 2, 2.5, 3, 3.5 and 4 mg/ml. As shown in Figure 2.1 A, the yield of CSNPs at all CS concentrations is higher that that of BSA-CSNPs, which probably results from the competitive reaction with chitosan between BSA molecules and TPP ions. Considering the big standard deviation, no remarkable influence of CS concentration on the yield of

CSNPs/BSA/CSNPs could be found. As the increase of CS concentration, particle size of CSNPs/BSA-CSNPs increases. Meanwhile, the particles polydispersity also increases, which means the formation of big particles or the appearance of aggregates. According to the size distribution diagrams (see appendix 1), both above mentioned issues are involved. Increasing CS concentration, increases the size of the particles and aggregates begin to appear. Besides, more small particles form as well during this process. All of these issues induce a wider size distribution at high CS concentration. The BSA encapsulation efficiency (EE) increases from 37% to 45% with the increase of CS concentration from 2.5 to 4 mg/ml. It's reasonable that more material and bigger particles could encapsulate more drug. However, Q. Gan et al. reported contrary result [100]. Besides, it is worth to notice that there is a drop of EE from the first and the second CS concentration which also shows in the case of particles yield. It applies that CSNPs prepared at the CS concentration below or above 2.5 mg/ml may show different EE trends, since besides of CS concentration, other factors could affect EE of particles, e.g. protein concentration and CS/TPP mass ratio. In other words, under our preparation conditions (CS/TPP mass ratio: 5/1, BSA concentration: 1.5 mg/ml, total reaction volume: 7 ml, CS/TPP volume ratio: 5/2), we found particles EE follows this trend.

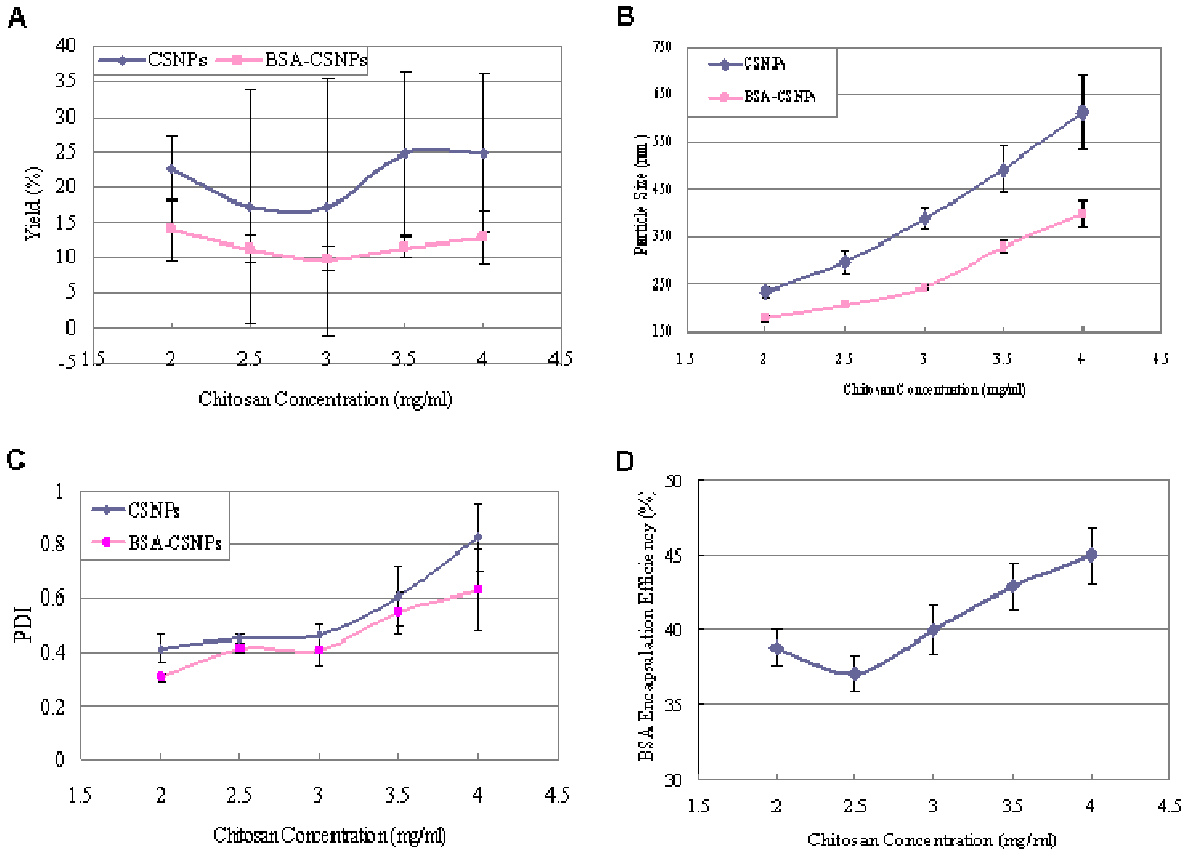

Fig. 2.2 The Effect of Chitosan Concentration on the A-Yield, B-Particle Size, C-Particle Size

Distribution and D-BSA Encapsulation Efficiency of CSNPs/BSA-CSNPs.

2.3.2 The Effect of CS/TPP Mass Ratio on the Particle Size and BSA Encapsulation Efficiency of CSNPs

In this section, 5 mass ratio values (3, 4, 5, 6, and 7) of CS/TPP were chosen to study its effect on the features of CSNPs. The other parameters were fixed at CS concentration: 3 mg/ml, BSA concentration 1.5 mg/ml. Weight analysis result shows that particles yield keeps going down as CS/TPP mass ratio increases. Particle size shows the contrary tendency with respect of particles yield. That is to say when the obtained CSNPs are becoming larger, less chitosan is gelated by TPP. As CS/TPP mass ratio rises, the size distribution also becomes wider. The incorporation of BSA affects the formation of CSNPs (see Fig. 2.2B and C). It is interesting to notice that when CS/TPP mass ratio comes from 3 to 4 a relative significant increase of particle size is observed. This happens to CSNPs and BSA-CSNPs, but when CS/TPP mass ratio continue to increase, particle size of BSA-incorporated CSNPs no longer increases significantly. The incorporation of BSA hinders the rise of polydispersity index compared to blank CSNPs. This observation implies that BSA hinders the gelation induced by TPP and when the amount of TPP is low enough, for instance when CS/TPP mass ratio rises to 4, the presence of BSA starts to play a dominant role. However, it is hard to demonstrate how BSA molecules interfere with the gelation process between chitosan and TPP. The EE of BSA-CSNPs decreases with the increasing CS/TPP mass ratio. One explanation is that high TPP mass at fixed chitosan concentration may cause a rise in solution pH value, with a consequential effect on increased overall negative surface charge carried by the protein molecules, which enhanced electrostatic interactions between chitosan and BSA molecules [101]. In the view of gelation density, higher TPP concentration results in more compact particlulate matrix. Consequently more protein molecules are entrapped.

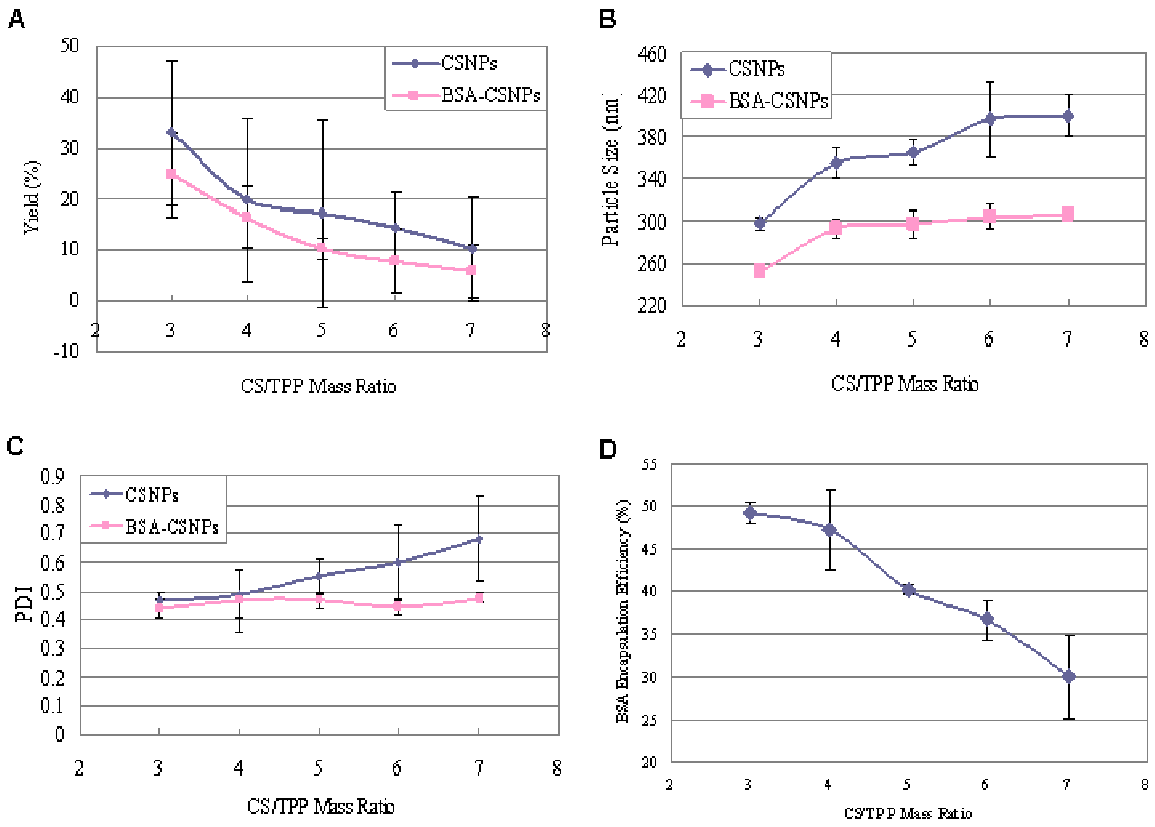

Fig. 2.3 The Effect of CS/TPP Mass Ratio on the A-Yield, B-Particle Size, C-Particle Size Distribution and D-BSA Encapsulation Efficiency of CSNPs/BSA-CSNPs.

2.3.3 The Effect of BSA Concentration on the Particle Size and BSA Encapsulation Efficiency of CSNPs

As discussed in last section, there is no clear mechanism by which protein molecules interfere the gelation process of CSNPs. In this section, a series of BSA concentration: 0.5, 1, 1.5, 2 and 2.5 mg/ml were set to study its effect on the features of CSNPs. As shown in Fig. 2.4A, BSA concentration shows no remarkable influence on the particles yield. It also shows weak influence on particle size of CSNPs (see Figure 2.4B and C). Figure 2.4D shows EE of CSNPs drops quickly from 55% to 38% with respect to BSA concentration 0.5 to 1.5 mg/ml. In the BSA concentration range of 1.5~2.5 mg/ml, particles EE shows a slight increase. Considering that the measuring range of Bradford protein assay is 0.1~1.4 mg/ml. From the last section we learn that at the constant CS concentration, smaller particles gelated by TPP with higher concentration show higher EE. This fits in the case what EE shows in the BSA concentration range 0.5~1.5 mg/ml.

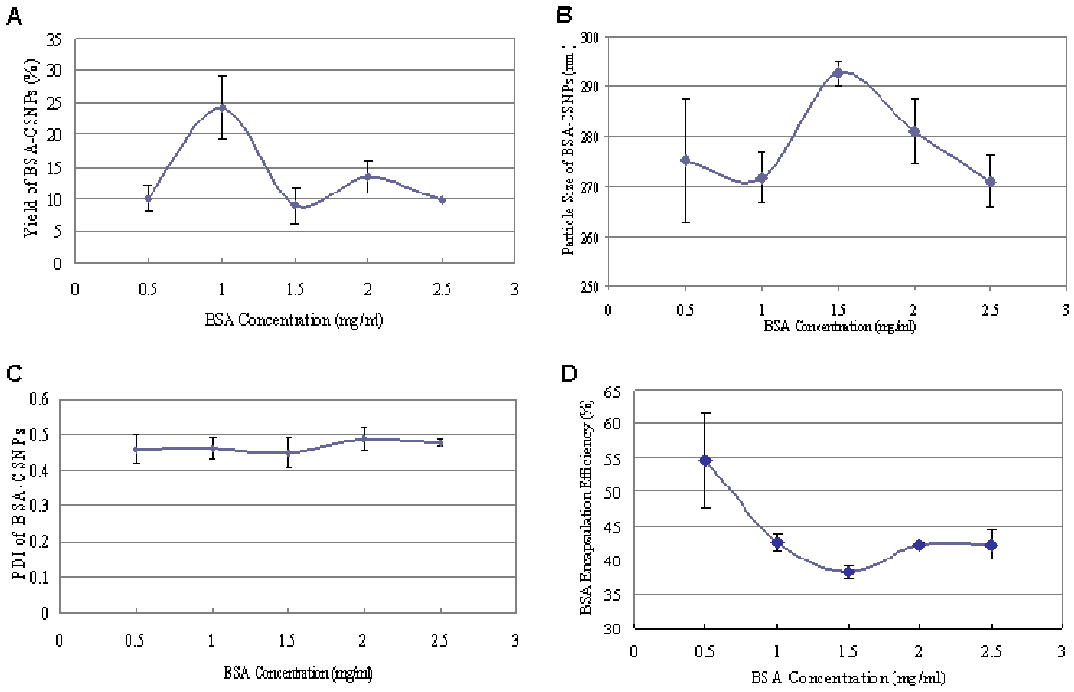

Fig. 2.4 The Effect of CS/TPP Mass Ratio on the A)Yield, B)Particle Size, C)Particle Size Distribution and D)BSA Encapsulation Efficiency of CSNPs/BSA-CSNPs.

2.3.4 The Effect of pH on the Formation and Encapsulation Efficiency of Chitosan Nanoparticles as Protein Nanocarrier

Chitosan is a natural polysaccharide composed of randomly distributed β (1 → 4)-linked glucosamine and N-acetylglucosamine units. Chitosan has found many applications in medical and pharmacological field in the forms of films, tablets, membranes, microparticles and nanoparticles due to its excellent biocompatible, biodegradable, mucoadhesive, non-toxic, antimicrobial, antiviral immunoadjuvant properties [102]. Chitosan is soluble in weakly acetic medium due to the protonation of primary amino groups on its chains. This makes chitosan to be a rare, cationic, natural polymer. Thanks to this, a variety of anions and negatively charged molecules could form complex or particles with chitosan and one of them is TPP. Since Calvo et al. firstly used TPP-cross-linked chitosan nanoparticles to deliver protein molecules in 1997 [98], a big number of researches have been conducted using CSNPs to deliver various drugs and bioactive molecules. Meanwhile, chitosan is always used as coating material to exert its hydrophilic, cationic, mucoadhesive properties [103-105]. Not to mention that numerous chtiosan derivatives which are modified up to various purposes have been applied to prepare CSNPs [106-108]. In short, the mild and convenient preparation conditions

make CSNPs very suitable to be a nanocarrier for bioactive molecules. Further more, excellent properties of chitosan such as cationic electric state, bioadhension facilitate the application of CSNPs in gene therapy and ocular, oral, pulmonary, gastrointestinal drug administration [102].

Even through several methods have been used to prepare CSNPs, i.e. ionic gelation, complex coacervation, microemulsion, emulsion-droplet coalescence, ionic gelation especially with TPP as cross-linker has been used most frequently so far. By this method, CSNPs are obtained via the electrostatic reaction between oppositely charged amino groups of chitosan and tripolyphosphoric ions from TPP. Some researchers have investigated the preparation parameters which influence the properties of CSNPs, i.e. chitosan molecular weight, concentration, mass ratio of chitosan to TPP, protein concentration, stirring rate, temperature and pH value. Among them, the molecular weight distribution of chitosan, mass ratio of chitosan to TPP and pH value are the major factors. With a low molecular weight chitosan solution filtered by a syringe filter, Fan and colleagues [109] obtained very monodispersed CSNPs (polidispersity index, PDI well below 0.05). Calvo and colleagues [98] revealed that CSNPs only generated in specific concentration range of chitosan and TPP at appropriate mass ratio. While, as respect to the effect of pH value, most studies were conducted on the influence of chitosan solution pH. Fan et al. [109] reported the critical mass ratio of chitosan to TPP for the formation of an opalescent suspension decreased with the pH decreasing and well monodispersed CSNPs only obtained in the pH range of 4.5-5.2. Gan et al. [110] reported a smallest particle size at pH 5.5 and the beginning of particles aggregation at pH 6.0, but the effect of chitosan solution pH on particle size did not follow any specific trends.

Since pH value has a significant influence on the size and electrical state of CSNPs. Whereas, particle size and zeta potential of CSNPs significantly affect the protein encapsulation and release. In this study, we further studied the effect of pH value on the formation and properties of CSNPs through strictly controlling the pH value of TPP solution. We characterize the CSNPs prepared under various pH conditions and attempt to understand the formation and protein encapsulation mechanisms of CSNPs better, eventually provid suggestions for avoiding ununiformity and initial burst release problems of CSNPs.

The Effect of pH on the Particle Size and Polydispersity of Chitosan Nanoparticles

The particle size of CSNPs could be affected by many factors such as chitosan molecular weight, deacetylation degree, concentration, TPP concentration, the mass ratio of chtosan to TPP, pH value, stirring rate and ambient temperature. In order to investigate the effect of pH on particle size of CSNPs,

the other parameters except for solution pH are fixed. Further more, the solution pH of chitosan and TPP was adjusted to the same value to reduce the alteration of resulting particles suspension pH.

In this study, a soluble chitosan salt chitosan hydrochloride (CSCL) was directly dissolved in deionized water to get 2 mg/ml solution. The pH of this initial CSCL solution was measured at pH 4.2. Two pH values of which one was below 4.2 (3.0) and one above (5.5) along with the initial 4.2 were set to prepare CSNPs. As shown in Table 2.2, particle size of CSNPs drops down remarkably as pH decreases from 5.5 to 3. At pH 5.5, aggregation happens when too much ionic cross-linking agent TPP is present (mass ratio of CS to TPP=3:1). It is worth noting that particle size drops down much more from pH 5.5 to 4.2 than that from pH 4.2 to 3. It is known that chitosan is a week polyelectrolyte with a pK_a around 6.5 and insoluble at neutral and alkaline pH values. In an acetic medium, the primary amino groups on chitosan polymer chains are protonated by hydrogen ions to confer to chitosan molecules a high charge density [112]. In this study, at the initial pH value (4.2), chitosan polymer chains extended well once upon CSCL was completely dissolved in water. When CSCL solution pH value was tuned to 5.5, partial NH_3^+ ions were deprontonized which led to the folding of chitosan chains [113]. Thus, fewer NH_3^+ ions were exposed, consequently fewer tripolyphosphric ions were involved in cross-linking chitosan, which resulted in a sparsely cross-linked chitosan polymer matrix and eventually a bigger particle size. On the other hand, when CSCL solution pH was tuned to 3 from initial 4.2, the amino groups on chitosan were further protonized which made the electric repulsion between chitosan molecules increase. Under this condition, more energy is needed to overcome the electrostatic repulsion between chitosan chains and form ionic linkages with TPP ions which resulted in the formation of CSNPs with small size. In addition, in the chitosan molecular conformation of view, more extended polymer chains at the lower pH value are prone to form more compact particles with small size.

Table 2.2 The Effect of pH on Particle size of Chitosan Nanoparticles.

Particle Size (nm)		Mass Ratio of CS/TPP		
		3	4	5
pH	5.5	▼	453.9±17	392.7±5
	4.2	166.9±1.9	155.9±1.5	157.9±1.7
	3.0	127.1±3.2	119.8±2.6	108.8±0.6

▼: Aggregation

In comparison with pH value, the mass ratio of chitosan to TPP has less predominant effect on the

particle size of CSNPs in this study, which also can be seen from Table 2.2. However, mass ratio of chitosan to TPP could contribute to affect the size distribution along with pH. As shown in Fig. 2.5, at low mass ratio of chitosan to TPP 3:1, namely more TPP, particle size distribution became wider from pH 3 to pH 4.2. Aggregation even happened when CSNPs were prepared at pH 5.5. At pH 4.2, polydispersity index (PDI) increased from 0.27±0.02 to 0.42±0.03. As shown in inset A (size distribution of CSNPs obtained at pH 4.2) and B (pH 5.5) in Fig. 2.5, at the same mass ratio of chitosan to TPP 4:1, it is prone to generate particles with big size at high pH value 5.5. Further more, particles are more likely to form aggregates comparing with that at low pH value 4.2. In the case of high pH, the aggregation of CSNPs mainly distributes to wide size distribution. On the other hand, at high mass ratio of chitosan to TPP 5:1, PDI increases from 0.27±0.01 at pH 5.5 and 0.25 at pH 4.2 to 0.34±0.04 at pH 3. At the same mass ratio of chitosan to TPP 4:1, the PDI of CSNPs increased from 0.27±0.02 to 0.39±0.01 when pH value was adjusted from 4.2 to 3. As shown in inset B (size distribution of CSNPs prepared at pH 4.2) and C (pH 3) in Fig.2.5, more small particles generated at pH 3 comparing with that at pH 4.2. Therefore, as shown in Fig. 2.5, pH value and mass ratio of chitosan to TPP collectively define an area in which formed CSNPs having a narrow size distribution. Otherwise, out of this area, wide size distribution could happen to CSNPs in the form of aggregation or a big number of small particles. Calvo et al. found in their research that CSNPs could only form in specific concentration range of chitosan and TPP [98]. In addition, Fan et al. found that when pH was below 4.5, it was not easy to produce nanoparticles with unimodal particle size distribution, while when pH was above 5.2, micro-particles were unavoidable present in suspension [109]. The above result in this study is generally in agreement with their data.

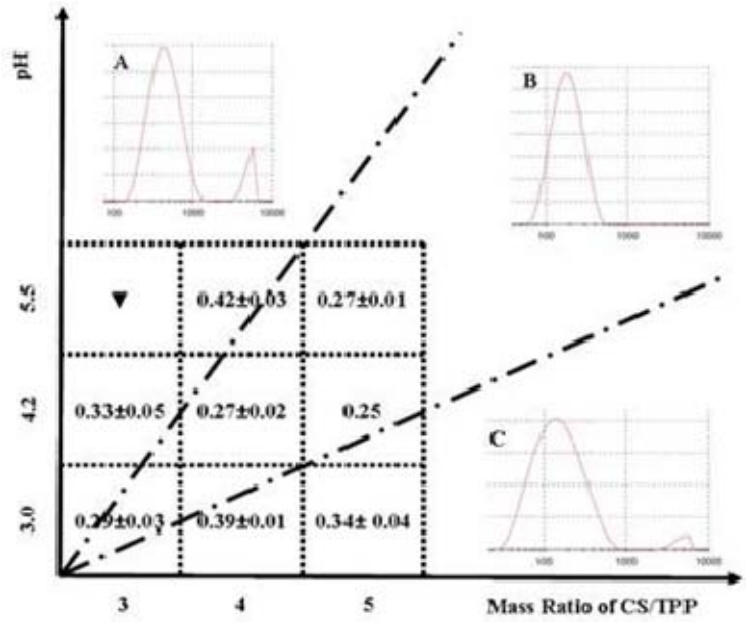

Fig. 2.5 The Effect of pH on Particle Size Distribution of Chitosan Nanoparticles. A, B, and C, the size distribution by intensity (light intensity in the unit of % against size in nanometer) of CSNPs prepared at pH 5.5, 4.2, 3.0 respectively (mass ratio of chitosan to TPP=4:1). The numbers in dash line squares are polydispersity indexes (PDI) of nanoparticles. ▼: Aggregation.

The Effect of pH on the Encapsulation Efficiency of Chitosan Nanoparticles

Chitosan molecules are positively charged in acetic medium. Therefore, they commonly used as carrier material to entrap or incorporate negatively charged macromolecules. In this study, BSA with an isoelectric point of 4.7 was used as model protein to investigate the effect of pH on the encapsulation efficiency (EE) of CSNPs. Since chitosan has a pKa of 6.5, 3 pH values (5, 5.5, 6) were set in the range of 4.7~6.5 to make electrostatic reaction happen between chitosan and BSA molecules.

As shown in Table 2.3, both particle size and PDI of CSNPs increased with the increasing solution pH value. However, when solution pH increased to 6, the resulting particles suspension was no longer stable. Aggregation of particles appeared which made only a part of small particles stay in suspension according to the size measurement. Gan et al. [110] studied the effect of solution pH on the particle size of CSNPs with raw chitosan by directly adjusting the pH of resulting particles suspension. They found a sharp increase of particle size of CSNPs at pH>6. In their further study on the surface charge density of CSNPs, particles showed a continual decrease in the positive zeta potential well before the pH value reached pH 6.0. Therefore, they concluded that deprotonation of the particle surface at pH > 6.0 induced decreasing electrostatic repulsion between particles thereby increasing the probability of particles aggregation. In this study, the particles aggregation happened at pH 6 may follow the same mechanism suggested by Gan et al..

After loading BSA, CSNPs showed a significant change in particle size, but no regular trends. It is difficult to interpret the influence of BSA encapsulation on particle size of CSNPs, because both the electoral states of chitosan and BSA molecules are changing with pH value. However, the particle size and size distribution of BSA-incorporated CSNPs (BSA-CSNPs) showed remarkable increase with the increasing pH value. Therefore, on the particle size point of view, the particle size of BSA-CSNPs increased as pH value increased, which suggests that pH value played a predominant role compared with BSA. With respect to size distribution, TPP cross-linked chitosan nanoparticle is actually one state of chitosan-TPP binary electrolyte system under specific conditions [113]. In the pH range of this study, negatively charged BSA molecules competed with TPP ions to electrostaticly react with chitosan. The shielding effect of counter ions, BSA molecules, disturbed the polymer network formed by chitosan

and TPP, which consequently reduced the monodispersity of CSNPs.

Table 2.3 Particle Size and Size Distribution of CSNPs/BSA-CSNPs Formed at Various pH Values.

Particle Size (nm)/PDI		CSNPs	BSA-CSNPs
pH	5.0	337.1±7.3/0.28	300±4.8/0.26±0.01
	5.5	381.2±5.8/0.32±0.04	499.2±18.7/0.49±0.03
	6.0	250.6±5.8/0.28±0.01※	450.1±15.4/0.55±0.07※

※: At this pH value, particles suspension was unstable and aggregates were present.

As shown in 2.6, pH value has a clear effect on the BSA encapsulation efficiency (EE) of CSNPs. The EE of CSNPs increased dramatically from 52% at pH 5 to 66% at pH 5.5 and almost 100% at pH 6. The increase of EE could be contributed to two effects induced by solution pH. Firstly, BSA molecules are further negatively charged with the increasing pH value, which favors the electrostatic reaction between chitosan and BSA molecules and consequential higher EE. On the other hand, particle size of CSNPs increased with the increasing solution pH, which improved the BSA encapsulating capability of particles.

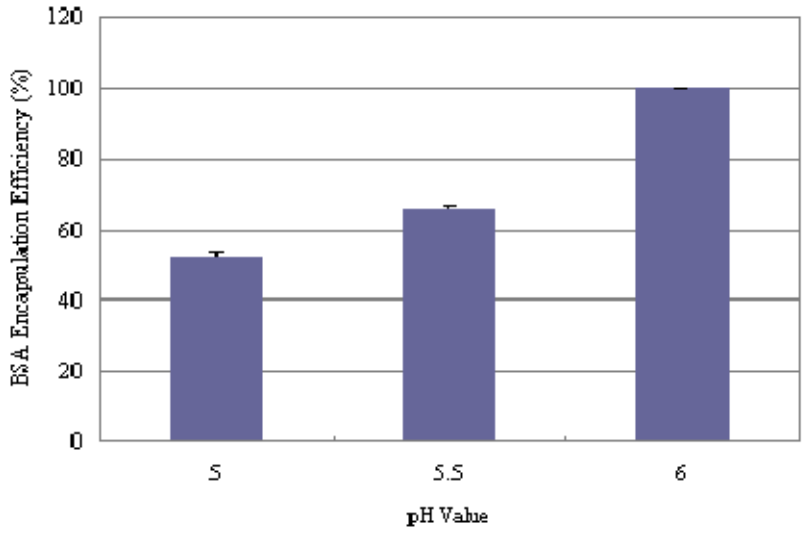

Fig. 2.6 The Influence of pH on BSA Entrapment Efficiency of CSNPs.

The Effect of TPP Solution pH on the Properties of Chitosan Nanoparticles

Chitosan is a cationic polymer which can form particles with negatively charged multivalent anions, such as sulfate [114], TPP [2]and deoxycholate [115], biomacromolecules such as DNA[116], siRNA [117] , lecithin [118] or polymers such as dextran sulphate [119], alginate [120] and hyaluronic acid

[121]. In addition, the deprotonation of charged amino groups on chitosan chains can results in precipitation of chitosan from aqueous solution and consequently leads to the formation of chitosan particles as well [122]. Mi et al. [123] reported TPP solution with different pH value could form chitosan beads with different interior structures via the coacervation effect of hydroxyl ions and ionic cross-linking of TPP ions. In this study, the effect of TPP pH value on the formation of chitosan nanoparticles is studied. Since the original TPP solution has a pH value around 9.5 in which OH^- and TPP ions coexist, the original TPP solution and a pH 5.5 TPP solution were chose to prepare CSNPs. The pH value of chitosan solution was set at 5.5.

As shown in Table 2.4, the CSNPs obtained with pH 9.5 TPP (9.5 blank) showed a bigger particle size, but a wider particle size distribution than that of CSNPs obtained with pH 5.5 TPP (5.5 blank). This could be interpreted that OH^- ions more easily penetrate chitosan gel matrix due to their smaller size compared with TPP ions, thus large amount of OH^- ions in pH 9.5 TPP solution induced the bend of chitosan chains firstly, consequently more intermolecular chitosan-TPP linkages formed, and eventually bigger particles generated. Meanwhile, the conjunct roles of OH^- and TPP on chitosan matrix result in nonhomogeneous and ionicly cross-linked particles [123]. Besides, 9.5 blank also has a bigger yield than that of 5.5 blank. The incorporation of BSA increased the particle size of CSNPs obtained with pH 5.5 TPP and polydispersity index (PDI) as well. However, for BSA-incorporated CSNPs obtained with pH 9.5 TPP (9.5 BSA), the incorporation of BSA make particles suspension unstable to precipitate out. Compared with 5.5 BSA, 9.5 BSA showed a higher yield and BSA encapsulation efficiency (EE). In the case of 9.5 BSA, even all of BSA was incorporated.

Table 2.4 The Properties of Chitosan Nanoparticles and BSA-incorporated Chitosan Nanoparticles.

	Particle Size (nm)		PDI		Yield (%)		EE (%)	
	9.5	5.5	9.5	5.5	9.5	5.5	9.5	5.5
CSNPs	495.3±21.7	386.4±8.6	0.46±0.05	0.27±0.04	36±4	30.7±2.3	-	-
BSA-CSNPs	※	433.8±5.7	※	0.43±0.04	29.5±1.6	27.6±3.3	100	71.7±0.5

※: Particles suspension was unstable and aggregates were present.

The obtained CSNPs and BSA-CSNPs were further characterized by FTIR-AIR spectrometry, DSC analysis and SEM. As shown in Fig. 2.7, chitosan hydrochloride (CSCL) showed characteristic absorbance peaks at 1632 cm^{-1} and 1514 cm^{-1} which indicate to the C=O stretching vibration of amide I and –NH stretching vibration of amino groups as reported previously [124]. The absorbance peaks of

BSA at 3282, 1644, and 1515 cm^{-1} are assigned to the stretching vibration of –OH, amide A (mainly –NH stretching vibration), amide I (mainly C=O stretching vibrations), and amide II (the coupling of bending vibrate of N–H and stretching vibrate of C–N) bands, respectively [125].

After the formation of 2 blank CSNPs and 2 BSA-CSNPs, the peak at 1514 cm^{-1} in CSCL shifted to 1535 cm^{-1}. The peak at 1624 cm^{-1} in CSCL shifted to 1632 cm^{-1} in 2 blank CSNPs. Besides, a new absorbance peak at 1204 cm^{-1} which indicates P=O stretching [126] shows up in the spectrum of all the 4 CSNPs. These suggest the amino groups on chitosan and TPP are involved in the formation of CSNPs. The absorbance peaks at 3282 cm^{-1}, 1644 cm^{-1} which are the characteristic absorbance peaks of BSA and the peaks at 1535 cm^{-1}, 1204 cm^{-1} which are assigned to CSCL are present in the 2 BSA-CSNPs. This suggests the encapsulation of BSA into CSNPs.

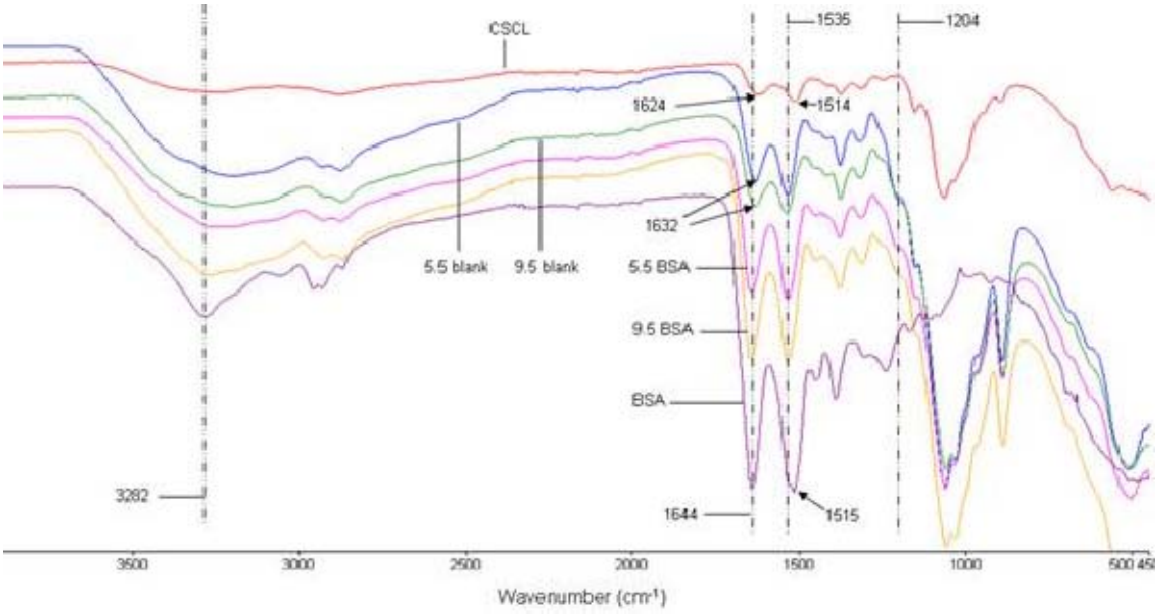

Fig. 2.7 FTIR Spectrums of Chitosan Nanoparticles and BSA-incorporated Chitosan Nanoparticles.

In order to understand the thermal behaviors of CSNPs ionicly cross-linked by TPP at different pH values, DSC analysis was performed. Fig. 2.8 shows the thermograms of CSCL, BSA, lyophilized CSNPs and BSA-CSNPs (the third thermal scan). Not like chitosan, the DSC curve of CSCL shows a wide endothermic peak centered at 228 ℃ which could be registered as the Tm of CSCL. The DSC curve of BSA shows a characteristic endothermic peak at about 222 ℃ [127]. Compared with CSCL, a wide endothermic peak centered around 235 ℃ with an onset at 187 ℃ appeared in the thermograms of 5.5 blank and 5.5 BSA which can be attributed to the breakdown of weak electrostatic interaction between chitosan and TPP [128]. Compared with 5.5 blank, this endothermic peak of 5.5 BSA shows a slightly bigger enthalpy change (ΔH). Further more, the exothermic peak of 5.5 BSA is

centered at a slightly higher temperature than that of 5.5 blank. These probably suggest a weak electrostatic interaction exist between BSA and chitosan. In addition, 5.5 BSA shows a wider exothermic peak comparing with 5.5 blank, which may be contributed to relatively inhomogeneous crystalline arrangement resulted from the encapsulation of BSA. This is also in agreement with that 5.5 BSA have a wider particle size distribution than that of 5.5 blank.

Intriguingly, two exothermic peaks appeared in the DSC curve of 9.5 blank, which suggests two crystalline arrangements exist in sample. Similar result also was previously reported by Liu et al. [128]. As shown in Fig. 2.8, one of the two exothermic peaks in 9.5 blank and 9.5 BSA is centered at a nearby temperature with that of 5.5 blank and 5.5 BSA. It suggests that similar crystalline arrangement exists in the CSNPs ionicly cross-linked by TPP at different pH values. Beside of this exothermic peak at around 260 ℃, another exothermic peak exists in the DSC curves of 9.5 blank and 9.5 BSA and is centered at lower temperature. Further more, the ΔH of this peak in 9.5 blank and 9.5 BSA is bigger than the peak centered at 260 ℃. It indicates the crystalline arrangement which refers to the peak located at relative low temperature has a predominant proportion in 9.5 blank and 9.5 BSA. In addition, both of the DSC curves of 9.5 blank and 9.5 BSA show a quite wide endothermic peak which is distinct with that of 5.5 blank and 5.5 BSA. It probably implies 9.5 blank and 9.5 BSA have less intensive chitosan-TPP linkages than that of 5.5 blank and 5.5 BSA.

In a weakly acetic environment, both of tripolyphosphoric and hydroxyl ions are present in chitosan-TPP gel system. But, the hydroxyl ions preferentially bind to $NH3^+$ binding sites on chitosan chains due to the their higher mobility compared with tripolyphosphoric ions, which causes polymer chain softens considerably [13]. In this study, the big amount of OH^- ions in pH 9.5 TPP solution soften chitosan polymer chains via the deprotonation of NH_3^+ resides, consequently leads to the folding of chitosan chains. In this way, less tripolyphosphoric ions are involved in the electrostatic interaction with chitosan. Further more, more ionic linkages are formed between folded chitosan molecules. However, as indicated by DSC analysis, there are still some crystalline arrangements which are similar with what could also found in CSNPs corss-linked by pH 5.5 TPP solution. One possible explanation to this phenomenon is that the CSNPs cross-linked by pH 9.5 TPP solution (pH5.5 blank and 9.5 BSA) are not completely cross-linked by TPP ions due to the folding of chitosan chains results from the deprotonation of OH^- ions. To be detailed, the folding of chitosan chains may hinder tripolyphophoric ions diffusing into the very center of particle gel matrix. Consequently, particle center is not fully cross-linked by TPP ions. The other explanation is that tripolyphosphoric and hydroxyl ions conjointly

play roles on the formation of chitosan nanoparticles, which induce the nonuniformity of particles. However, in regardless of which reason inferred above, the relatively loose chitosan matrix which is cross-linked by relatively fewer TPP ions in the case of TPP solution at higher pH results in high BSA encapsulation.

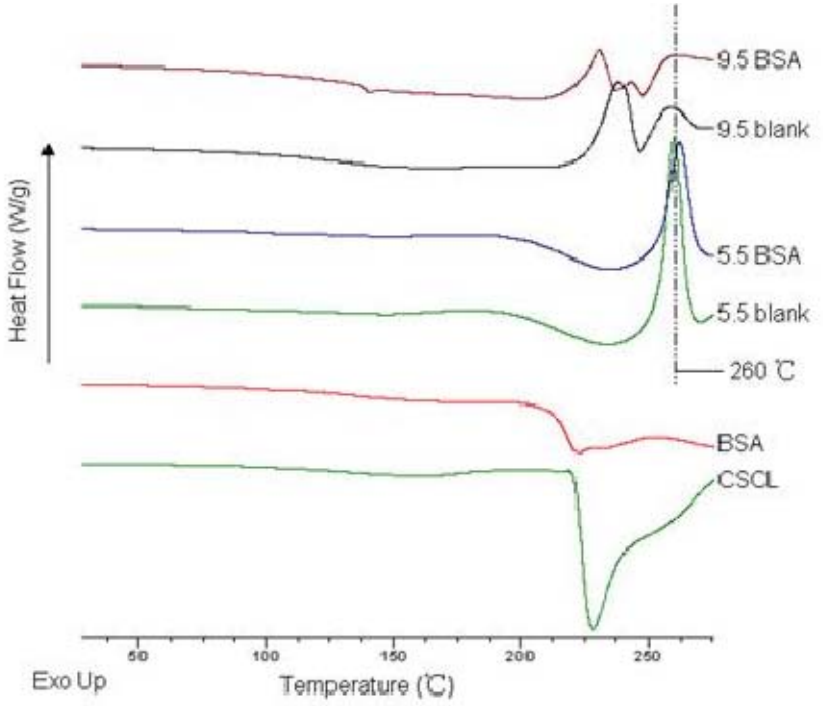

Fig. 2.8 DSC Thermograms of CSNPs and BSA-CSNPs.

In order to verify the above inferred reasons, the morphology of chitosan nanoparticles was checked using SEM. As shown in Fig. 2.9 A and C, particles in 9.5 blank and 9.5 A are irregular-shaped, loose and inhomogeneous. On the contrary, as shown in B and D, particles in 5.5 blank and 5.5 BSA are nearly spherical, compact and homogeneous. The compact particles formed with pH 5.5 TPP solution are also in accordance with the interpretation proposed in the first section. That is, more extended chitosan chains form more compact particles at low pH value. Since many small particles are also present in 9.5 blank and 9.5 BSA, the latter interpretation discussed in DSC analysis part seems more reasonable. That is, tripolyphosphoric and hydroxyl ions conjointly affect the formation of chitosan nanoparticles, which could result in the nonuniformity of particles.

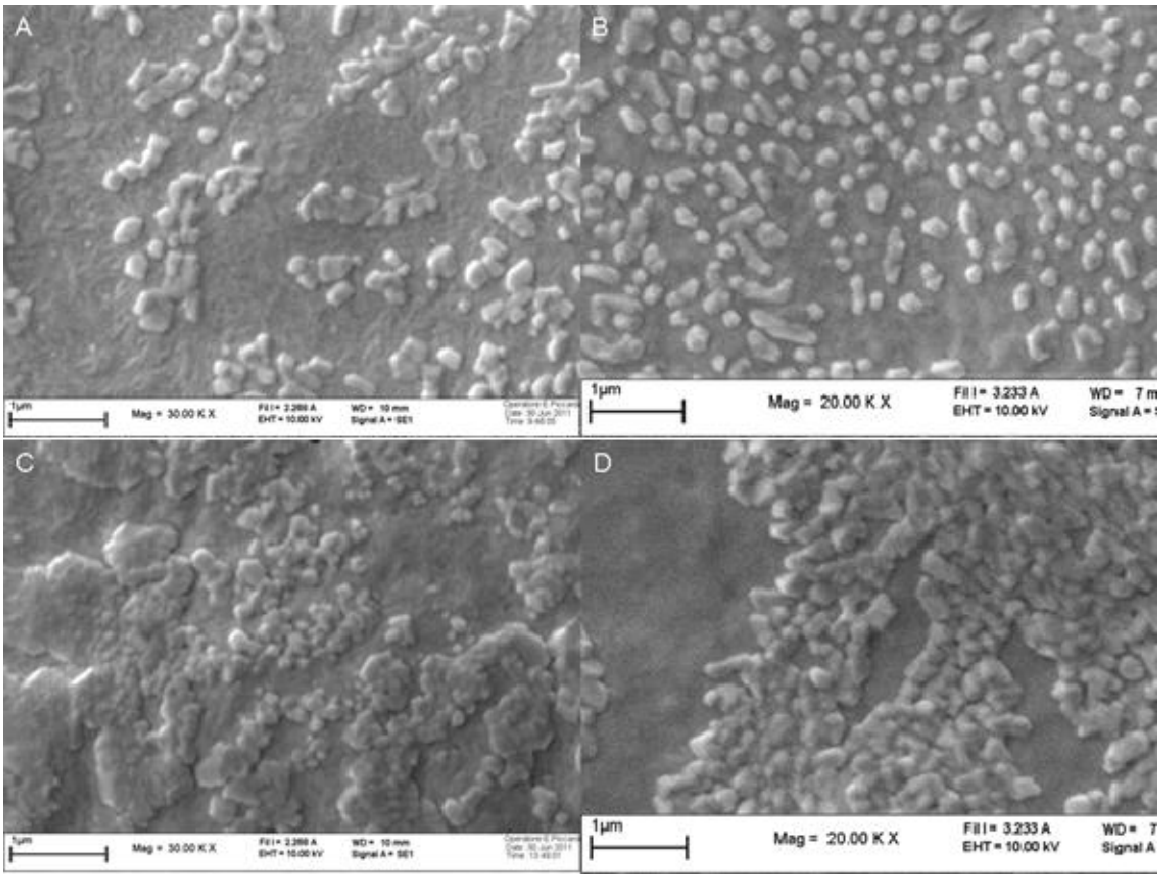

Fig. 2.9 SEM Microphotographs of CSNPs and BSA-CSNPs Cross-linked by TPP at Different pH Value. A, 9.5 blank, B, 5.5 blank, C, 9.5 BSA, D, 5.5 BSA. Scale Bars represent 1 μm.

The FTIR spectrometry confirms the encapsulation of BSA into chitosan nanoparticles. The DSC analysis confirms the electrostatic interaction between CSNPs and BSA molecules, even though this interaction is weak. Seen from the SEM photographs of BSA-incorporated CSNPs, the encapsulation of BSA gives CSNPs ununiformity. In other words, a charged biomolecules—BSA disturbed chitosan-TPP gel system and make the situation more complicated. As seen above, higher solution or TPP solution pH gives higher BSA encapsulation efficiency. Here, we studied the in vitro BSA release profiles of two BSA-CSNPs cross-linked by TPP solutions at different pH values.

As shown in Fig. 2.10, 5.5 BSA shows an initial burst release in the first hour in pH 7.4 PBS at 37 ℃ followed by a slow release in the following 24 hours. Gan et al. [129] investigated the in vitro release of BSA from CSNPs. They concluded that the burst is more likely a consequential effect of rapid surface desorption of large amount of protein molecules from a huge specific surface area provided by large numbers of particles at nano-scale, and a larger proportion of protein molecules may not truly embedded in the nanoparticles' inner structure. Compared with 5.5 BSA, 9.5 BSA only released ~20% of BSA in the first hour and then a sustained release in the next 6 hours. However, totally only <70% BSA were release after 24 hours. It is probably contributed to two reasons. On one

hand, 9.5 BSA have a big particle size which extends the diffusion pathway of BSA molecules. On the other hand, the bending conformation of chitosan chains under this condition may hinder the diffusion of BSA molecules in particles. In this sense, for 5.5 BSA, their polymer chains are more extended, which provide more NH_3^+ binding sites for TPP. Therefore, more compact polymer network forms for particles. Since BSA molecules also have a large dimension (an ellipsoid of revolution with major and minor axes 13.8 and 4.6 nm) [130], compact internal structure may limit the distribution of BSA molecules inside particles. Eventually, most of BSA molecules absorb on particle surface, which results in an initial burst release effect.

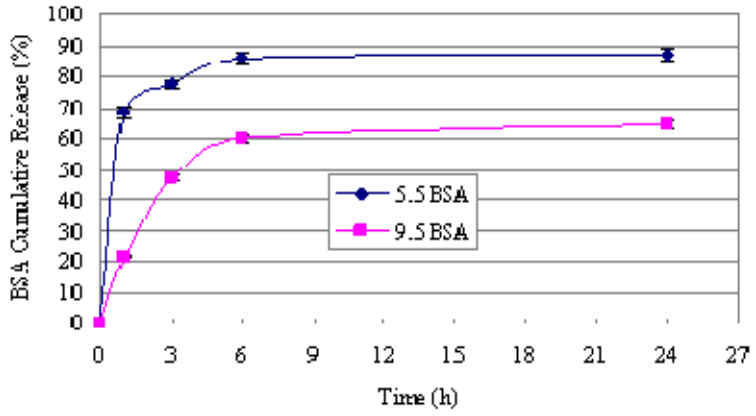

Fig. 2.10 The in vitro BSA Release of BSA-CSNPs. TPP 9.5/TPP 5.5, BSA-CSNPs gelated by pH 9.5/5.5 TPP solution. The pH value of chitosan solution was 5.5 for the both cases.

2.3.5 VEGF-incorporated CSNPs for the Regeneration of Peripheral Nerves

In this section, VEGF-incorporated CSNPs are prepared to preserve the bioactivity and control the release of VEGF in a hydrogel for peripheral regeneration. The particle size and yield of blank CSNPs/ VEGF-CSNPs are shown in Table 2.5. Figure 2.11 shows the particle size distribution of blank CSNPs and VEGF-CSNPs. VEGF-CSNPs show smaller particle size in comaprison with that of blank CSNPs. It suggests that the incorporation of VEGF disturbed the formation of CSNPs. The obtained particles were observed under TEM (see Figure 2.12). At the chitosan (LMWCS) concentration of 2 mg/ml, CS/TPP mass ratio of 3/1 and solution pH 5, nanoscale coacervates form and are prone to fuse with each other (see Figure 2.12A). At high magnification, small particles are visible inside the coacervates (see Figure 2.12B). For VEGF-CSNPs, no particles with size above 100 nm in disagreement with the particle size data based on DLS. Probably because coacervates formed at this preparation conditions. This coacervates could be detected by DLS in solution, but could not be seen by TEM at the dry

environment. A few small nanoparticles are visible (see Figure 2.12C),with deep color in the core and on the surface (in accordance to what Fan et al. observed [131]). Besides, small pieces of irregular shaped coacervates are present in the whole picture. However, the in vitro release of VEGF-CSNPs showed a rapid initial burst release effect (see Figure 2.13). The burst release effect results from the week electrostatic interaction between VEGF molecules and CSNPs. Since chitosan is a cationic polymer, negatively charged protein molecules are supposed to be encapsulated more efficiently. Whereas, VEGF is a basic protein molecule with an isoelectric point of 8.5. This may explain why VEGF-CSNPs show a burst release effect of VEGF.

Table 2.5 Particle size and Yield of VEGF-CSNPs.

	Particle Size (nm)	PDI	Yield (%)
Blank CSNPs	281.6±6.1	0.22±0.02	78.9±5.3
VEGF-CSNPs	250.1±3.2	0.20±0.04	87.7±3.0

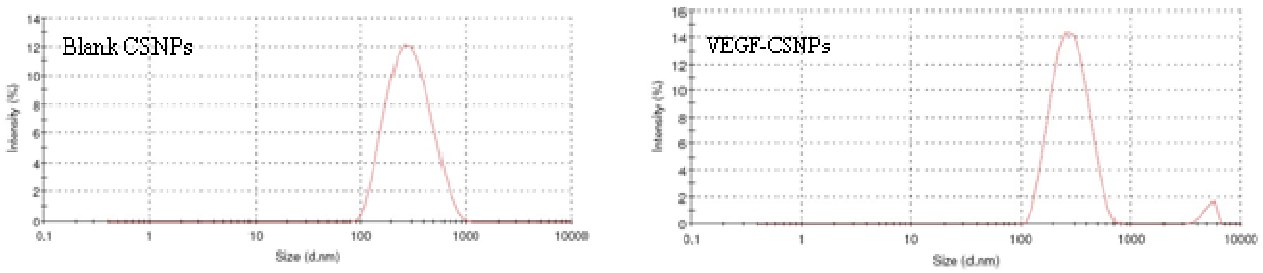

Fig. 2.11 Particle Size Distribution of CSNPs/VEGF-CSNPs.

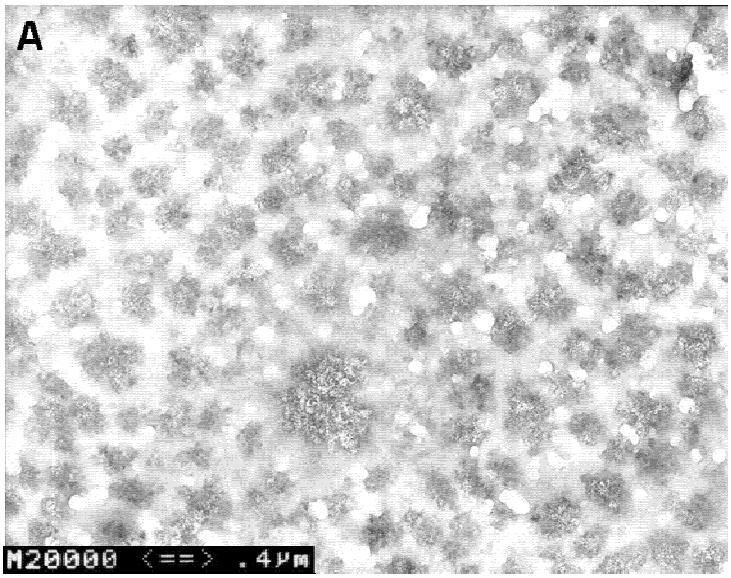

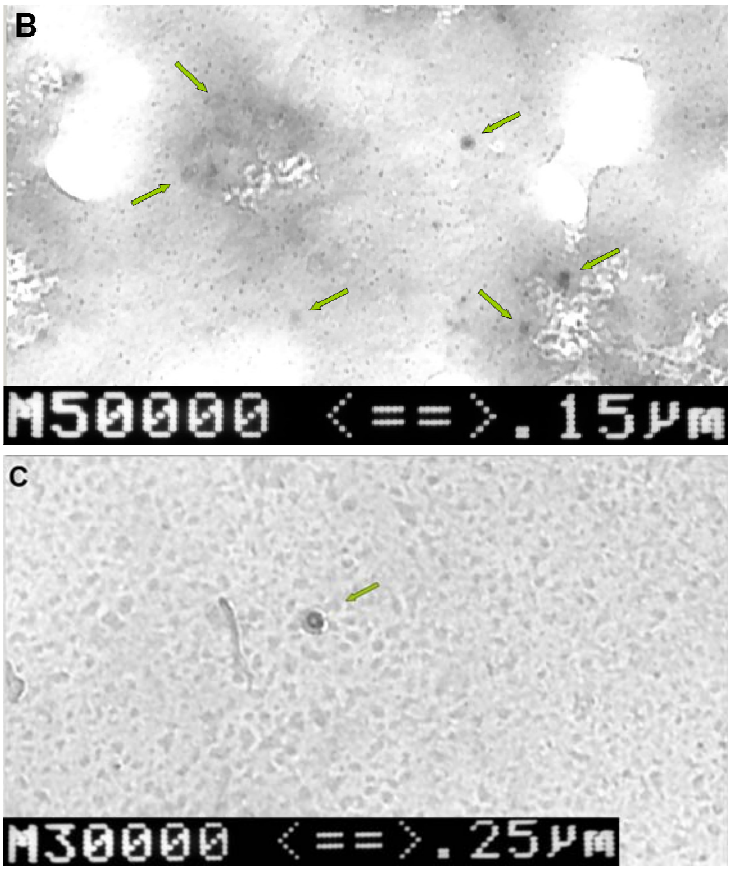

Figure 2.12 TEM Photographs of CSNPs and VEGF-CSNPs. A, CSNPs, B, CSNPs at High Magnification, C, VEGF-CSNPs. Green arrows indicate nanoparticles.

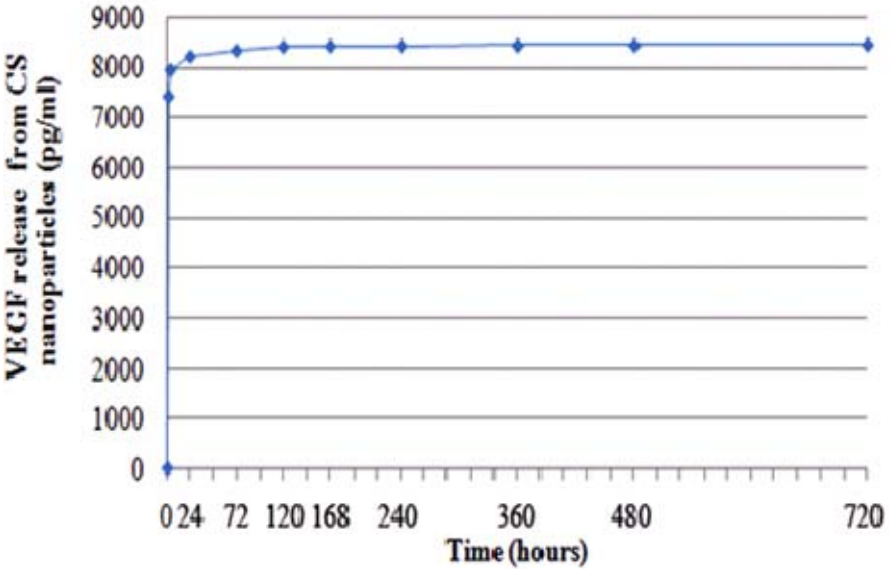

Figure 2.13 The in vitro release of VEGF from VEGF-CSNPs. Performed by Francesca Ruini and Chiara Tonda Turo.

2.4 Conclusion and Perspective

In this chapter, chitosan nanoparticles are prepared for the delivery and controlled release of protein molecules. The main factors which affect the particle size, protein loading and release properties of CSNPs are studied. Increasing polymer concentration, particle size of CSNPs increases, but a wider size distribution is obtained. Protein encapsulation efficiency rises with increasing CS concentration, but only in the CS concentration range above 2.5 mg/ml. When CS/TPP mass ratio increases, that is, when TPP decreases, particles yield decreases, but particle size increases. Thus, the presence of smaller particles results in the decrease of particles EE. The presence of BSA shows an influence on the particles formation. The particle size data reveals that TPP plays a dominant role on the formation of CSNPs at the CS/TPP mass ratio 3/1. When this ratio goes up, BSA starts to affects the particle size more than CS/TPP mass ratio.Consequently, particle size and size distribution stop increasing remarkably. It can be attributed to the competitive interaction between BSA molecules and TPP ions with chitosan. BSA concentration does not significantly affect particles yield and size. A decrease in particles EE when BSA concentration increases from 0.5 to 1.5 mg/ml is detected. Kaloti et al indicated that phase transition was involved in the chitosan-TPP polyelectrolytes system [132]. Therefore, the effect of these parameters on the size and drug encapsulation of CSNPs should take this issue in consider.

This work studied the effect of pH value on the formation of TPP-ionic-gelated chitosan nanoparticles and protein its encapsulation efficiency. To be different with previous studies, this study studied the influence of pH value on the formation of chitosan nanoparticles considering both the pH values of chitosan and TPP solution. In order to do this, the pH of ionic cross-linker—TPP was adjusted to the same value to that of chitosan solution. In addition, the influence of TPP pH on the formation of CSNPs and its protein encapsulation efficiency were also studied. Thus, this study is favorable to better understand how to get monodispersed chitosan nanoparticles, how to achieve a high protein encapsulation efficiency and how to prolong the release of protein from chitosan nanoparticles.

Firstly, pH value has a significant effect on the particle size of CSNPs. The lower pH value is, the smaller the particle size is. This because chitosan chains are more extended at lower pH value due to the protonation of amino groups on chitosan chains. Under this condition, more NH_3^+ are exposed to be cross-linked by tripolyphosphoric ions, consequently more compact chitosan polymer network forms and eventually smaller particle size is achieved. In comparison with the mass ratio of chitosan to TPP,

pH value plays a predominant role on particle size. Nevertheless, pH value affects particle size distribution of CSNPs along with this ratio. It is found that monodispersed CSNPs only form in a domain which is defined by pH value and mass ratio of chitosan to TPP. Under the conditions which are outside this domain, CSNPs are unstable with a big size distribution or aggregates.

BSA was used as a protein model in this study. Various pH values which fell in the pH range between the Ip (~4.7) of BSA and pKa (~6.5) of amino groups on chitosan were set for BSA encapsulation experiments. Both the particle size and size distribution of CSNPs and BSA-incorporated CSNPs increased with the increasing pH value. However, when pH value retched 6, particles suspension became unstable. In addition, in comparison with blank CSNPs, the influence of BSA encapsulation on particles size of BSA-CSNPs did not follow any certain roles, which probably because the electrical states of all the components in chitosan-TPP gel system could be affected by solution pH. Even so, the encapsulation efficiency of CSNPs increased dramatically when pH value increased. This could be contributed to the larger particle size at higher pH, which makes encapsulating more BSA possible. This could be also contributed to more negative charges BSA molecules bear at higher pH, which leads to stronger electrostatic attraction between BSA and chitosan.

In the end, the effect of TPP solution pH on the properties of chitosan nanoparticles was studied. Two TPP solutions at different pH were used: one original TPP solution at pH 9.5 and the other tuned to pH 5.5 which was the same with that of chitosan solution used for both cases. Results indicated that chitosan nanoparticles prepared with pH 9.5 TPP solution had a bigger particle size, wider size distribution, higher yield and BSA encapsulation efficiency comparing with that of particles prepared with pH 5.5 TPP solution. FTIR microscopy proved the formation of particles and encapsulation of BSA, but did not reveal any reaction between chitosan and BSA. The further thermal analysis of two particles with DSC revealed that two crystalline arrangements existed in the particles prepared with TPP 9.5 TPP solution. Together with SEM analysis in which 9.5 blank and 9.5 BSA particles showed irregular-shaped, ununiform, and loose appearance, we concluded that hydroxyl ions and tripolyphophoric ions conjointly reacted with chitosan chains (see Fig. 2.14). Since DSC result revealed that BSA had a weak electric reaction with chitosan, here, the conformation of chitosan chains played a predominant role in the formation of chitosan nanoparticles and BSA encapsulation. As shown in Fig.7, when an acetic TPP solution is used to cross-link chitosan, chitosan chains can hold the extended state thereby a compact chitosan polymer network which is fully cross-lined by TPP ions forms. In this case, considering the dimensions of chitosan nanoparticles and BSA molecules, a big amount of BSA

molecules would rather absorb on the particle surface than are entrapped inside particles, which is also verified in BSA release profile in this study. For the case of chitosan nanoparticles prepared with a basic TPP solution, tripolyphosphoric ions react with chitosan along with hydroxyl ions. Nevertheless, hydroxyl ions preferentially react with chitosan via deprotonizing NH_3^+ on chitosan due to their high mobility. The deprotonation of NH_3^+ not only softens chitosan chains but also decreases the number of NH_3^+, which results in few and far ionic linkages between chitosan and TPP. Therefore, large, loose and inhomogeneous particles are obtained as seen under SEM. However, a small amount of small particles inevitably generate as well, since both hydroxyl ions and tripolyphosphric ions are present, which is also the reason why two crystalline arrangements were detected by DSC analysis in this study. In this case, loose and large particles are capable to encapsulate a big amount of BSA molecules. Further more, the big particle size also provide a long distance diffusion path for encapsulated BSA molecules and in sequential a sustained release of BSA.

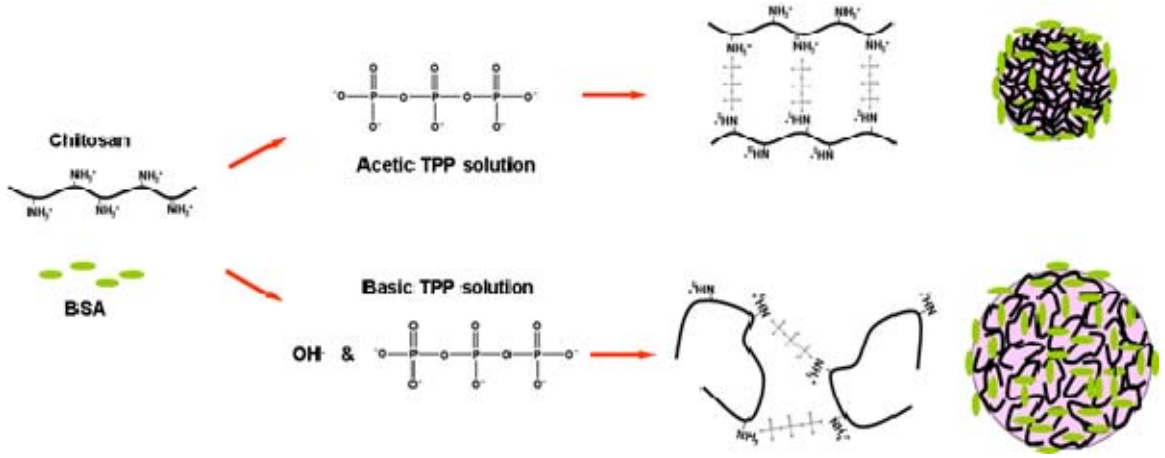

Fig. 2.14 Schematic Presentation of Chtisan Nanoparticles Cross-linked by TPP with Different pH Values.

To sum up, in order to obtain monodispersed chitosan nanoparticles, an acetic TPP solution should be used to cross-link chitosan; in order to achieve a high protein encapsulation efficiency, an as high as possible pH value should be adopted; in order to achieve a long and sustained protein release, the dimension of protein molecules and the effect of pH value on the formation of chitosan chains should be taken into account.

VEGF is intended to be encapsulated into chitosan nanoparticles to preserve its bioactivity and realize stable release in a chitosan/gelatine blend hydrogel. The in vitro release profile of this VEGF-CSNPs shows a initial burst release in a few hours. The electric state of VEGF is very likely to be responsible for this phenomenon in the consideration of CSNPs are preferable to carry anionic drugs.

The nature of the structures visible (Fig. 2.10A and C) in the CSNPs gelated by pH-untuned TPP is not completely clear, The possibility that the irregular-shaped blocks are aggregates of small CSNPs can be excluded, because if they were, the temperature of their exothermic peak should be located at higher temperature which is not the case. It can be also supposed that these are the result of the gelation of different tripolyphosphic ions ($P_3O_{10}^{5-}$, $H_2P_3O_{10}^{3-}$, and $HP_3O_{10}^{4-}$), since in any pH range three forms of ions coexist in TPP solution. This possibility is not strongly supported, because all these ions have equal chances to react with chitosan, thus it is not likely to get two crystal structures. The most reasonable explanation is that these blocks are the result of coacervation induced by hydroxyl ions in pH-untuned (~9.5) TPP solution. Chitosan particles coacervates by other salts e.g. Na_2SO_4 are usually irregular-shaped. For this reason, a control experiment could be set to confirm the .

Even through the advantage of TPP gelated CSNPs in encapsulating bioactive molecules, its fast release profile could be a barrier for certain applications. For this reason, several other chitosan based derivatives have been proposed to overcome this drawback. For instance, thiolated chitosan which can be used to cross-link chitosan via covalent bonds could be a means to achieve a more sustainable release [133]. On the other hand, alternative drug encapsulation strategies can be also considered. For example, microemulsion containing interior chitosan aqueous phase can be formulated to entrap the drug [134]. During the study of section 3.3.5, when pH value of the mixture of TPP and BSA came to 2~3, the mixture started to become turbid. Some of this suspension was checked by SEM and coacervate complexes were visible. In order to exclude the possible formation of salt crystals, controlled trials were performed. NaCl (HCl was used to tune solution pH) and TPP solution were deposited to undergo SEM observation. Results indicated that no such regular complexes could be visible in NaCl and TPP samples (see Appendix 4). The controlled trials of individual titration of BSA and TPP solution are also negative (data not shown). Afterwards, a set of BSA/TPP mass ratios were adopted to obtain monodispersed BSA/TPP coacervate complexes. As shown in Figure 2.16, single nanoscaled BSA/TPP coacervates are already visible at BSA/TPP mass ratio 2/1. If the solution pH was tuned back to a neutral or basic pH value, this complex form redissolved into solution, but not in pure water. Thus, this BSA/TPP coacervate complex provided a possible way to more effective BSA encapsulation. As shown in Figure 2.15, a considerable amount of BSA is entrapped in subsurface layer of chitosan particles and able to diffuse out of particle quickly. Whereas, if BSA molecules were condensed as the particles core covered by a layer of polymer shell as shown in the right model, this diffusion course could be prolonged. Considering the electric state of BSA/TPP coacervate complex, an

anionic shell material e.g. alginate could be alterative.

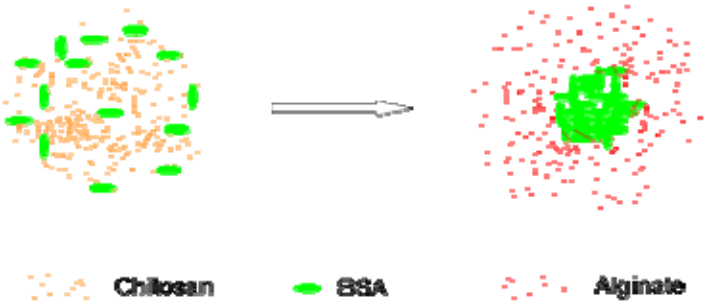

Fig. 2. 15 The Schematic of BSA Encapsulation Form by CSNPs.

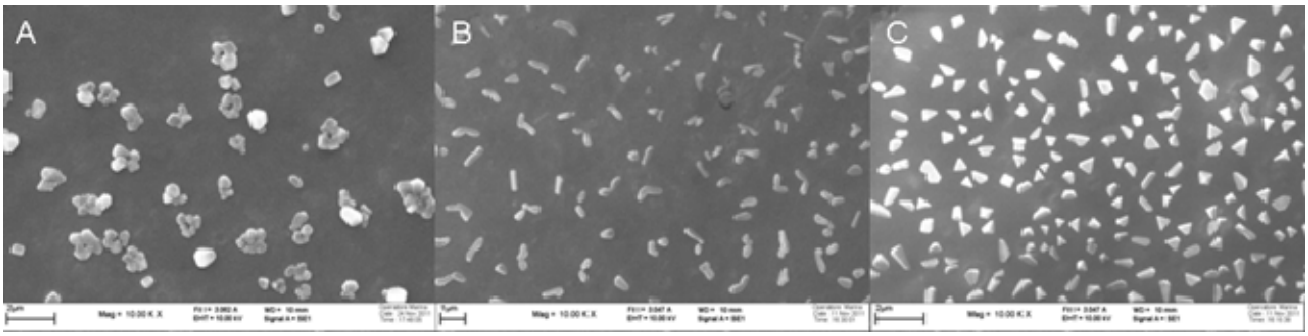

Fig. 2.16 The BSA/TPP Complex Formed at Low pH Value. The mass ratio of BSA/TPP of A), B), and C) is 2/1, 3/1, 5/1 respectively. Magnification: 10, 000X.

Chapter 3 Chitosan Microparticles for the Controlled Release of Proteins

3.1 Aim of the Study

In this section, CSMPs were prepared to realize prolonged and stable protein release based on conventional emulsification and coacervation method. Since particle size, homogeneity and surface morphology significantly affect the protein loading and release properties, a set of preparation parameters are systemically investigated to understand their effects on these features. On the purpose to overcome the serious aggregation problem encountered in the preparation of TPP-gelated CSMPs, a microemulsion of TPP as gelation reagent are proposed. The final goal of this section is aimed to load CSMPs into bioengineering scaffolds to achieve the extended and stable release of tissue growth factors. However, organic solvents, rigorous shear forces result from homogenization used in this conventional method could compromise the bioactivity of protein molecules. Therefore, CSNPs formulated in chapter 1 are proposed to be used to encapsulate proteins due to their mold preparation conditions. Afterwards, these protein-incorporated CSNPs were intended to be encapsulated into microparticles (MPs) in which chitosan or polylactic acid would be used as particles matrix. A set of porous chitosan scaffolds are prepared by freeze-drying of chitosan hydrogel (pre-gelled with dibasic sodium phosphate at 37°C).

3.2 Materials and Methods

3.2.1 Materials

Low molecular weight chitosan (product code: 448869) with a deacetylation degree (DD) of 75-85% and viscosity of 20-300 cP (1% in 1% acetic acid), medium molecular weight chitosan (448877) with a DD of 75-85% and viscosity of 200-800 cP (1% in 1% acetic acid) were ordered from Sigma. The molecular weight is approximately 50,000-190,000 /190,000-310,000 Da for low/medium molecular weight chitosan based on viscosity. Octane, Span 85, Tween 80, Na_2SO_4, Fluorescein isothiocyanate (FITC) isomer I, dibasic sodium phosphate, and other reagent grade chemicals were supplied by Sigma. The information on other materials can be found in section 2.2.1.

3.2.2 Instruments

Homogenizer (ULTRA-TURRAX T.25 BASIC) was purchased from IKA Corporation. Fluorescence spectrometer is the product of Perkin Elmer Corporation. Fluorescence microscope (Axiovert 40) is the product of Zeiss Corporation. The information of other instruments could be found in section 2.2.2.

3.2.3 Methods

Preparation of Chitosan Microparticles

Chitosan microparticles (CSMPs) were prepared according to an emulsification and ionotropic gelation method adopted by L. Y. Lim et al. [135] with some modification. In brief, low/medium molecular weight chitosan was completely dissolved in water containing 1% (v/v) acetic acid to a concentration of 2% (m/v). Two milliliters of a chitosan solution were added into 20ml octane containing 4% Span 85 as emulsifier under constant homogenization at 5 Krpm for 5 min to get a homogeneous emulsion. Then 2ml 1 M NaOH solution was added to resulting emulsion with extended homogenization for 10 min. In order to study the influence of preparation conditions on the formation of CSMPs, various parameters such as concentration of chitosan, BSA, Span 85, stirring rate etc. were applied, meanwhile, the other parameters were fixed (for section 3.3.1-3.3.4, the preparation parameters of CSMPs were presented in Table 3.1). The resulting particles suspension was centrifugation at 3000 rpm for 10 min at room temperature. After discarding the supernatant, particles sediment was washed repeatedly by acetone to remove the residual octane solvent. This washing step was repeated with water to remove residual salts. Finally, the obtained CSMPs were vacuuming dried at room temperature.

Table 3.1 Preparation Parameters of Chitosan Microparticles.

Sample Code	Chitosan Concentration (%)	w/o Volume Ratio	Span 85 Concentration (%)	Homogenization Speed (Krpm)	Times of Addition[1]	Coacervation Agent	Emulsifier	Chitosan Molecular Weight	BSA Incorporation (%)
A	1	2/10	4	5	3	NaOH	Span 85	LMW	0
B	2	2/10	4	5	3	NaOH	Span 85	LMW	0

C	3	2/10	4	5	3	NaOH	Span 85	LMW	0
D	2	1/10	4	5	3	NaOH	Span 85	LMW	0
E	2	3/10	4	5	3	NaOH	Span 85	LMW	0
F	2	2/10	2	5	3	NaOH	Span 85	LMW	0
G	2	2/10	6	5	3	NaOH	Span 85	LMW	0
H	2	2/10	4	8	3	NaOH	Span 85	LMW	0
I	2	2/10	4	10	3	NaOH	Span 85	LMW	0
J	2	2/10	4	5	1	NaOH	Span 85	LMW	0
K	2	2/10	4	5	5	NaOH	Span 85	LMW	0
L	2	2/10	4	5	3	Na_2SO4	Span 85	LMW	0
M	2	2/10	4	5	3	TPP	Span 85	LMW	0
N	2	2/10	4	5	3	NaOH	T+S[2]	LMW	0
O	2	2/10	4	5	3	NaOH	S+S[3]	LMW	0
P	2	2/10	4	5	3	NaOH	Span 85	MMW	0
Q	2	2/10	4	5	3	NaOH	Span 85	LMW	0.5
R	2	2/10	4	5	3	NaOH	Span 85	LMW	1
S	2	2/10	4	5	3	NaOH	Span 85	LMW	2

1. Adding the same volume of NaOH in 10 min. 2. 4% Tween 80 in chitosan solution. 3. Span 80/Span 85=1/1 (v/v).

Particle Size Measurement and Morphology Observation of CSMPs

Fresh-made CSMPs was resuspended in acetone to dehydrate. Then one drop of CSMPs suspension was deposited on carbon stub followed by coating with gold before SEM observation. SEM

microphotographs were taken at magnification of 300X, 500X, 1000K to check mondispersity and 5000X to study the surface morphology of CSMPs. Particle size analysis was performed using a image analysis software Image-Pro Plus 6.0 (version 6.0.0.260, Media Cybernics, Inc.). 50~90 particles were measured for every sample (as a example, see Fig. 3.1), then the size data was analyzed using Excel.

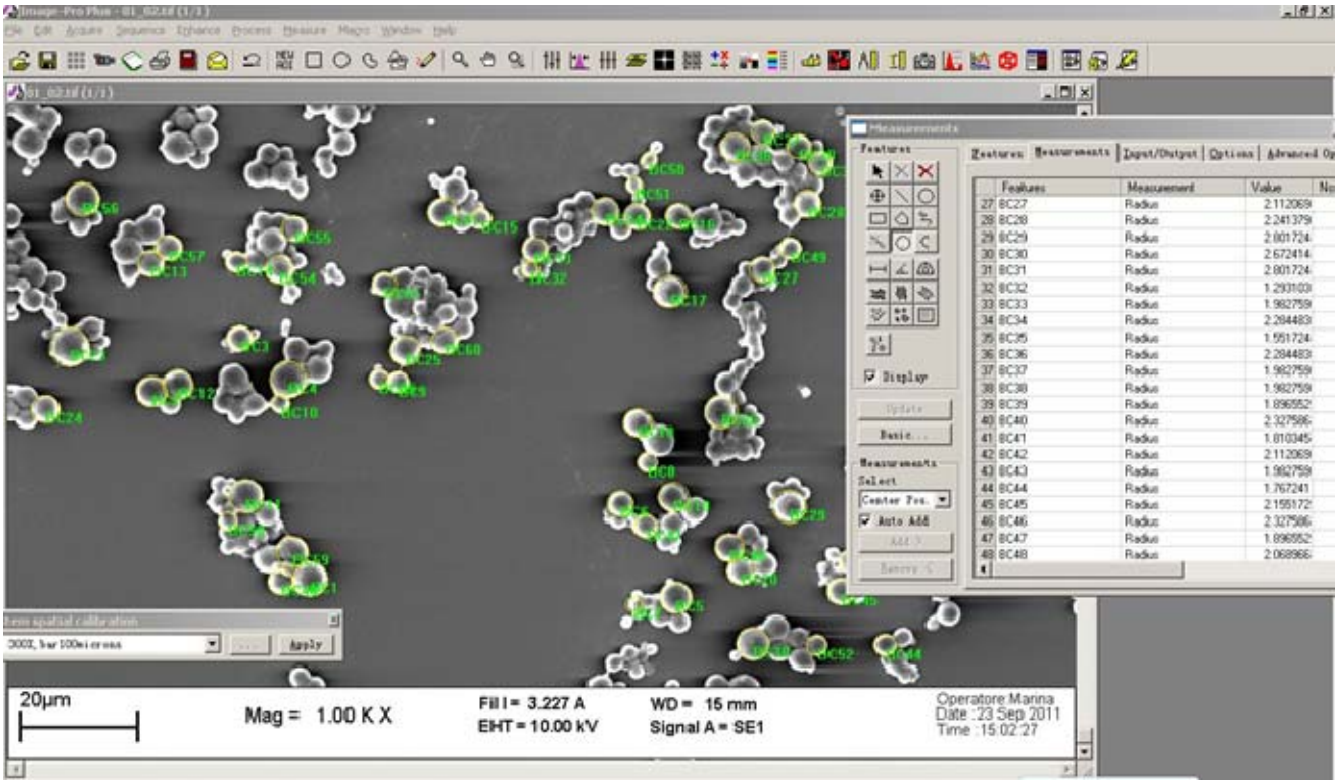

Fig. 3.1 CSMPs Particle Size Analysis by Image Analysis Software. Software: Image-Pro Plus 6.0 (version 6.0.0.260, Media Cybernics, Inc.). Sample: Sample A in Table 3.1.

Preparation of TPP-gelated CSMPs

The preparation of chitosan emulsion was prepared by the same way as that of NaOH-gelated CSMPs. 10% TPP solution was prepared followed by tuning the pH value to 2. 2 ml of this TPP solution was added into 20 ml octane containing 2% Span 85 with homogenization at 15 Krpm for 5 min to form TPP microemulsion. Then specified amount of this TPP microemulsion was added into chitosan emulsion prepared before with continuous homogenization at 5 Krpm for 10 min. The mixed emulsion was standed for 4 hours. The resulting microparticles were collected by centrifugation at 3000 rpm for 10min. Then the obtained particles were washed by acetone and water repeatedly to remove residual octane and TPP followed by vacuuming dried at room temperature.

Fluorescence Labeling of CSNPs

CSNPs/BSA-CSNPs were prepared according to section 2.2.3 with chitosan hydrochloride. The main preparation parameters are as follows: CSCL concentration 2mg/ml, CS/TPP mass ratio 5/1, BSA concentration 0.5 mg/ml, total reaction solution volume 98 ml, and stirring speed 600 rpm. The fluorescence labeling of CSNPs was performed according to the method Zhao et al. [136] described previously. Briefly, 0.4 mg of freeze-dried CSNPs was resuspended in 5 ml DMSO followed by the addition of 0.5 ml 0.1 M NaOH solution. Then FITC was dissolved in DMSO at 10.0 mg/ml concentration, and was slowly added to the suspension of CSNPs. The reaction between the isothiocyanate groups of FITC and the amino groups of D-glucosamine residue on chitosan was allowed to proceed for 10 hours in the dark at room temperature. FITC-labeled chitosan nanoparticles were centrifugated and washed with DMSO several times until the free FITC could not be detected in the supernatant by fluorescence spectrophotometer.

Preparation of CSNPs-incorporated CS/PLA-MPs

For the preparation of CSNPs-incorporated chitosan microparticles (CSNPs-CSMPs), 4 mg CSNPs/BSA-CSNPs were completely resuspended in 2 ml 2% chitosan hydrochloride solution by homogenization. This suspension was then added to 20 ml octane containing 2% Span 85 with continuous homogenization at 5 Krpm for 5 min. Afterwords, 2 ml 1 M NaOH solution was added to gelate microparticles under extended homogenization for 10 min. The resulting microparticles were collected by centrifugation at 3,000rpm for 10 min, repeatedly washed by acetone and water, and finally vacuuming dried at room temperature. For verifying the successful incorporation of CSNPs, the FITC-labeled BSA-CSNPs were incorporated into CSMPs.

For the preparation of CSNPs-incorporated PLA microparticles (CSNPs-PLAMPs), a double s/o/w emulsification method was used. In brief, 8 mg CSNPs/BSA-CSNPs was collected by centrifuging the particles suspension. Then the obtained humid particles pellet was resuspended in 4ml dichloromethane containing 1% PLA and 1% Span 85 by homogenization at 15 Krpm to form the first emulsion. Then this emulsion was added into 20 ml 4% PVA under homogenization at 5 Krpm for 10 min. The resulting suspension was stirred overnight to evaporate solvent. After being collected by centrifugation, repeated washing with 0.1% PVA and water, the resulting particles were vacuum dried at room temperature.

Preparation of Chitosan Scaffold

The wide pore spongy chitosan scaffold was prepared according to the method adopted by B. Yang et al. [137]. Low/medium molecular weight Chitosan was dissolved in 0.5% acetic acid solution under continuous stirring for 48 h at room temperature. The resulting solution was filtered and stored at 4°C for further use. Autogelling solutions were prepared by adding dropwise 0.8 ml dibasic sodium phosphate (500 mg/ml) into 8 ml chitosan solution underwent continuous stirring in ice bath. Finally, the autogelling solutions were transferred into 24-well plate (2 ml per well) and incubated at 37°C overnight to obtain a chitosan hydrogel. The obtained chitosan hydrogel was stored in a refrigerator at -80 °C for 24 h and lyophilized in a freeze dryer for 48 h. A series of chitosan scaffolds were obtained with various chitosan molecular weight and concentration. The three-dimensional morphology of chitosan scaffold was recorded with a digital camera.

3.3 Results and Discussion

3.3.1 The Effect of Chitosan Dispersed Phase on the Formation of CSMPs

The Effect of Chitosan Molecular Weight on the Formation of CSMPs

Low molecular weight (LMWCS, 50~190KDa, 20-300 cP) and medium molecular weight chitosan (MMWCS, 190~310KDa, 200-800 cP) were used to prepare chitosan microparticles to study the effect of molecular weight on the formation of CSMPs. The mean diameter (calculated by number) of CSMPs prepared with LMWCS/MMWCS is 9.4±1.9 and13.6±10.5μm respectively. However, the mean diameter does not cover the size feature of the later due to its wide size distribution (see Figure 3.4P). A big number of small particles coexist along with few big particles in sample P, which is also evidenced on Figure 3.2P. The viscosity of dispersed phase significantly affects the particle size of emulsion droplets and the lower the viscosity of dispersed phase the smaller the size of emulsion droplets [135]. Thus, MMWCS with a higher viscosity compared with LMWCS forms CSMPs with bigger size. The size distribution of CSMPs depends on the energy distribution throughout the mixing vessel and the turbulence induced by high stirring speed gives the emulsion droplet a wider size distribution [135]. We speculate that the energy distribution in MMWCS emulsion system is less homogeneous than that in LMWCS emulsion system since bigger particles formed with MMWCS result in more turbulence, then wider size distribution. Deformed (Appendix 5) and hollow big particles (Figure 3.2P) were found in sample P which prepared with MMWCS. Besides, some smaller particles are embedded onto big particles (Figure 3.2P& Figure 3.3P). These probably because high viscosity of MMWCS dispersed

phase hinders or slows down the diffusion of gelation agent. Consequently less gelation occurs to interior matrix. Thereby, these big particles formed with MMWCS show weak mechanic strength.

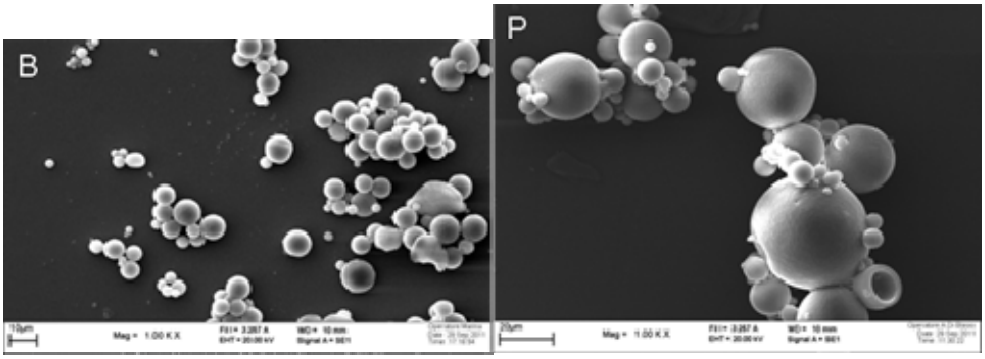

Fig. 3.2 SEM Photographs of CSMPs Prepared with Different Molecular Weight. B, low molecular weight (Sigma, product code: 448869) B, medium molecular weight (Sigma, product code: 448877) P. Magnification: 1000X. Scale Bar represents 10μm in B and 20 μm in P.

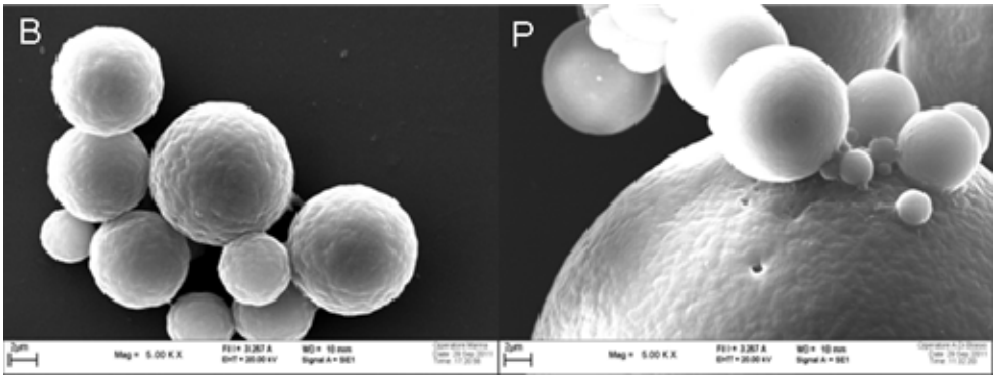

Fig. 3.3 The Surface Morphology of CSMPs Prepared with Different Molecular Weight. B, low molecular weight (Sigma, product code: 448869) P, medium molecular weight (Sigma, product code: 448877). Magnification: 5000X. Scale Bars represent 2μm.

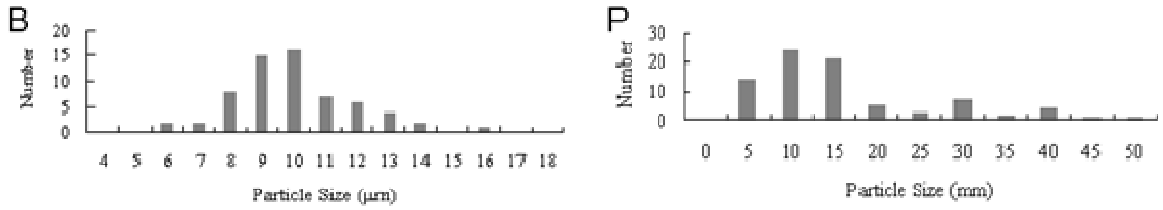

Fig. 3.4 Particle Size Distribution of CSMPs Prepared with Different Molecular Weight. B, low molecular weigh (Sigma, product code: 448869), P, medium molecular weight (Sigma, product code: 448877).

The Effect of Chitosan Concentration on the Formation of CSMPs

CSMPs were prepared with varying chitosan concentrations to study the effect of chitosan concentration on the formation of CSNPs. Figure 3.5 shows that particle size of CSMPs increases with

increasing chitosan concentration. Because the lower the viscosity of chitosan dispersed phase the smaller the chitosan emulsion droplets and the lower the chitosan concentration the lower the viscosity of chitosan dispersed phase, so chitosan aqueous phase with lower concentration is prone to form smaller emulsion droplet. Eventually CSMPs with smaller size form at the low chitosan concentration. This trend is also confirmed by the size analysis with software (see Figure 3.7). The particle size ranges of CSMPs are 3~7, 6~14, 10~50 μm and mean diameters are 4.3±0.9, 9.4±1.9, 20.1±7.1 μm with respect to 1%, 2% and 3% (m/v) chitosan respectively. Besides, particle size shows wider size distribution at high chitosan concentration. With 3% chitosan, smaller particles form compared with the concentration 1% and 2%. As discussed above, this wide size distribution effect of high chitosan concentration probably is contributing to the energy distribution in the emulsion system which is affected by turbulence. Nevertheless, big particles forming with high chitosan concentration are able to result in more turbulence than the small particles do. On the other hand, with 1% chitosan, fusion of particles appears. With the 1 % chitosan solution, the dispersed chitosan droplets in octane had a low chitosan volume, resulting in weak microparticles upon interaction with NaOH because of the relatively thin wall of gelled chitosan. Collision of the particles with each other may cause tearing at the point of contact on the weak wall, resulting in the fusion of ungelled material between the particles [135]. All the three CSMPs show smooth surface as seen in Figure 3.6.

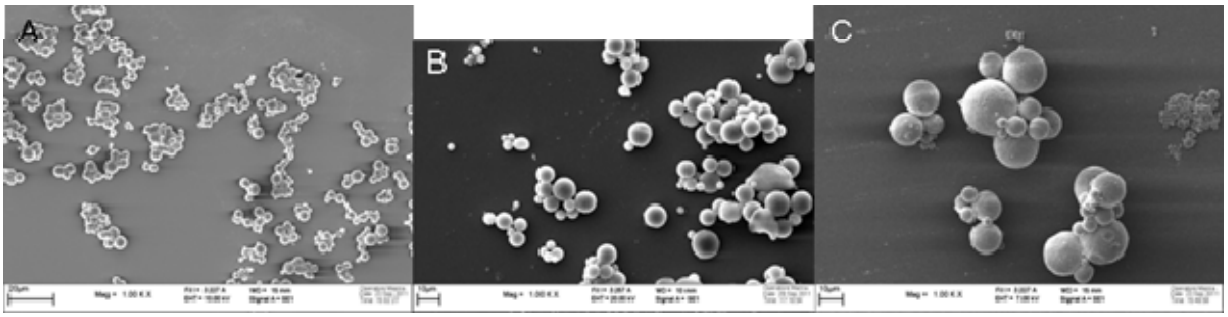

Fig. 3.5 SEM Photographs of CSMPs Prepared with Different Chitosan Concentration. A, 1%, B, 2%, C, 3%. Magnification: 1000X. Scale Bar represents 20μm in A and 10 μm in B and C.

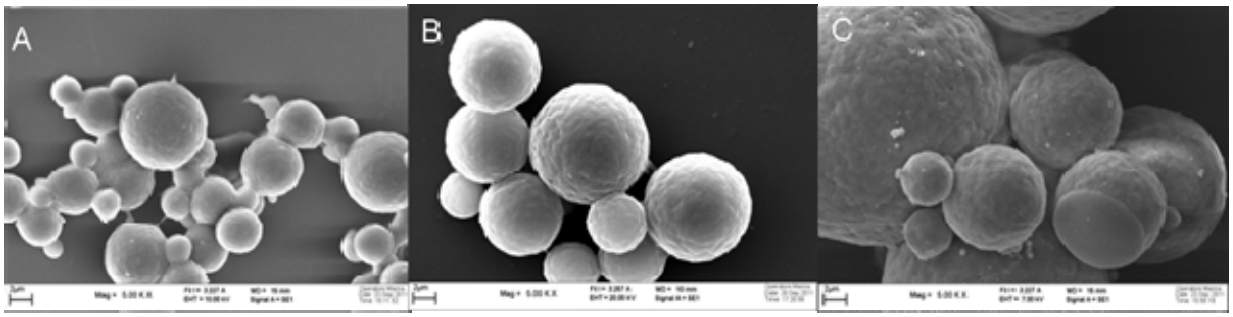

Fig. 3.6 The Surface Morphology of CSMPs Prepared with Different Chitosan Concentration. A, 1%, B, 2%, C, 3%. Magnification: 5000X. Scale Bars represent 2μm.

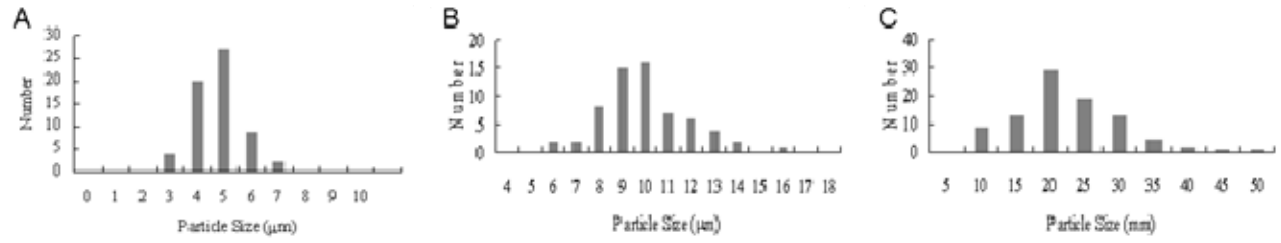

Fig. 3.7 Particle Size Distribution of CSMPs Prepared with Different Chitosan Concentration. A, 1%, B, 2%, C, 3%.

3.3.2 The Effect of Emulsification Parameters on the Formation of CSMPs

The Effect of w/o Volume Ratio on the Formation of CSMPs

The mean diameter of CSMPs prepared with varying w/o volume ratio at 1/10, 2/10 and 3/10 is 8.1±2.3, 9.4±1.9 and 9.2±2.3μm respectively. The size distribution shows no obvious change as the increasing w/o volume ratio and the size of most particles is in the range of 3~17μm (see Figure 3.10). However, w/o volume ratio influences the surface morphology of CSMPs. Rough surface (Figure 3.9) and deformed particles (Appendix 6) were found in sample D which was obtianed with low w/o volume ratio. This effect probably results from the relative big ratio of surfactant to chitosan dispersed phase in sample D with 1/10 w/o volume ratio compared with sample B 2/10 and sample E 3/10. Thus, excess of surfactant dramatically reduces the interfacial tension between oil and water phase and consequently results in irregular shape or rough surface of particles.

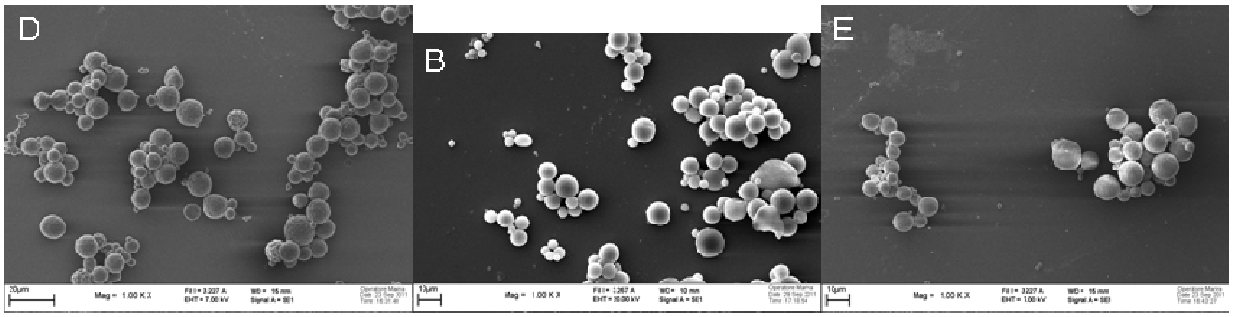

Fig. 3.8 SEM Photographs of CSMPs Prepared with Different w/o Volume Ratio. D, 1/10, B, 2/10, E, 3/10. Magnification: 1000X. Scale Bar represents 10μm in D and B, 10 μm in E.

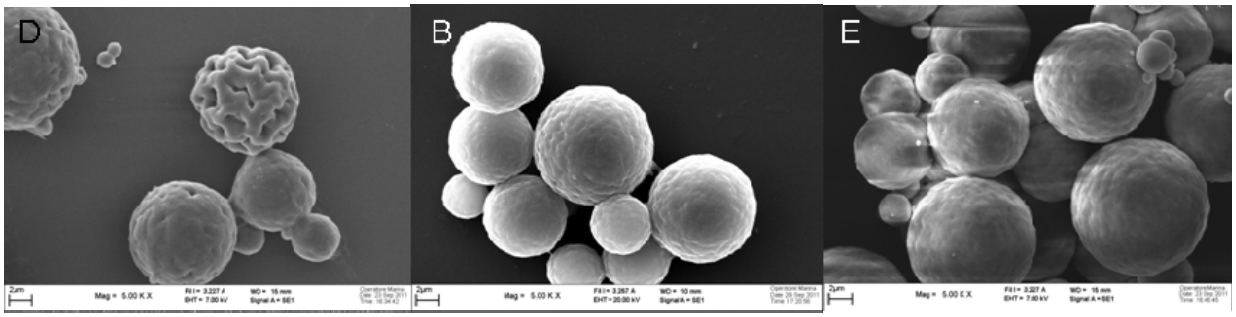

Fig. 3.9 The Surface Morphology of CSMPs Prepared with Different w/o Volume Ratio. D, 1/10, B, 2/10, E, 3/10. Magnification: 5000X. Scale Bars represent 2μm.

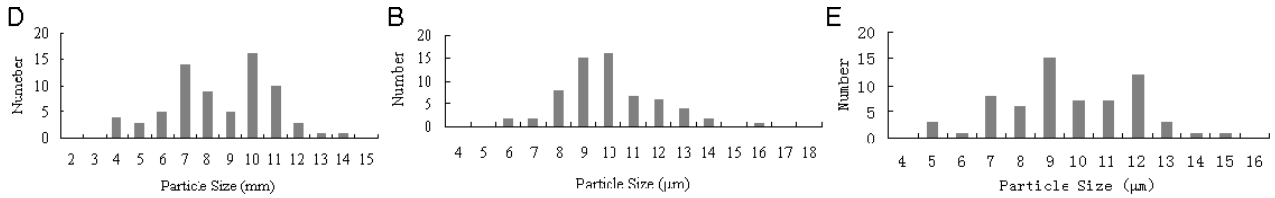

Fig. 3.10 Particle Size Distribution of CSMPs Prepared with Different w/o Volume Ratio. D, 1/10, B, 2/10, E, 3/10.

The Influence of Emulsifier on the Formation of CSMPs

In this section we studied the effect of various emulsifiers on the formation of CSMPs. Single surfactant or the combination of two surfactants are used. The mean diameter of Sample B with only Span 85 as emulsifier, Sample N with 2% Span 80 and 2% Span 85 in continuous phase, Sample O with 2% Tween 80 in chitosan dispersed phase and 2% Span 85 in continuous phase is 9.4±1.9, 6.5±2.4 and 6.6±2.5μm respectively. The addition of Tween 80 in the dispersed phase results in the reduction of particle size and wide size distribution (see Figure 3.13N) compared with Sample B only with Span 85 as emusifier. Tween 80 is not effective in boosting the emulsion stability, on the contrary, much fusion of particles and rough particle surface appear (see Figure 3.12N). For the surfactants combination of Span 80 and Span 85 in Sample O, the particles size is reduced but smaller particles appear compared to Sample B (see Figure 3.13O). The particle surface of Sample O is smooth (see Figure 3.12N). Span 80 is also a hydrophobic surfactant but with higher Hydrophile-Lipophile Balance Number (HLB) compared with Span 85. The higher the HLB number the more hydrophilic the surfactant is. Thus, the combination of Span 80 and Span 85 with a higher HBL number reduces particle size.

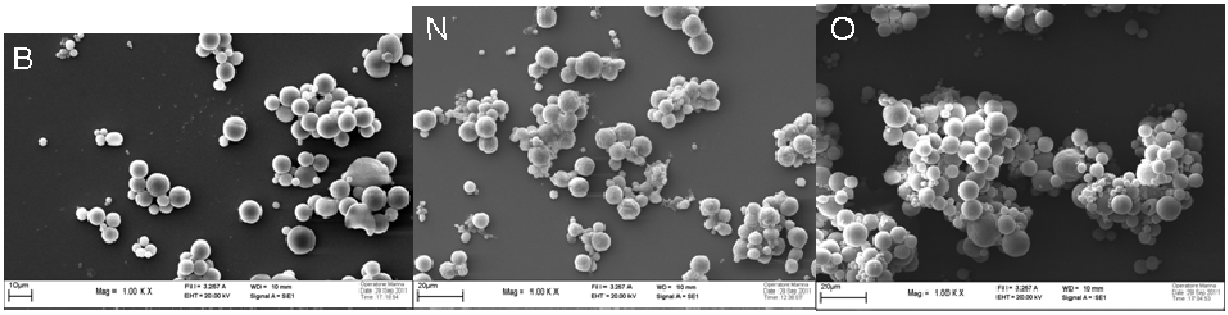

Fig. 3.11 SEM Photographs of CSMPs Prepared at Different Emulsifier Combinations. B, Span 85, N, 4%Tween 85 in chitosan solution, O, 2% Span 80+2% Span 85. Magnification: 1000X. Scale Bar represents 10μm in B and 20 μm in N and O.

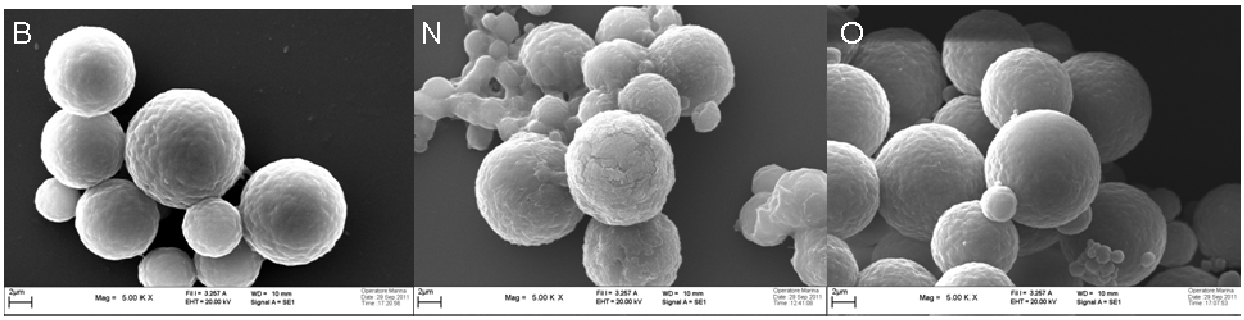

Fig. 3.12 The Surface Morphology of CSMPs Prepared with Different Emulsifier Combinations. B, Span 85, N, 4%Tween 85 in chitosan solution, O, 2% Span 80+2% Span 85. Magnification: 5000X. Scale Bars represent 2μm.

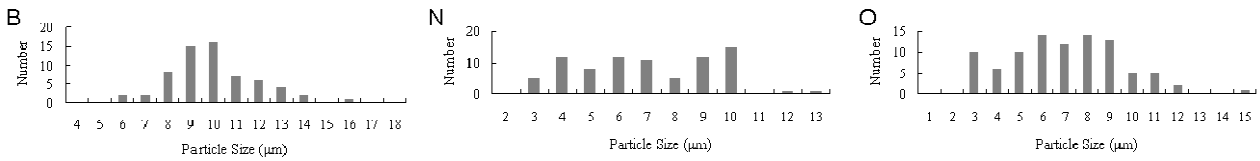

Fig. 3.13 Particle Size Distribution of CSMPs Prepared with Different Emulsifier Combinations. B, Span 85, N, 4%Tween 85 in chitosan solution, O, 2% Span 80+2% Span 85.

The Effect of Emulsifier Concentration on the Formation of CSMPs

The mean diameter of CSNPs prepared with varying Span 85 concentration of 2%, 4% and 6% is 9.9±2.6, 9.4±1.9, 6.3±2.8μm respectively. All the three CSMPs show good size distribution (see Figure 3.14 and 3.16). The particle size of CSMPs decreases with increasing Span 85 concentration. This result is probably due to high surfactant concentration, which reduces the interfacial tension at the interface between dispersed phase and continuous phase and thus particles with small size form. However, when the surfactant concentration is too high, for example Sample G prepared with 6% Span 85, some collapsed and deformed particles appear (Figure 3.14G). All the three CSMPs show a smooth

surface (Figure 3.15).

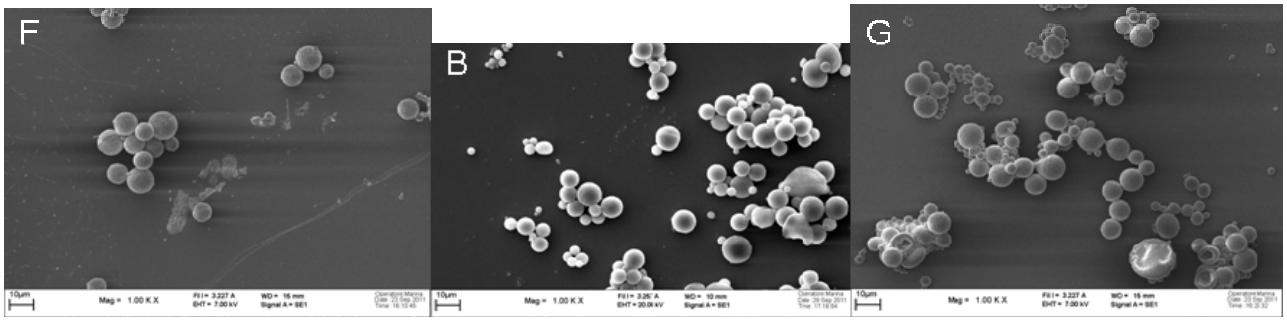

Fig. 3.14 SEM Photographs of CSMPs Prepared with Different Span 85 Concentration. F, 2%, B, 4%, G, 6%. Magnification: 1000X. Scale Bars represent 10μm.

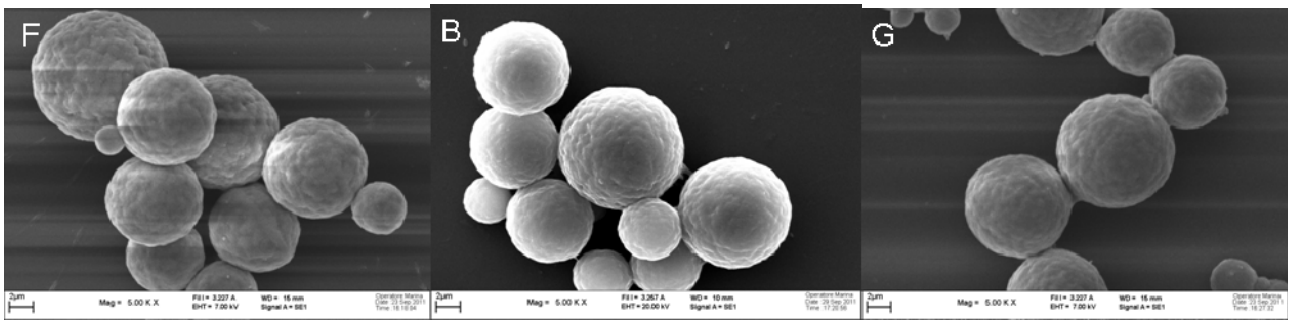

Fig. 3.15 The Surface Morphology of CSMPs Prepared with Different Span 85 Concentration. F, 2%, B, 4%, G, 6%. Magnification: 5000X. Scale Bars represent 2μm.

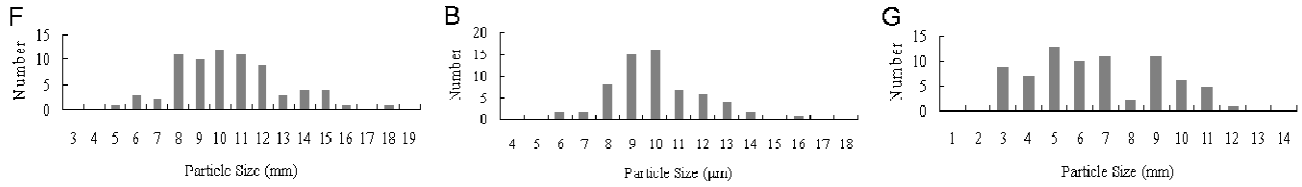

Fig. 3.16 Particle Size Distribution of CSMPs Prepared with Different Span 85 Concentration. F, 2%, B, 4%, G, 6%.

The Effect of Homogenization Speed on the Formation of CSMPs

CSMPs prepared with homogenization speed at 5, 8, 10 Krpm show a mean diameter of 9.4±1.9, 5.0±1.5, and 3.5±1.2μm respectively. High homogenization speed e.g. Sample H and I with 8 and 10 Krpm give a slightly wider size distribution compared with Sample B with 5 Krpm. The particle size of CSMPs decreases with increasing homogenization speed. This probably results from high shear force at high homogenization speed tears the dispersed phase into small emulsion droplets. As discussed above, high stirring speed results in turbulences and these turbulences induce the heterogeneous energy

distribution in emulsion system and eventually particles with wide size distribution form [138]. However, very high stirring speed results in vigorous collision between particles. Therefore, it is unfavorable for the formation of regular-shaped particles. As shown in Figure 3.18, with homogenization speed at 5 Krpm, Sample B shows very spherical appearance. Increasing the speed to 8 Krpm (Sample H) some particles start to lose the spherical appearance (Figure 3.18H) and become ellipsoidal, irregularly shaped (Figure 3.17H). When the speed is increased to 10 Krpm, fusion between particles appears (Figure 3.18I).

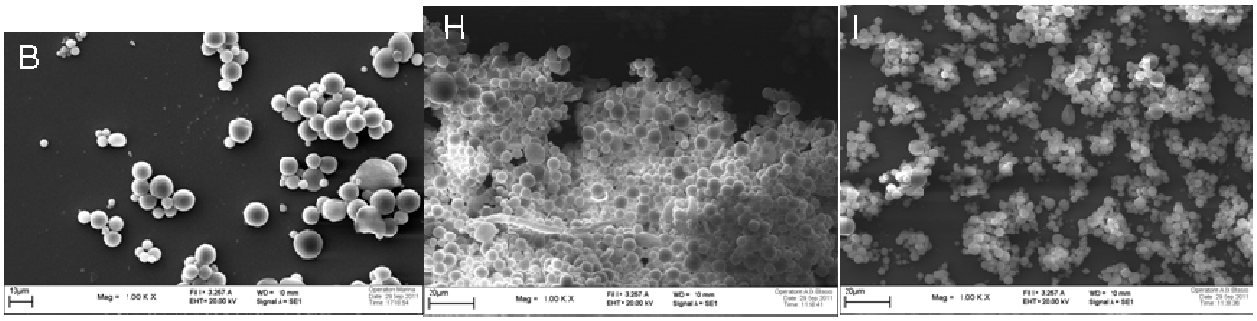

Fig. 3.17 SEM Photographs of CSMPs Prepared with Different Homogenization Speed. B, 5000 rpm, H, 8000 rpm, I, 10000 rpm. Magnification: 1000X. Scale Bar represents 10μm in B and 20 μm in H and I.

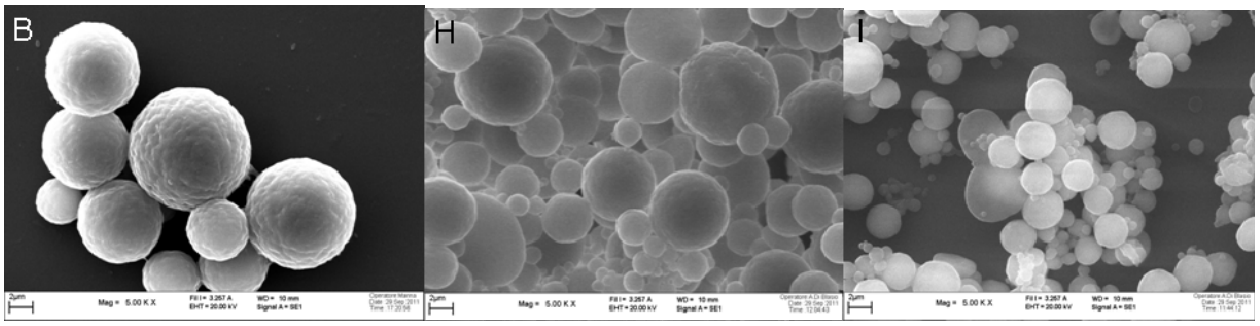

Fig. 3.18 The Surface Morphology of CSMPs Prepared with Different Homogenization Speed. B, 5000 rpm, H, 8000 rpm, I, 10000 rpm. Magnification: 5000X. Scale Bars represent 2μm.

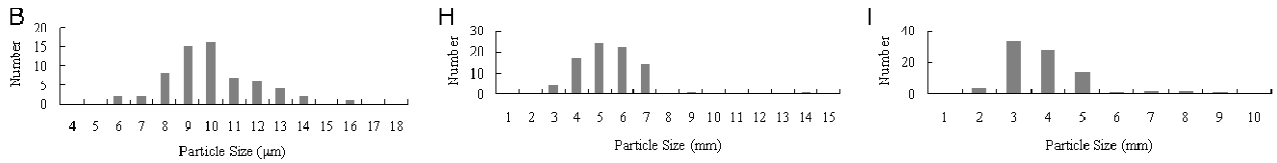

Fig. 3.19 Particle Size Distribution of CSMPs Prepared with Different Homogenization Speed. B, 5000 rpm, H, 8000 rpm, I, 10000 rpm.

3.3.3 The Influence of Coacervation Agents on the Formation of CSMPs

The Influence of Coacervation Agents on the Formation of CSMPs

In this section, NaOH, Na_2SO_4, and TPP were used as gelling agents to study their influence on the formation of CSMPs. However, when TPP was added to gelate chitosan emulsions, a big amount of aggregates formed and could not be redispersed (Sample M in Table 3.1). Aggregation also occurred when Na_2SO_4 was used as coacervation agent of CSMPs (Figure 3.20L). Particle surface observation indicates that fusion between particles is present throughout the whole Sample L (Figure 3.20L). We speculate that different formation mechanisms of particles may be underneath the gelation process with different coacervation agents, since hydroxyl ion is a monovalent anion, whereas sulfate and tripolyphosphic ions are multivalent anions. The gelation of chitosan emulsion droplets induced by OH^- results from the deprotonation of primary amino groups on chitosan chains. Na_2SO_4, and TPP induce the gelation of chitosan emulsion droplets via the formation of ionic linkages between SO_4^{2-}/$P_3O_{10}^{5-}$ and amino groups on chitosan chains. Thus, residual OH^- ions are not able to make the already gelated chitosan particles undergo further aggregation or fusion unless the CSMPs are not completely gelated which sometimes occurs to the non-gelated interior matrix of CSMPs. Nevertheless, multivalent anions- SO_4^{2-}/$P_3O_{10}^{5-}$, are able to react with already formed CSMPs and then aggregation or fusion of particles occurs.

The mean diameter of CSMPs gelated by NaOH and Na_2SO_4 is 9.4±1.9 and 9.1±2.1 μm respectively. The CSMPs gelated by NaOH and Na_2SO_4 show similar size and size distribution (Figure 3.22).

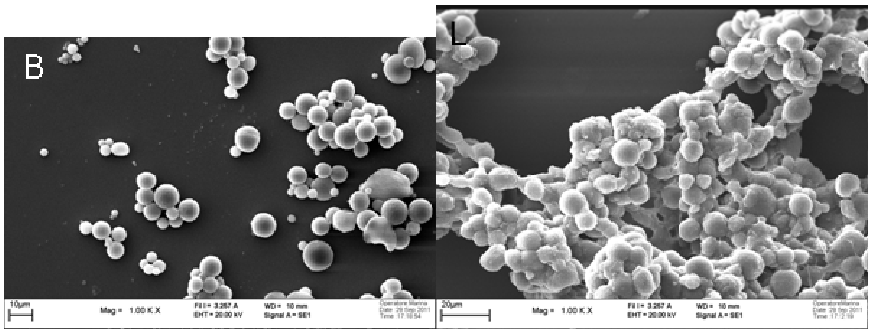

Fig. 3.20 SEM Photographs of CSMPs Prepared with Different Coacervation Agents. A, NaOH, B, Na_2SO_4. Magnification: 1000X. Scale Bar represents 10μm in B and 20 μm in L.

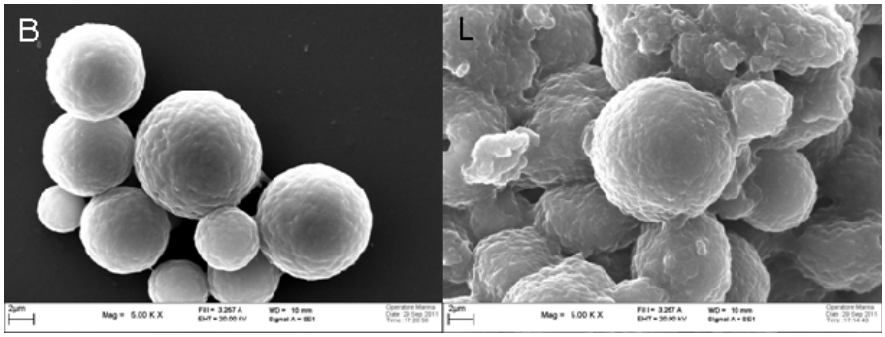

Fig. 3.21 The Surface Morphology of CSMPs Prepared with Different Coacervation Agents. B, NaOH, L, Na_2SO_4. Magnification: 5000X. Scale Bars represent 2μm.

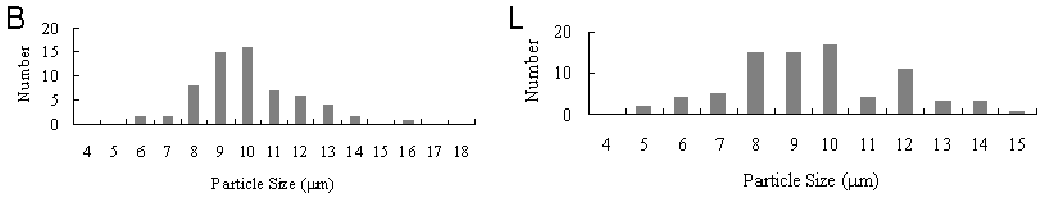

Fig. 3.22 Particle Size Distribution of CSMPs Prepared with Different Coacervation Agents. B, NaOH, L, Na_2SO_4.

The Influence of NaOH Adding Rate on the Formation of CSMPs

The addition of NaOH solution destabilizes the chitosan emulsion. In order to reduce this unfavorable effect, the addition rate of NaOH was studied. In 10 min, 2 ml 1 M NaOH solution was added all at once, 2/3 ml every 3 min and 2/5 ml every 2 min to chitosan emulsion system to prepare CSMPs. The mean diameter of obtained CSMPs is 6.4±2.3, 9.4±1.9, 6.3±2.2 μm respectively. In comparison with Sample B which is obtained by adding NaOH in 3 times, both Sample J in 1 time and Sample K in 5 times show wider size distribution (Figure 3.25). Figure 3.23 indicates that Sample B is the most discrete sample in the 3 samples. Figure 3.24 shows the surface morphology of these 3 samples. For Sample J in which NaOH was added all at once, much fusion of particles are found. For Sample K in which NaOH was added 0.4ml per 2 min, all particles are irregularly shaped and show a rough surface. These indicate that neither too fast nor too slow addition of coacervation agent-NaOH is favorable to get uniform and diepersedparticles. Therefore, the NaOH adding rate of Sample B is adopted for the preparation of all samples.

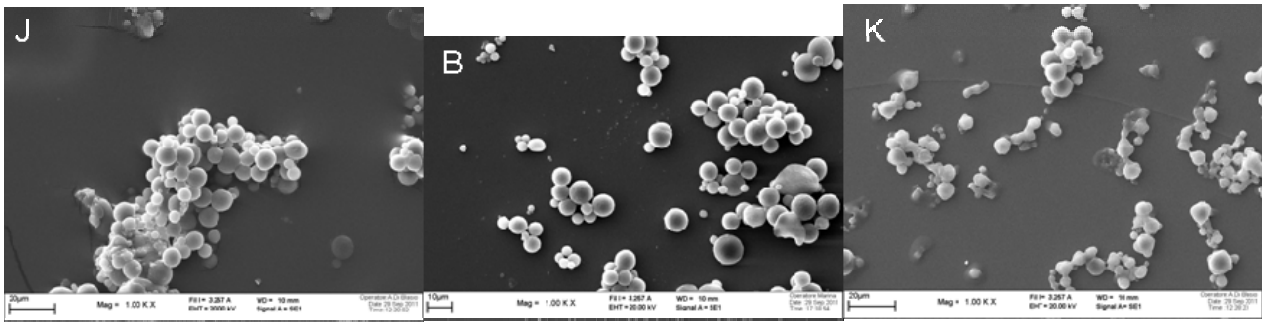

Fig. 3.23 SEM Photographs of CSMPs Prepared at Different NaOH Adding Rate. J, all at once in 10 min, B, 3 times in 10 min, K, 5 times in 10 min. The amount of NaOH solution was kept consistent. Magnification: 1000X. Scale Bar represents 10μm in B and 20 μm in J and K.

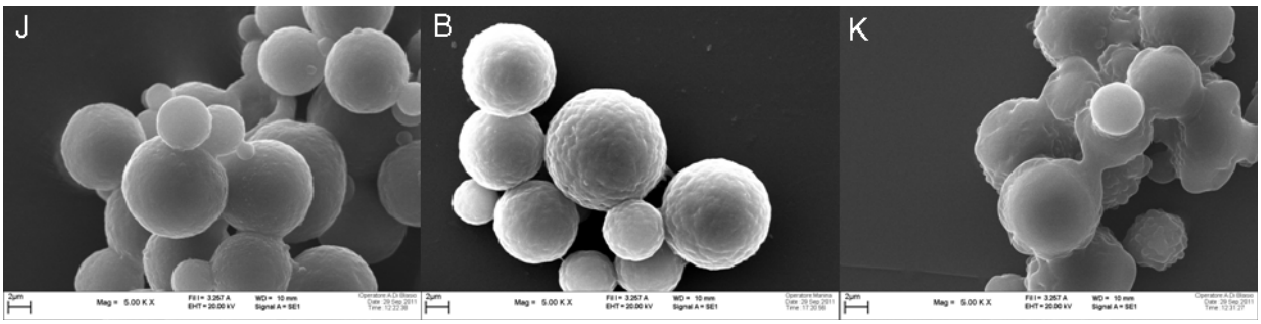

Fig. 3.24 The Surface Morphology of CSMPs Prepared with Different NaOH Adding Rate. J, 1 time in 10 min, B, 3 times in 10 min, K, 5 times in 10 min. Magnification: 5000X. Scale Bars represent 2μm.

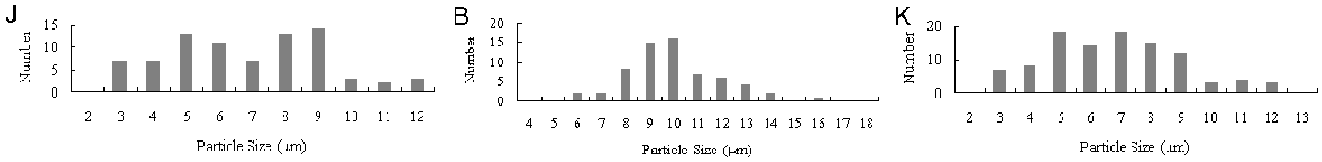

Fig. 3.25 Particle Size Distribution of CSMPs Prepared with Different NaOH Adding Rate. J, 1 time in 10 min, B, 3 times in 10 min, K, 5 times in 10 min.

3.3.4 The Influence of Protein Encapsulation on the Formation of CSMPs

The monodispersity and morphology significantly affect drug encapsulation and release. In turn, protein encapsulation also affects the monodispersity and morphology of particles. In this section, BSA with 3 concentrations-0.5%, 1%, 2% were incorporated into CSMPs to study the influence of protein encapsulation on the formation of CSMPs. As shown in Figure 3.26, only Sample Q with a BSA concentration of 0.5% shows dispersed appearance. When increasing BSA concentration from 0.5% to

1%, many ellipsoidal particles show up and all of particle form aggregates. When BSA concentration increases to 2%, particle size increases, but particles are still present as aggregates. Figure 3.27 indicates that there is no obvious difference in the surface morphology of blank CSMPs (Sample B) and 0.5% BSA-loaded CSMPs (Sample Q), but some cracked particles exist in the latter sample. As shown in Figure 3.28, Sample Q shows smaller particle size in mean diameter of 6.1±2.4 μm and wider size distribution compared with Sample B with a mean diameter of 9.4±1.9μm. The diameter of most particle are in a range of 8~13μm, 3~10μm, 5~11μm and 7~12μm for blank, 0.5%, 1% and 2% BSA-loaded CSMPs. Therefore, BSA encapsulation results in the decrease of particle size and increased size distribution.

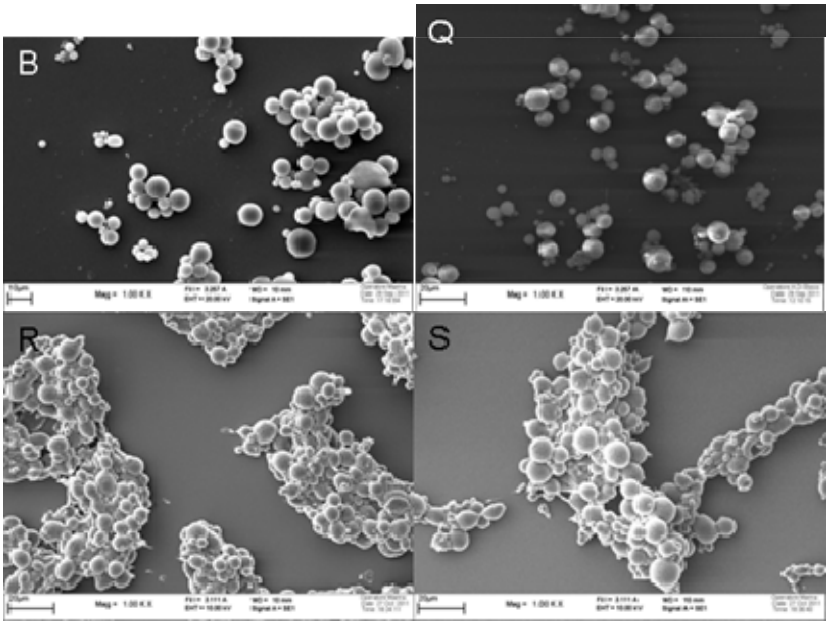

Fig. 3.26 SEM Photographs of CSMPs Prepared with Different BSA Loading Concentrations. B, 0%, Q, 0.5%, R, 1%, S, 2%.

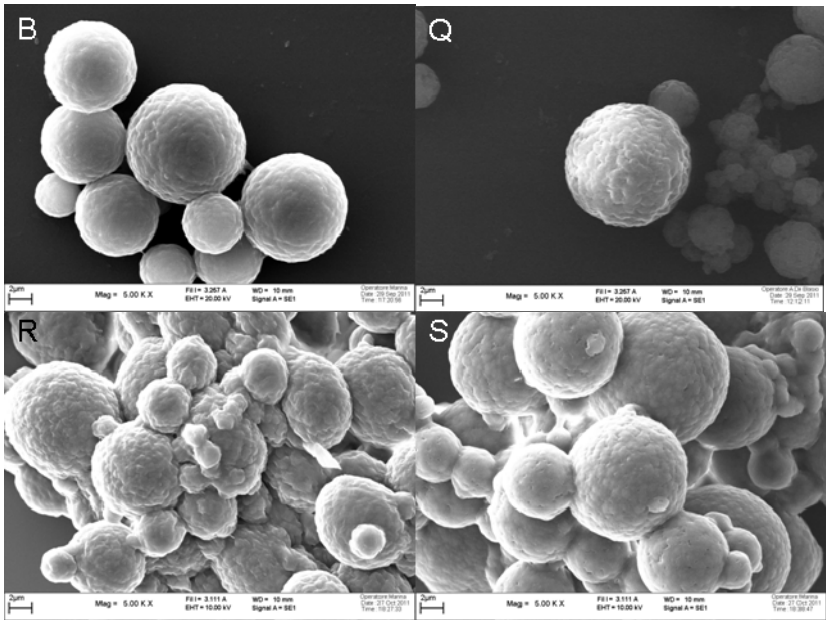

Fig. 3.27 The Surface Morphology of CSMPs Prepared with Different BSA Loading Concentrations. B, 0%, Q, 0.5%, R, 1%, S, 2%.

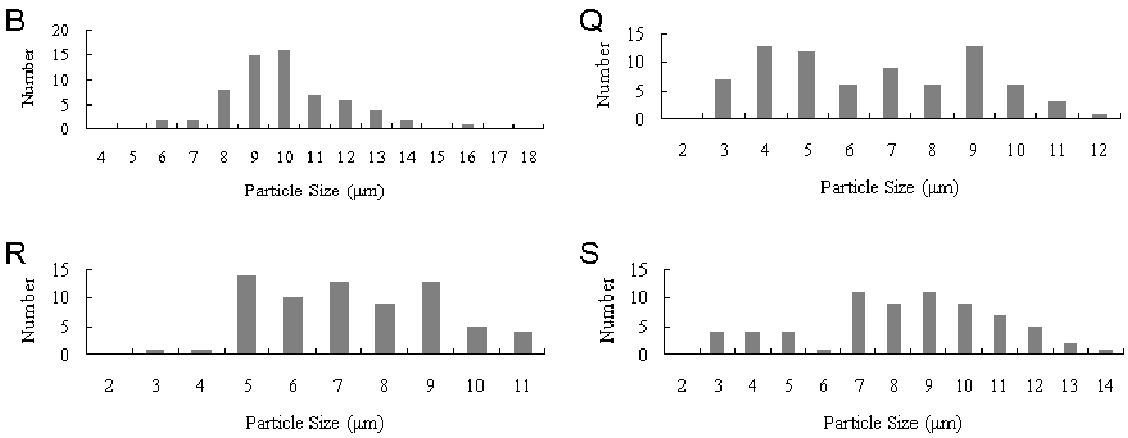

Fig. 3.28 Particle Size Distribution of CSMPs Prepared with Different Different BSA Loading Concentrations. A, 0%, B, 0.5%, C, 1%, D, 2%.

3.3.5 Optimization of the Preparation Condition of TPP Gelated CSMPs

The drug release kinetics of CSMPs coacervated by NaOH is different with that of TPP-gelated counterpart. The former releases entrapped drugs via swelling and erosion of particles. For the latter, the chitosan matrix gelated by TPP is the primary barrier on the diffusion route of the entrapped drug. The preparation of TPP-gelated CSMPs had the purpose to 1) avoid using NaOH as coacervation agent which may compromise the bioactivity of protein molecules, 2) compare the protein release property of

the two CSMPs to have more options when they are used in various practical applications. However, serious aggregation happened when TPP was used as particles coacervation agent based on the conventional emulsification-coacervation method (Sample M in Table 3.1). Previous literature also reported the same phenomenon [135, 138]. This probably results from the direct addition of TPP solution which destabilizes the chitosan emulsion. Previous investigations on chitosan microparticles usually use glutaraldehyde as crosslinker [139, 140]. Glutaraldeyhyde is a liposoluble crosslinker, therefore, it can diffuse into chitosan emulsion (w/o) droplets to cross-link the interior chitosan matrix. For this reason, usually small quantity of glutaraldehyde was added to the chitosan emulsion, thus, its influence on the emulsion stability is negligible. However, glutaraldehyde is toxic to human body, moreover it is also able to crosslink proteins since protein molecules are also rich in amino groups. For this reason, it is not suitable for our goal here in which chitosan microparticles are going to be used as protein carriers. Hereof, we proposed to prepare a microemulsion of TPP to gelate chitosan emulsion without disturbing emulsion stability (see the schematic in Figue 3.29).

The preliminary experiment showed dispersed CSMPs were obtained (Figure 3.30). At the CS/TPP mass ratio 1/2 (Figure 3.30A) and 3/2(Figure 3.30B), only few microparticles form along with a big number of small particles. At the CS/TPP mass ratio 3/1 (Figure 3.30C), the number of formed microparticles increases, but some porous particles also exit. Figure 3.31 shows the surface morphology of TPP-gelated CSMPs with CS/TPP mass ratio at 2/1. The small, round, sunk parts on the surface of CSMPs may verify the cross-linking process of TPP-gelated CSMPs. When small TPP microemulsions collide with big chitosan emulsion droplet, TPP microemulsion fuses into chitosan emulsion droplet quickly and then cross-link chitosan matrix (Figure 3.30). There are several kinds of particles in the CSMPs sample prepared with CS/TPP mass ratio 3/1. As shown in Figure 3.32, Figure 3.32A probably show an incompletely cross-linked microparticle. The cross-linking almost has been done in the CSMP shown in Figure 3.32B. Whereas, Figure 3.32C shows a TPP-gelated CSMPs with relatively small particle size. On the base of porous particles which still exist in the CSMPs sample gelated with a CS/TPP mass ratio 3/1, it means gelation time is not enough or the amount of TPP microemulsion is not enough. The small particles shown in Figure 3.30A and B are probably the result of big particles which did not encounter enough TPP microemulsion droplets.

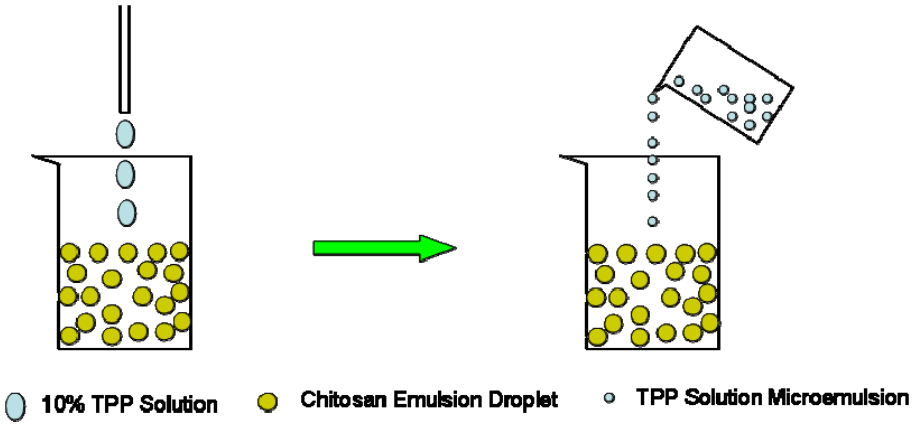

Fig. 3.29 Schematic of Optimized Preparation of TPP-cross-linked CSMPs.

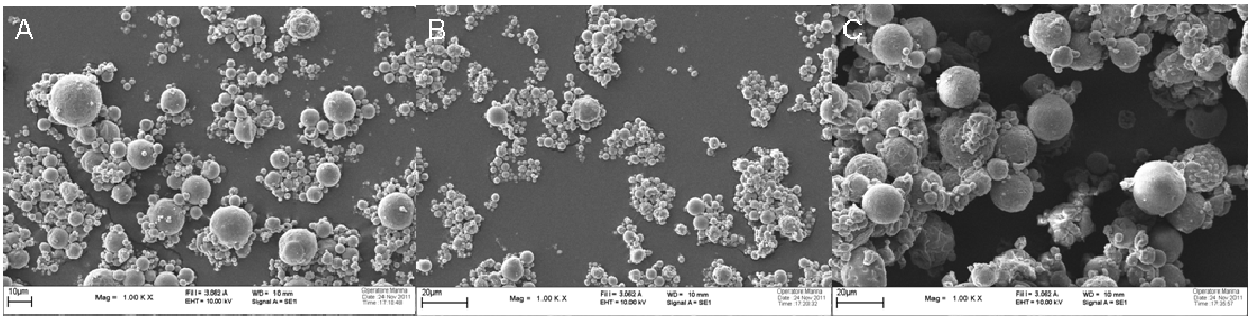

Fig. 3.30 SEM Photographs of TPP-cross-linked CSMPs with Various Amount of TPP microemulsion. A, 0.5ml, B,1.5ml, C, 3ml. Magnification: 1000X. Scale bar represents 10μm in A and 20μm in B and C.

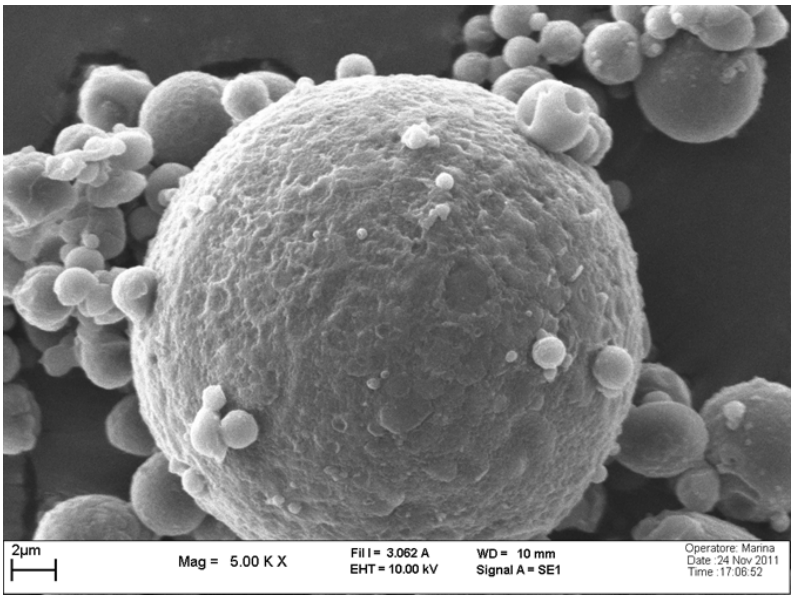

Fig. 3.31 SEM Photograph of TPP-cross-linked CSMPs with CS/TPP mass ratio 2/1. Scale bar represents 2μm.

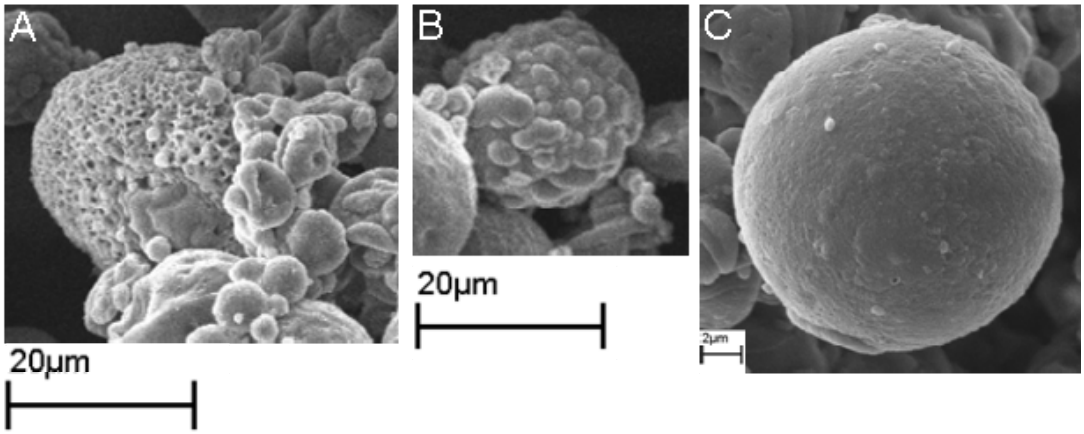

Fig. 3.32 The Surface Morphology of TPP-cross-linked CSMPs with CS/TPP mass ratio 1/3. Scale bar represents 20μm in A and B, 2μm in C.

3.3.6 The Construction of NPs/MPs Composite Particulate System for the Controlled Release of Proteins

As shown in chapter 2, chitosan nanoparticles showed an unfavorable initial release effect due to their nanoscale size and week electrostatic reaction with protein molecules, even though they are superior in preserving the bioactivity of protein molecules. As discussed in chapter 3, the use of organic solvents and strong shear force results from high-speed homogenization could compromise the bioactivity of protein molecules. However, in comparison with NPs, generally MPs possess higher drug payload and more extended drug release course. The strategy to construct a nanoparticles/microparticles composite system takes the advantages of the two and minimizes their drawbacks to achieve at one hand a long and stable drug release course and on the other hand effective protection of protein bioactivity. On this purpose, the CSNPs-containing CS/PLAMPs (CSNPs-CS/PLA MPs) were attempted to be constructed in this section to realize prolonged and stable protein release profile.

Fresh chitosan nanoparticles/BSA-incorporated chitosan nanoparticles prepared in chapter 2 with particle size of 389.7±6.5/432.5±6.3 nm, BSA loading capacity of 35.1±0.3% were encapsulated to chitosan microparticles. Chitosan microparticles were prepared according to the preparation parameters of Sample B (Table 3.1). As shown in Figure 3.33, chitosan nanoparticles-incorporated chitosan microparticles (CSNPs-CSMPs) show a smaller particle size compared with the blank CSMPs. The size range of blank CSMPs, CSNPs-CSMPs and BSA-CSNPs-CSMPs is 5.6±1.9, 3.7±1.1, 4.5±1.3μm

respectively (see Figure 3.34). As shown in Figure 3.35, all of the three particles show smooth surface. There is no obvious difference among blank CSMPs and the two composite particles. In order to verify the successful incorporation of CSNPs into CSMPs, the BSA-CSNPs were labeled with FITC. Then the FITC-labeled BSA-CSNPs were incorporated to CSMPs and observed with a fluorescence microscope. As shown in Figure 3.36, both discrete and clustered fluorescent spots are visible in composite particles. It indicates that BSA-CSNPs have been incorporated in CSMPs successfully. However, the distribution of CSNPs in chitosan microparticles is not uniform and some aggregates of CSNPs could be seen inside CSMPs. It's probably due to an incomplete redispersion of CSNPs by homogenization. Figure 3.36 also shows that the discrete CSNPs are preferentially located in the sub layer of some microparticles. It suggests that the interior matrix of these chitosan microparticles were not completely gelated.

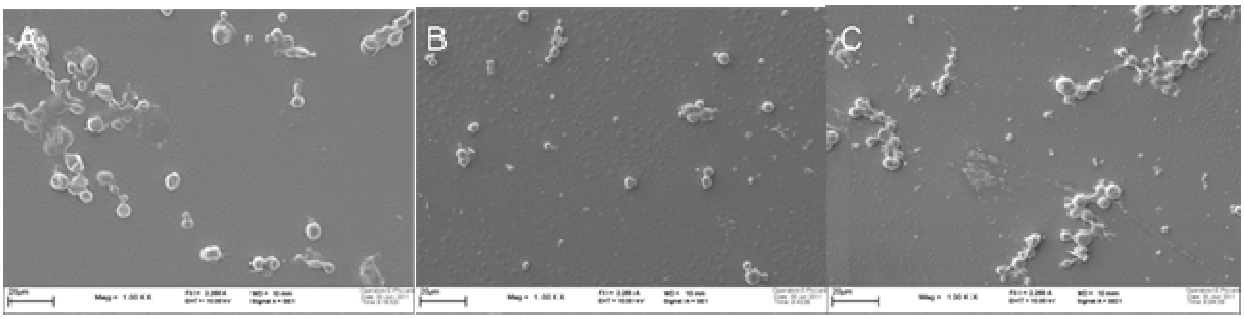

Fig. 3.33 SEM photographs of A, CSNP-CSMPs and B, BSA-CSNP-CSMPs. Magnification: 1000X. Bar represents 20μm in A and 10μm in B.

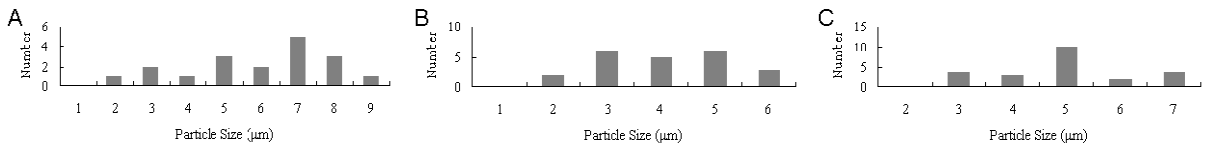

Fig. 3.34 Particle Size Distribution of CSMPs/BSA-CSMPs. A, blank CSMPs, B, blank CSNPs-incorporated CSMPs.

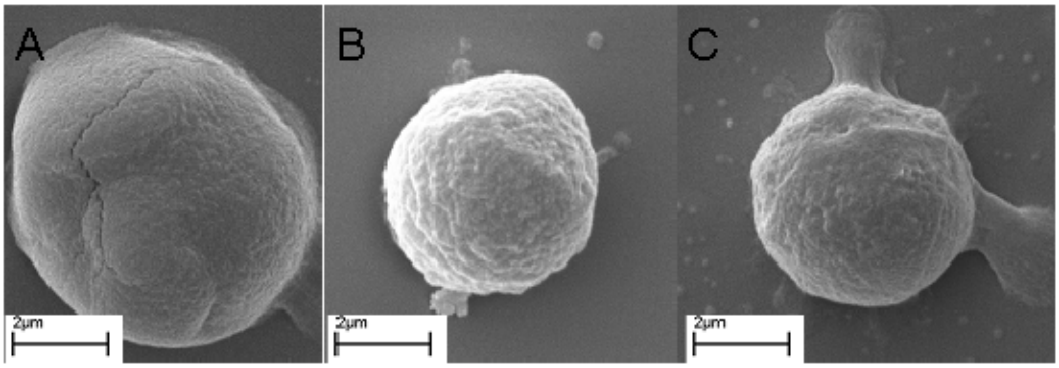

Fig.3.35 SEM Photographs of Particle Surfaces. A, CSMPs, B, CSNPs-CSMPs, C, BSA-CSNPs-CSMPs. Scale bars represent 2μm.

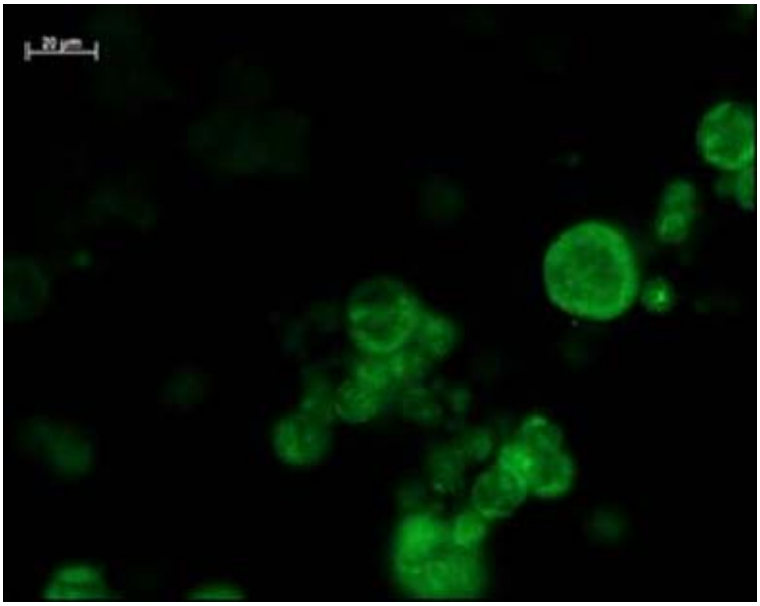

Fig. 3.36 The Incorporation of BSA-CSNPs into CSMPs under Fluoresence Microscope. Bar represents 20μm.

Considering that CSNPs show a fast initial burst release once they contact with aqueous medium, some BSA may already leak into chitosan microparticles matrix during CSNPs dispersion in the chitosan phase for emulsification. Even though these BSA leaks into the CSMPs matrix and have little chance to get out of the peripheral chitosan dispersed phase, the leakage could compromise the protein activity. To avoid this, we attempted to incorporate CSNPs into PLA to form chitosan nanoparticles-incorporated PLA microparticles (CSNPs-PLAMPs), since the leaking effect does not likely happen if CSNPs are incorporated into a hydrophobic dispersed phase. The preparation procedue of chitosan nanoparticles encapsulated PLA composite particles is shown in Fig. 3.37.

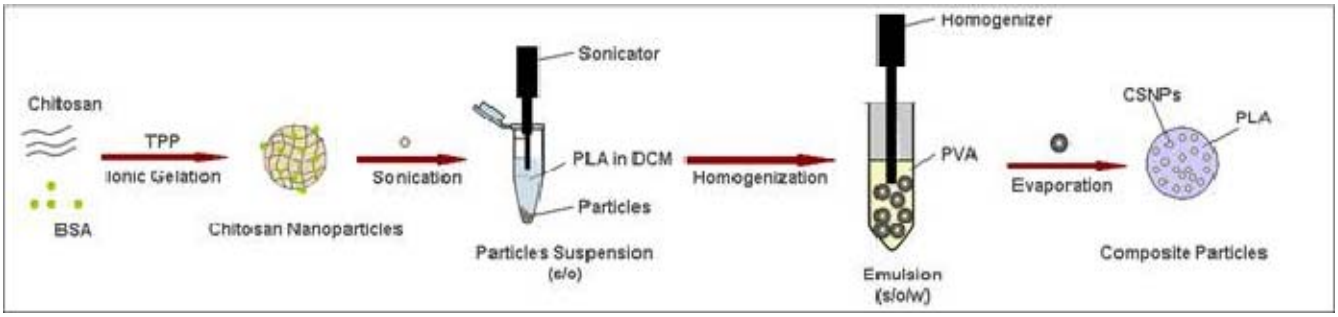

Fig. 3.37 The Schematic Presentation of the Preparation of Chitosan Nanoparticles Encapsulated PLA Composite Particles.

As shown in Figure 3.38, the obtained blank CSNPs incorporated PLA micropaticles show a mean diameter of 1.7±0.3 μm. The composite PLA particles have a very spherical morphology and smooth surface. Some small pores are present on the surface of some composite particles. Some composite are partially imperfect. The pores and defects observed on some composite particles are probably the result of the degradation of chitosan nanoparticles which distributed on the surface or surface layer of composite particles.

Fig. 3.38 SEM Photographs of CSNP-PLAMPs. Magnification: 3000X. Bar represents 20μm.

Fig. 3.39 shows the PLA composite particles under fluorescent microscope. Some bright spots can be seen in the frame of microparticles, which indicates the encapsulation of chitosan nanoparticles inside PLA external layer.

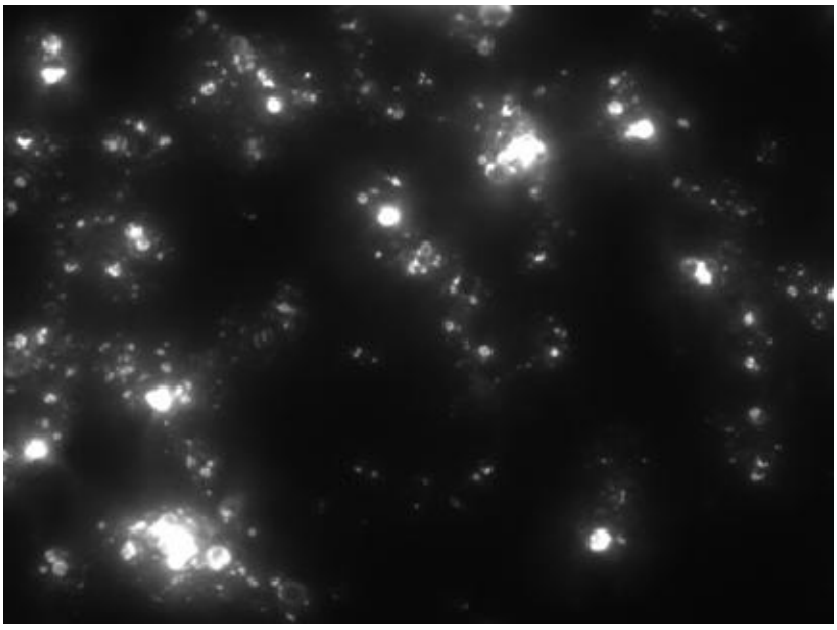

Fig. 3.39 Fluorescent Microphotograph of CSNP-PLAMPs. Phase contrast mode.

3.4 Conclusion and Perspective

Chitosan microparticles have found many applications as a proteins/peptides carrier for the delivery of therapeutic proteins/peptides via nasal, pulmonary, and parenteral administration [139]. In this chapter, we aim to prepare chitosan microparticles and composite particulate system to control the release of proteins.

Firstly, the preparation parameters of a conventional emulsification-coacervation method which is used in this study for the preparation of CSMPs are studied to obtain discrete, uniform, and spherical chitosan microparticles. For the dispersed phase, CSMPs obtained with medium molecular weight show bigger particle size than that with low molecular weight. But CSMPs formed with MMWCS show much wider size distribution compared with that with LMWCS. As the increase of chitosan concentration, particle size of CSMPs increases, meanwhile, the size distribution gets wider. However, at the chitosan concentration of 1%, fusion of particles occurs. The effect of chitosan molecular weight and concentration on the particle size and dispersity of CSMPs could contribute to the viscosity of the chitosan dispersed phase. Many emulsification parameters could influence the characters of CSMPs. w/o volume ratio shows no obvious effect on the particle size but some influence on particles morphology. At the w/o volume ratio of 1/10, obtained CSMPs show a rough surface and deformed particles appear. Above this ratio, obtained particles show a smooth surface. The addition of Tween 80 in chitosan dispersed phase does not help to stabilize the chitosan emulsion, on the contrary, rough particle surface and deformed particles appear. The combination of Span 85 and Span 80 as emulsifier with a higher HBL number reduces the particle size of CSMPs compared to only with Span 85 as emulsifier. The particle size of CSMPs decreases with the increasing Span 85 concentration. However, when it is too high (6%), some collapsed and deformed particles appear. High homogenization speed induces decreased particle size, but with the increase of homogenization speed, CSMPs are not able to keep spherical shape and begin to deform and fuse with each other. Results indicate that the multivalent anions are not favorable to give CSMPs good dispersity and morphology. TPP induced serious aggregation of particles. With Na_2SO_4 as coacervation agent, deformed particles and aggregate appear. According to the morphology of obtained CSMPs, the addition of 2/3 ml NaOH per 3 min was found the favorable addition rate. With either faster or slower addition, particles fusion, irregular shape or

rough surface appears. In the end, various amounts of BSA were encapsulated. The results indicate that only BSA-incorporated CSMPs with 0.5% BSA are discrete. The encapsulation of BSA reduces the particle size and increases size distribution of CSMPs. The ‘Sample B’ (see Table 3.1) which is always used as a control for other samples gives CSMPs with the best features in this study.

In order to avoid unfavorable preparation conditions and achieve more sustainable release, a modified preparation method was adopted to prepare TPP-glated CSMPs. A microemulsion of TPP was used to coacervate chitosan emulsion to minimize the interaction with the chitosan emulsion. Results show that discrete TPP-gelated CSMPs could be obtained in this way. Based on the analysis of obtained particles, increasing the amount of TPP microemulsion and extending the reaction time are able to obtain more uniform CSMPs.

In the end, a nanoparticles containing chitosan/PLA composite particulate system was realised. The preliminary experiments indicate CSNPs are able to be entrapped into chitosan or PLA microparticles. This composite particulate system which combines the advantages of chitosan nanoparticles and microparticles is a promising protein carrier.

As a prospect, in the future, the NaOH coacervated-chitosan microparticles, optimized TPP-gelated particles would be compared to study their controlled release property of proteins. In the end, these microparticles and the composite particles would be loaded onto a tissue engineering scaffold (e.g. chitosan scaffold as shown in Figure 3.40) to realize prolonged and stable release of growth factors.

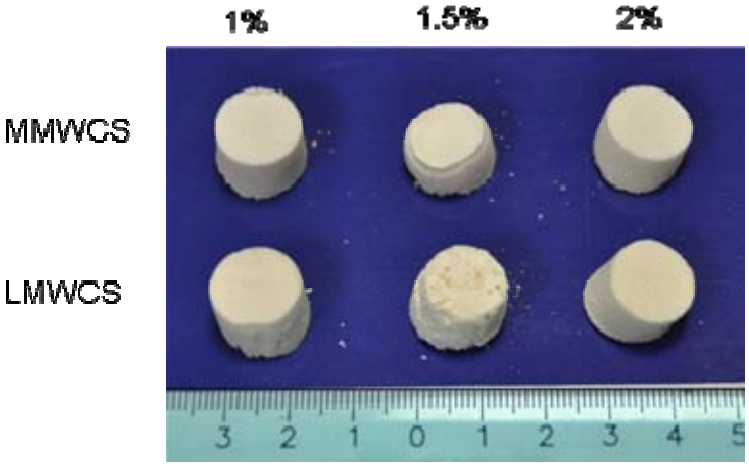

Fig. 3.40 Photographs of Chitosan Scaffolds.

Final Conclusion and Perspective

Chitosan (CS) is a rare cationic natural polymer. The primary amino groups on chitosan chains enable chitosan to interact with a big number of chemicals, biomolecules and polymers. For example, deprotonated amino groups interact with polyanions to form chitosan nanoparticles which is also one topic of this thesis. The formed chitosan nanoparticles can be used to delivery nuclear acids, peptides and proteins based on the electrostatic interaction between chitosan and these biomolecules. Additionally, the cationic and mucous permeability enhancing properties of chitosan are always used to develop oral, optical, pulmonary, and gastrointestinal administration formulations. Chitosan microparticles studied in this thesis is one of the formats in which these formulations are developed.

In chapter 2, chitosan nanoparticles (CSNPs) were prepared by the ionic gelation of polyanions-tripolyphosphate (TPP) to encapsulate protein molecules. BSA was used as a model protein. In order to get desirable particle size, dispersity, protein loading and release properties, the effect of primary preparation parameters on these characters of CSNPs were studied. Particle size measurement results indicated that both particle size and size distribution of CSNPs increased with increasing

chitosan concentration and inversely with the decreasing CS/TPP mass ratio. However, BSA concentration did not show a clearly detectable effect on the particle size within the studied concentration range, but stopped the rise of polydispersity of CSNPs with increasing CS/TPP mass ratio. This result indicates the competitive interaction between BSA molecules and TPP with chitosan. There's no obvious effect of chitosan and BSA concentration on the yield of CSNPs, but particles yield decreased with the increasing CS/TPP mass ratio. Besides, the encapsulation of BSA also resulted in the decrease of particles yield. The encapsulation efficiency (EE) of CSNPs increased with increasing chitosan concentration and decreased with increasing CS/TPP mass ratio. The EE of CSNPs reduced remarkably at the BSA concentration range 0.5~1.5 mg/ml (chitosan 3mg/ml, CS/TPP mass ratio 5/1).

In the past few decades, tripolyphosphate (TPP)-cross-linked chitosan nanoparticles (CSNPs) have been widely applied for the delivery of various biomacrimolecules such as nucleic acids, peptides and proteins due to their mild and convenient preparation conditions. However, ununiformity and burst release effect are always the major drawbacks of CSNPs and limit their application to some extent. In this study, we investigated the effect of pH value on the formation and protein encapsulation of CSNPs. The results revealed that the particle size of CSNPs dropped down dramatically with the decreasing pH value. However, the size distribution was conjointly influenced by pH vale and the mass ratio of chitosan to TPP. BSA was chose as the protein model in the study. The results indicated that BSA encapsulation efficiency (EE) of CSNPs increased significantly with the increasing pH value. In the end, the influence of cross-linker—TPP pH on the properties of CSNPs was studied. The results showed that the CSNPs prepared with a basic TPP solution (~ pH 9.5) had larger size, higher yield and BSA EE compared with that of the CSNPs obtained with a acetic TPP solution (~pH 5.5). The further characterization with FTIR spectrometry, DSC, SEM and in vitro BSA release test revealed that TPP solution pH might influence the formation and BSA encapsulation via changing the conformation of chitosan chains. In conclusion, this study gives a glance of the formation of CSNPs and protein encapsulation mechanisms from the pH value point of view. Thus, it is helpful to overcome the major drawbacks of CSNPs as a protein nanocarrier mentioned above.

Preliminary in vitro experiment showed a obvious initial burst release effect by VEGF-incorporated CSNPs. This is probably due to the electric state of VEGF in solution that hinders an efficient encapsulation by cationic CSNPs.

In chapter 3, chitosan microparticles (CSMPs) were prepared to control the release of proteins. Firstly, the preparation parameters were studied to get desirable particle size, dispersity and

morphology. Results indicated that high molecular weight and concentration of chitosan dispersed phase formed CSMPs with big size and wide size distribution. The study on the emulsification parameter found that w/o volume ratio mainly affected the surface morphology of CSMPs. Low w/o volume ratio (1/10) resulted in a rough particle surface. The addition of another surfactant into chitosan dispersed phase did not help to stabilize the emulsion. A combination of Span 80 and Span 85 as emulsifier with a higher hydrophile-lipophile balance (HLB) number can reduce the particle size compared with the CSMPs only with Span 85 as emulsifier. High speed homogenization reduced the particle size of CSMPs, but deformed particles and aggregates began to form. The concentration of Span 85 as a surfactant slightly reduced the particle size of CSMPs, but at high concentration of Span 85 particles began to deform. As gelation agents, multivalent anions SO_4^{2-} and $P_3O_{10}^{5-}$ did not give good monodispersity and regular shape to CSMPs. The result showed that adding NaOH solution by 2/3 ml every 3 min, obtained CSMPs showed the best dispersity and morphology. BSA encapsulation resulted in a wider size distribution compared with BSA-unloaded CSMPs. Results indicated that dispersed CSMPs could not be obtained with a BSA concentration above 1%. Afterwards, we optimized the preparation method of TPP-gelated CSMPs to realize a desirable protein release. A microemulsion of TPP solution was proposed to gelate the chitosan dispersed phase. The preliminary experiments indicated that this optimization could work to obtain dispersed CSMPs. In order to avoid the undesirable fast burst release of CSNPs and unfavorable preparation conditions of CSMPs, chitosan nanoparticles were incorporated in chitosan/PLA microparticles. Preliminary experiments verified the incorporation of CSNPs into Chitosan microparticles.

In the future, the controlled protein release properties of the NaOH-coacervated and TPP-gelated CSMPs could be compared. The chitosan nanoparticles incorporated PLA microparticles could be further engineered.and the protein release properties from this composite particulate system further investigated. In the end, all the three-nano, micro, and nano/micro particles could be loaded onto a bioengineering scaffold to test their protein release properties. During the study of chitosan nanoparticles, we found that protein molecules (BSA) could form nanoscaled complex with polyanions (TPP) at low solution pH. Therefore, it is possible to construct a core-shell nanovehicle to get a more sustainable protein release.

Acknowledgment

First I want to thank my thesis advisor - Professor Gianluca Ciardelii. He is not only a supervisor for me, but also a good friend. Thanks for his firm encourage, solid support, wise acedmic guidence, respect for acadmic freedom, tolerance for misticks from which I benefit a lot and hold my strength to finish my Ph.D. work.

Thank all of my colleges- Piergiogio, Chiara, Clara, Antonella, Marina, Monica, Anna, Valeria, Susana...Without your support I can't finish my work. Thank Fabiana, Cristina and Simone from Biosolar lab, because you are always happy to give me help. Thank all the colleagues in the Department of Mechanics; we have a good time together. All of you treat me like a member in a big family and together with you I never felt alone studing in abroad.

Thank my families; you are always near to me.

Thank all the people who ever helped me and gave me advices.

References

[1] M. Biondi et al. Advanced Drug Delivery Reviews 60 (2008) 229-242.

[2] Yasuhiko Tabata. Drug Discovery Today 10, (2005) 1639-1646.

[3] Journal of Controlled Release, Perspective, 120 (2007) 1-3.

[4] R.A. Freitas. Nanomedicine: Nanotechnology, Biology, and Medicine 1 (2005) 2–9.

[5] C.Nithya shanthi et al /Int.J. PharmTech Res.2010, 2(1).

[6] Expert Rev Vaccines. Author manuscript; available in PMC 2011 July 1.

[7] Panyam J, Labhasetwar V. Adv Drug Deliv Rev 2003; 55(3):329–347.

[8] Elamanchili P, Diwan M, Cao M, Samuel J. Vaccine 2004; 22(19):2406–2412.

[9] Cui Z, Mumper RJ. J Controlled Release 2002; 81(1–2):173–184.

[10] Tobío M, Gref R, Sánchez A, Langer R, Alonso MJ. Pharm Res 1998; 15(2):270–275.

[11] Patel PB, Shastri DH, Shelat PK, Shukla AK. Syst Rev Pharm 2010;1:113-20.

[12] Doherty MM, Hughes PJ, Kim SR. Int J Pharm 1994;111:205-11.

[13] Leucuta SE. Int J Pharm 1989; 54:71-8.

[14] Dhaliwal S, Jain S, Singh HP, Tiwary AK. AAPS J 2008;10:322-30.

[15] Michael I. Ugwoke, Ingrid J. Vereyken, and Henrik Luessen

[16] Suphiya Parveen, MS, Ranjita Misra, MS, Sanjeeb K. Sahoo. Nanoparticles: a boon to drug delivery, therapeutics, diagnostics and imaging. Nanomedicine: Nanotechnology, Biology, and Medicine 8 (2012) 147–166.

[17] Maeda H, Bharate GY, Daruwalla J. Polymeric drugs for efficient tumor-targeted drug delivery based on EPR-effect. Eur J Pharm Biopharm 2009;71:409-19.

[18] Gullotti E, Yeo Y. Extracellularly activated nanocarriers: a new paradigm of tumor targeted drug delivery. Mol Pharm 2009;6:1041-51.

[19] Kocbek P, Obermajer N, Cegnar M, Kos J, Kristl J. Targeting cancer cells using PLGA nanoparticles surface modified with monoclonal antibody. J Control Release 2007;120:18-26.

[20] Dakrong Pissuwan, Takuro Niidome, Michael B. Cortie. The forthcoming applications of gold nanoparticles in drug and gene delivery systems. Journal of Controlled Release 149 (2011) 65–71.

[21] Timothy Jamieson, Raheleh Bakhshi, Daniela Petrova, Rachael Pocock, Mo Imani, Alexander M. Seifalian. Biological applications of quantum dots. Biomaterials 28 (2007) 4717–4732.

[22] Sherief Essa, Jean Michel Rabanel, Patrice Hildgen. Effect of polyethylene glycol (PEG) chain organization on the physicochemical properties of poly(D, L-lactide) (PLA) based nanoparticles. European Journal of Pharmaceutics and Biopharmaceutics 75 (2010) 96–106.

[23] Tapan K. Dash, V. Badireenath Konkimalla. Poly-ϵ-caprolactone based formulations for drug delivery and tissue engineering: A review. Journal of Controlled Release 158 (2012) 15–33.

[24] Fabienne Danhier, Eduardo Ansorena, Joana M. Silva, Régis Coco, Aude Le Breton, Véronique Préat. PLGA-based nanoparticles: An overview of biomedical applications. Journal of Controlled Release 161 (2012) 505–522.

[25] Sunil A. Agnihotri, Nadagouda N. Mallikarjuna, Tejraj M. Aminabhavi. Recent advances on chitosan-based micro- and nanoparticles in drug delivery. Journal of Controlled Release 100 (2004) 5–28.

[26] Heidi Vogt Sæther, Hilde K. Holme, Gjertrud Maurstad, Olav Smidsrød, Bjørn T. Stokke. Polyelectrolyte complex formation using alginate and chitosan. Carbohydrate Polymers 74 (2008) 813–821.

[27] Kayser O, Lemke A, Hernandez-Trejo N. The impact of nanobiotechnology on the development of new drug delivery systems. Curr Pharm Biotechnol 2005;6:3-5.

[28] Rainer H. MuÈller, Karsten MaÈder, Sven Gohla. Solid lipid nanoparticles (SLN) for controlled

drug delivery-a review of the state of the art. European Journal of Pharmaceutics and Biopharmaceutics 50 (2000) 161-177.

[29] Rahul P. Bagwe, Lisa R. Hilliard, and Weihong Tan. Surface modification of silica nanoparticles to reduce aggregation and non-specific binding. Langmuir. 2006 April 25; 22(9): 4357–4362.

[30] Zhanhu Guo, Tony Pereira, Oyoung Choi, Ying Wang and H. Thomas Hahn. Surface functionalized alumina nanoparticle filled polymeric nanocomposites with enhanced mechanical properties. J. Mater. Chem., 2006, 16, 2800–2808.

[31] Gupta Shipra Mital & TRIPATHI Manoj. A review of TiO2 nanoparticles. Chinese Sci Bull June (2011) Vol.56 No.16.

[32] Badley RD, Ford WT, McEnroe FJ, Assink RA. Surface modification of colloidal silica. Langmuir 1990;6:792-801.

[33] G. F. Goya, V. Grazú, M. R. and Ibarra. Magnetic Nanoparticles for Cancer Therapy. Current Nanoscience, 2008, 4, 1-16.

[34] For a comprehensive review on magnetic fluid applications see: Odenbach S. J. Phys.: Condens. Matter., 2004, 16, R1135.

[35] Dilnawaz F, Singh A, Mohanty C, Sahoo SK. Dual drug loaded superparamagnetic iron oxide nanoparticles for targeted cancer therapy. Biomaterials 2010;31:3694-706.

[36] Torchilin VP, Trubetskoy VS, Whiteman KR, Caliceti P, Ferruti P, Veronese FM. New synthetic amphiphilic polymers for steric protection of liposomes in vivo. J Pharm Sci 1995; 84:1049-53.

[37] Croy SR & Kwon GS. Polymeric micelles for drug delivery. Curr Pharm Des. 2006;12(36):4669-84.

[38] Ruth Duncan & Lorella Izzo. Dendrimer biocompatibility and toxicity. Advanced Drug Delivery Reviews 57 (2005) 2215– 2237.

[39] D.A. Tomalia, H. Baker, J. Dewald, M. Hall, G. Kallos, S. Martin, J. Roeck, J. Ryder, P. Smith, A new class of polymers: starburst-dendritic macromolecules, Polym. J. 17 (1985) 117–132.

[40] Valérie D, Vinod DV. Pharmaceutical applications of chitosan. Pharm Sci Technol Today 1998;1:246–53.

[41] Inez M. van der Lubben, J. Coos Verhoef, Gerrit Borchard, Hans E. Junginger. Chitosan and its derivatives in mucosal drug and vaccine delivery. European Journal of Pharmaceutical Sciences 14 (2001) 201–207.

[42] Kean T, Thanou M. Chitin and chitosan—sources, production and medical applications. In:

Williams PA, Arshady R, editors. Desk reference of natural polymers, their sources, chemistry and applications. London: Kentus Books; 2009. p. 327–61.

[43] Funkhouser JD, Aronson Jr NN. Chitinase family GH18: evolutionary insights from the genomic history of a diverse protein family. BMC Evol Biol 2007;7:96–112.

[44] Kean T, Thanou M. Biodegradation, biodistribution and toxicity of chitosan. Adv Drug Deliv Rev 2009;62:3–11.

[45] Yang YM, Hu W, Wang XD, Gu XS. The controlling biodegradation of chitosan fibers by N-acetylation in vitro and in vivo. J Mater Sci Mater Med 2007;18:2117–21.

[46] Xu J, McCarthy SP, Gross RA, Kaplan DL. Chitosan film acylation and effects on biodegradability. Macromolecules 1996;29:3436–40.

[47] Sevda Senela & Susan J. McClureb. Potential applications of chitosan in veterinary medicine. Advanced Drug Delivery Reviews 56 (2004) 1467– 1480.

[48] Smith, J., Wood, E., Dornish, M., 2004. Effect of chitosan on epithelial cell tight junctions. Pharm. Res. 21, 43–49.

[49] A. Bacon, J. Makin, N. Chatfield, A novel mucosal influenza vaccine, Res. Immunol. 149 (1998) 98.

[50] E.A. McNeela, D. O'Connor, I. Jabbal-Gill, L. Illum, S.S. Davis, M. Pizza, S. Peppoloni, R. Rappuoli, K.H.G. Mills, A mucosal vaccine against diptheria: formulation of cross reacting material (CRM 197) of diptheria toxin with chitosan enhances local and systemic antibody and Th2 responses following nasal delivery, Vacccine 19 (2001) 1198– 1199.

[51] H. Le Buanec, C. Vetu, A. Lachgar, M.A. Benoit, J. Gillard, S. Paturance, J. Aucouturier, V. Gane, D. Zagury, B. Biizzini, Induction in mice of anti-Tat mucosal immunity by the intranasal and oral routes, Biomed. Pharmacother. 55 (2001) 316–320.

[52] M.A.J. Westerink, S.L. Smithson, N. Srivastava, J. Blonder, C. Coeshott, G.J. Rosenthal, Projuvantk (Pluronic F127/chitosan) enhances the immune response to intranasally administered tetanus toxoid, Vaccine 20 (2002) 711 –723.

[53] Jumaa M, Furkert FH, Muller BW. A new lipid emulsion formulation with high antimicrobial efficacy using chitosan. Eur J Pharm Biopharm 2002;53:115–23.

[54] M. Dasha, F. Chiellini a, R.M. Ottenbriteb, E. Chiellini a. Chitosan—A versatile semi-synthetic polymer in biomedical applications. Progress in Polymer Science 36 (2011) 981–1014.

[55] Seol YJ, Lee JY, Park YJ, Lee YM, Young K, Rhyu IC, Lee SJ, Han SB, Chung CP. Chitosan

sponges as tissue engineering scaffolds for bone formation. Biotechnol Lett 2004;26:1037–41.

[56] Wu Y, Chen N, Liu LK, Yuan H, Li QL, Chen SH. Chitosan/alginate multilayer scaffold encapsulating bone marrow stromal cells in situ on titanium. J Bioact Compat Polym 2009;24:301–15.

[57] Lahiji A, Sohrabi A, Hungerford DS, Frondoza CG. Chitosan supports the expression of extracellular matrix proteins in human osteoblasts and chondrocytes. J Biomed Mater Res 2000;51:586–95.

[58] Lindahl U, Hook M. Glycosaminoglycans and their binding to biological macromolecules. Annu Rev Biochem 1978;47:385–417.

[59] Li J, Pan J, Zhang L, Guo X, Yu Y. Culture of primary rat hepatocytes within porous chitosan scaffolds. J Biomed Mater Res A 2003;67:938–43.

[60] Kim IY, Seo SJ, Moon HS, Yoo MK, Park IY, Kim BC, Cho CS. Chitosan and its derivatives for tissue engineering applications. Biotechnol Adv 2008;26:1–21.

[61] Li F, LiuWG,Yao KD. Preparation of oxidized glucose-crosslinked Nalkylated chitosan membrane and in vitro studies of pH-sensitive drug delivery behaviour. Biomaterials 2002;23:343–7.

[62] Narayan Bhattarai1, Jonathan Gunn1, Miqin Zhang. Chitosan-based hydrogels for controlled, localized drug delivery. Progress in Polymer Science 36 (2011) 981–1014.

[63] Sunil A. Agnihotri, Nadagouda N. Mallikarjuna, Tejraj M. Aminabhavi. Recent advances on chitosan-based micro- and nanoparticles in drug delivery. Journal of Controlled Release 100 (2004) 5–28.

[64] Hennink WE, van Nostrum CF. Novel crosslinking methods to design hydrogels. Adv Drug Deliv Rev 2002;54:13–36.

[65] Ueno H, Mori T, Fujinaga T. Topical formulations andwoundhealing applications of chitosan. Adv Drug Deliv Rev 2001;52:105–15.

[66] Obara K, Ishihara M, Ishizuka T, Fujita M, Ozeki Y, Maehara T, Saito Y, Yura H, Matsui T, Hattori H, Kikuchi M, Kurita A. Photocrosslinkable chitosan hydrogel containing fibroblast growth factor-2 stimulates wound healing in healing-impaired db/db mice. Biomaterials 2003;24:3437–44.

[67] Omid Veiseh, Jonathan W. Gunn, Miqin Zhang. Design and fabrication of magnetic nanoparticles for targeted drug delivery and imaging. Advanced Drug Delivery Reviews 62 (2010) 284–304.

[68] Lee CM, Jeong HJ, Kim SL, Kim EM, Kim DW, Lim ST, Jang KY, Jeong YY, Nah JW, Sohn MH. SPION-loaded chitosan-linoleic acid nanoparticles to target hepatocytes. Int J Pharm 2009;371:163–9.

[69] Kumar MN, Muzzarelli RA, Muzzarelli C, Sashiwa H, Domb AJ. Chitosan chemistry and

pharmaceutical perspectives. Chem Rev 2004;104:6017–84.

[70] V.R. Sinha, A.K. Singla, S. Wadhawan, R. Kaushik, R. Kumria, K. Bansal, S. Dhawan. Chitosan microspheres as a potential carrier for drugs. International Journal of Pharmaceutics 274 (2004) 1–33.

[71] Skaugrud, O., 1991. Chitosan—new biopolymer for cosmetics and drugs. Drug Cosmetic Ind. 148, 24–29.

[72] Akbuga J, Durmaz G. Preparation and evaluation of crosslinked chitosan microspheres containing furosemide. Int J Pharm 1994;111:217–22.

[73] Bayomi MA, al-Suwayeh SA, el-Helw AM, Mesnad AF. Preparation of casein-chitosan microspheres containing diltiazem hydrochloride by an aqueous coacervation technique. Pharm Acta Helv. 1998 Dec;73(4):187-92.

[74] Li YH, Fan MW, Bian Z, Chen Z, Zhang Q, Yang HR. Chitosan-DNA microparticles as mucosal delivery system: synthesis, characterization and release in vitro. Chin Med J (Engl). 2005 Jun 5;118(11):936-41.

[75] He P, Davis SS, Illum L. Chitosan microspheres prepared by spray drying. Int J Pharm 1999;187:53–65.

[76] Agnihotri SA, Aminabhavi TM. Controlled release of clozapine through chitosan microparticles prepared by a novel method. J Control Release 2004;96:245–59.

[77] Mansouri S, Cuie Y, Winnik F, Shi Q, Lavigne P, Benderdour M, Beaumont E, Fernandes JC. Biomaterials. Characterization of folate-chitosan-DNA nanoparticles for gene therapy.2 006 Mar;27(9):2060-5. Epub 2005 Oct 3.

[78] Ülker Guliyeva, Filiz Öner, Şule Özsoy, Rıfkı Haziroğlu. Chitosan microparticles containing plasmid DNA as potential oral gene delivery system. European Journal of Pharmaceutics and Biopharmaceutics 62 (2006) 17–25.

[79] I.M. van der Lubben, J.C. Verhoef, A.C. van Aelst, G. Borchard, H.E. Junginger. Chitosan microparticles for oral vaccination: preparation, characterization and preliminary in vivo uptake studies in murine Peyer's patches. Biomaterials 22 (2001) 687-694.

[80] Mi Lan Kang, Chong Su Cho, Han Sang Yoo. Application of chitosan microspheres for nasal delivery of vaccines. Biotechnology Advances 27 (2009) 857–865.

[81] M.L. Lorenzo-Lamosa, C. Remunan-Lopez, J.L. Vila-Jato, M.J. Alonso. Design of microencapsulated chitosan microspheres for colonic drug delivery. Journal of Controlled Release 52 (1998) 109–118.

[82] K. Mladenovska, R.S. Raicki, E.I. Janevik, T. Ristoski, M.J. Pavlova, Z. Kavrakovski, M.G. Dodov, K. Goracinova. Colon-specific delivery of 5-aminosalicylic acid from chitosan-Ca-alginate microparticles. International Journal of Pharmaceutics 342 (2007) 124–136.

[83] El-Shabouri MH. Positively charged nanoparticles for improving the oral bioavailability of cyclosporin-A. Int J Pharm. 2002 Dec 5;249(1-2):101-8.

[84] Tokumitsu H, Ichikawa H, Fukumori Y. Chitosan-gadopentetic acid complex nanoparticles for gadolinium neutron-capture therapy of cancer: preparation by novel emulsion-droplet coalescence technique and characterization. Pharm Res. 1999 Dec;16(12):1830-5.

[85] Calvo P, Remunan-L opez C, Vila-Jato JL, Alonso MJ. J Polym Sci 63:125–132 (1997).

[86] Hu Y, Jiang X, Ding Y, Ge H, Yuan Y and Yang C, Biomaterials 23:3193–3201 (2002).

[87] Tarane Gazori, Mohammad Reza Khoshayand, Ebrahim Azizi, Parisa Yazdizade, Alireza Nomani, Ismaeil Haririan. Evaluation of Alginate/Chitosan nanoparticles as antisense delivery vector: Formulation, optimization and in vitro characterization. Carbohydrate Polymers 77 (2009) 599–606.

[88] Saranya N, Moorthi A, Saravanan S, Devi MP, Selvamurugan N. Chitosan and its derivatives for gene delivery. Int J Biol Macromol. 2011 Mar 1;48(2):234-8. Epub 2010 Dec 4.

[89] Kim J-H, Kim Y-S, Kim S, Park JH, Kim K, Choi K, et al, J Control Rel 111:228–234 (2006).

[90] Sarmento B, Ribeiro A, Veiga F, Sampaio P, Neufeld R and Ferreira D, J Nanosci Nanotechnol 7:2833–2841 (2007).

[91] Zang H, Wu S, Tao Y, Zang L and Su Z, J Nanomater 2010:898910 (2010).

[92] Al-Qadi S, Grenha A, Carrión-Recio D, Seijo B, Remuñán-López C. Microencapsulated chitosan nanoparticles for pulmonary protein delivery: in vivo evaluation of insulin-loaded formulations. J Control Release. 2012 Feb 10;157(3):383-90. Epub 2011 Aug 12.

[93] Shahnaz G, Vetter A, Barthelmes J, Rahmat D, Laffleur F, Iqbal J, Perera G, Schlocker W, Dünnhaput S, Augustijns P, Bernkop-Schnürch A. Thiolated chitosan nanoparticles for the nasal administration of leuprolide: bioavailability and pharmacokinetic characterization. Int J Pharm. 2012 May 30;428(1-2):164-70. Epub 2012 Mar 5.

[94] de la Fuente M, Seijo B, Alonso MJ. Novel hyaluronic acid-chitosan nanoparticles for ocular gene therapy. Invest Ophthalmol Vis Sci. 2008 May;49(5):2016-24.

[95] Zheng-Shun Wen, Ying-Lei Xu, Xiao-Ting Zou, Zi-Rong Xu. Chitosan Nanoparticles Act as an Adjuvant to Promote both Th1 and Th2 Immune Responses Induced by Ovalbumin in Mice. Mar. Drugs 2011, 9, 1038-1055.

[96] Katas H, Alpar HO. Development and characterisation of chitosan nanoparticles for siRNA delivery.J Control Release. 2006 Oct 10;115(2):216-25. Epub 2006 Jul 25.

[97] Chih-Hui Yang, Keng-Shiang Huang, Po-Wen Lin, Yu-Cheng Lin. Using a cross-flow microfluidic chip and external crosslinking reaction for monodisperse TPP-chitosan microparticles. Sensors and Actuators B 124 (2007) 510–516.

[98] Calvo, P., Remunan-Lopez, C., Vila-Jato, J.L., Alonso, M.J., 1997a. Chitosan and chitosan/ethylene oxide–propylene oxide block copolymer nanoparticles as novel carriers for proteins and vaccines. Pharm. Res. 14, 1431-1436.

[99] Bradford, M. M., 1976. A Rapid and Sensitive Method for the Quantitation of Microgram Quantities of Protein Utilizing the Principle of Protein-Dye Binding. Analytical Biochemistry 72, 248-254.

[100] Q. Gan, T. Wang, 2007. Chitosan nanoparticle as protein delivery carrier-Systematic examination of fabrication conditions for efficient loading and release. Colloids and Surfaces B: Biointerfaces 59, 24-34.

[101] I.A. Alsarra, S.H. Neau, 2004. M.A. Howard, Effects of preparative parameters on the properties of chitosan hydrogel beads containing Candida rugosa lipase, Biomaterials 25, 2645-2655.

[102] Peniche, H. & Peniche, C. (2011). Chitosan nanoparticles: a contribution to nanomedicine. Polymer International, 60, 883–889.

[103] I. Bravo-Osuna, G. Ponchel, C. Vauthiera, European Journal of Pharmaceutical Sciences 30 (2007) 143-154.

[104] G.-Y. Li et al., Colloids and Surfaces A: Physicochem. Eng. Aspects 320 (2008) 11-18.

[105] F. Atyabi et al., Carbohydrate Polymers 74 (2008) 59-67.

[106] J. Zhang et al., Nanomedicine: Nanotechnology, Biology, and Medicine 3 (2007) 258-265.

[107] A.M.M. Sadeghi et al., International Journal of Pharmaceutics 355 (2008) 299-306.

[108] A. Anitha et al., Carbohydrate Polymers 78 (2009) 672-677.

[109] W. Fan, W Yan, Z. Xu, H. Ni, Colloids and Surfaces B: Biointerfaces 90 (2012) 21-27.

[110] Q. Gan et al. Colloids and Surfaces B: Biointerfaces 44 (2005) 65-73.

[111] Bradford, M. M., 1976. Analytical Biochemistry 72, 248-254.

[112] K.W. Leong, H.Q. Mao, V.L. Truong-Le, J. Control. Release 53 (1998) 183-193.

[113] M. Kaloti, H.B. Bohidar, Colloids and Surfaces B: Biointerfaces 81 (2010) 165-173.

[114]I.S. Tavares et al., Colloids and Surfaces B: Biointerfaces 90 (2012) 254-258.

[115] A. Cadete et al., European Journal of Pharmaceutical Sciences 45 (2012) 451-458.

[116] R. Jayakumar et al., Carbohydrate Polymers 79 (2010) 1-8.

[117] W.E. Rudzinski, T.M. Aminabhavi, International Journal of Pharmaceutics 399 (2010) 1-11.

[118] F. Sonvico et al., International Journal of Pharmaceutics 324 (2006) 67-73.

[119] A. Anitha et al., Carbohydrate Polymers 84 (2011) 1158-1164.

[120] T. Gazori et al., Carbohydrate Polymers 77 (2009) 599-606.

[121] F.A. Oyarzun-Ampuero et al., International Journal of Pharmaceutics 381 (2009) 122-129.

[122] Tokumitsu H, Ichikawa H and Fukumori Y, Pharm Res 16:1830-1835 (1999).

[123] F. Mi, S. Shyu, T. Wong, S. Jang, S. Lee, K. Lu. Journal of Applied Polymer Science, 74, (1999) 1093-1107.

[124] Zhang, H., Oh, M., Allen, C., Kumacheva, Biomacromolecules 5 (2004) 2461-2468.

[125] Peng Huang, Zhiming Li, Hengyao Hu, and Daxiang Cui, Journal of Nanomaterials, Volume 2010 (2010), Article ID 641545, 6 pages

[126] Qi, L., Z. Xu, Z. (2004). Colloids and Surfaces, A: Physiochemical and Engineering Aspects, 251(1-3), 183-190.

[127] B. Luppi et al., European Journal of Pharmaceutical Sciences 44 (2011) 559-565.

[128] Y. Liu et al., Carbohydrate Polymers 83 (2011) 1162-1168.

[129] Q. Gan, T. Wang, Colloids and Surfaces B: Biointerfaces 59 (2007) 24-34.

[130] A.K. Wright, M.R. Thompson, Biophysical journal, 15 (1975) 137-141.

[131] W. Fan et al., 2012. Colloids and Surfaces B: Biointerfaces 90, 21-27.

[132] M. Kaloti, H.B. Bohidar, 2010. Colloids and Surfaces B: Biointerfaces 81, 165-173.

[133] A.B. Schnurch, A. Heinrich, A. Greimel, 2006. Development of a novel method for the preparation of submicron particles based on thiolated chitosan. European Journal Pharmaceutics and Biopharmaceutics 63, 166-172.

[134] Leong YS and Candau F, J Phys Chem 86:2269-2271 (1982).

[135] L. Y. Lim, Lucy S. C. Wan, and P. Y. Thai, 1997. Chitosan microspheres prepared by emulsification and ionotropic Gelation. Drug Development and Industrial Pharmacy 23 (10), 981-985.

[136] J. Y. Zhao et al. Chinese Journal of Analytical Chemistry, 2006, 34(11): 1555-1559.

[137] B. Yang et al. Carbohydrate Polymers 80 (2010) 860-865.

[138] O. Skaugrud, Manuf. Chem., 60, 31-35 (1989).

[139] Somasundaram Ramachandran et al /Int.J. PharmTech Res.2011,3(1).

[140] Ida Genta, a, Monica Costantinib, Annalia Astic, Bice Contia, Luisa Montanarib